TARGETED ACTIVITY OF HISTONE DEACETYLASE INHIBITION IN SYNOVIAL SARCOMA

by:

Aimée Nicole Laporte

B.Sc. Honours, Queen's University, 2010
M.Sc., University of Ottawa, 2012

A THESIS SUBMITTED IN PARTIAL FULFILLMENT OF
THE REQUIREMENTS FOR THE DEGREE OF

DOCTOR OF PHILOSOPHY

in

THE FACULTY OF GRADUATE AND POSTDOCTORAL STUDIES

(Interdisciplinary Oncology)

THE UNIVERSITY OF BRITISH COLUMBIA
(Vancouver)

August 2017

ABSTRACT

Synovial sarcoma is an aggressive soft tissue cancer affecting primarily adolescents and young adults and characterized by the known chimeric fusion oncoprotein SS18-SSX resulting from a t(X;18) translocation. Oncoprotein-mediated interactions with chromatin-modification proteins are known to influence transformation; however targeted therapies are not currently available. Patients remain at high-risk for local recurrence and metastasis and see a 10-year survival rate of approximately 50%. Accordingly, it was hypothesized that therapeutic compounds able to disrupt the SS18-SSX driving complex would be clinically effective against synovial sarcoma. The proximity ligation assay was employed to study the drug-mediated disruption of the key SS18-SSX-mediated protein interactions that drive sarcomagenesis, and was developed for use to demonstrate targeted drug efficacy. Results identified HDAC inhibitors as potent in disrupting the oncogenic protein complex. The combination of HDAC and proteasome inhibitors was further found to be synergistic against synovial sarcoma. This pre-clinical study was used as support for a novel clinical trial proposal for translocation-associated soft tissue sarcomas. The effects of HDAC inhibition on genome-wide transcription patterns was further assessed by RNA-seq analysis. Uniquely to synovial sarcoma, it was revealed that HDAC inhibition elicits loss of the SS18-SSX oncoprotein and provokes significant pro-apoptotic *BIK* expression correlating to *CDKN2A* reactivation. From this, the contributing role of *CDKN2A* reactivation and reactive oxygen species accumulation in HDAC-inhibitor mediated apoptosis in synovial sarcoma was demonstrated.

LAY ABSTRACT

Synovial sarcoma is an aggressive soft tissue cancer affecting primarily adolescents and young adults. It is known to be caused by a mutation called SS18-SSX; however therapies targeted against this cancer-causing protein are not currently available. Patients remain at high-risk for local recurrence and metastasis and only half are still alive 10 years after diagnosis. Cancer therapies able to inhibit SS18-SSX should provide better treatment options for synovial sarcoma. Experiments were employed to study the drug-mediated inhibition of SS18-SSX, revealing a drug class known as HDAC inhibitors to be effective. Furthermore another drug class known as proteasome inhibitors was found to effectively work in combination with HDAC inhibitors, enhancing activity against synovial sarcoma. This pre-clinical study was used as support for a novel clinical trial proposal for translocation-associated soft tissue sarcomas.

PREFACE

The contents of chapter 2 are modified from the published paper: "**A.N. Laporte**, J.X. Ji, L. Ma, T.O. Nielsen, B.A. Brodin. 2016. Identification of cytotoxic agents disrupting synovial sarcoma oncoprotein interactions by proximity ligation assay. *Oncotarget* 7(23):34384-34394". My contributions include development of the proximity ligation assay for use in the synovial sarcoma cell model and adapting it for high-throughput experiments, performing the majority of the validation experiments, undertaking the 16 000-compound drug library screen and all functional drug studies, as well as writing of the manuscript. The FFPE PLA study was performed by Jennifer Ji. Experiments using CME-1 cell line were performed by Dr. Bertha Brodin with assistance by Limin Ma.

The contents of chapter 3 are modified from the published paper: "**A.N. Laporte**, J.J. Barrott, R.J. Yao, N.M. Poulin, B.A. Brodin, K.B. Jones, T.M. Underhill, T.O. Nielsen. 2017. Combination of HDAC and proteasome inhibitors synergize in the activation of pro-apoptotic factors in synovial sarcoma. *PLoS ONE.* 12(1): e0169407". My contributions include development of the drug combination and mechanism of synergy concept, performing the majority of the experiments and writing of the manuscript. The animal studies were performed by Drs. Jared Barrett and Kevin Jones. The primary cell line experiment was performed by Dr. Bertha Brodin. Dr. Neal Poulin assisted with drug screen data configuration. Robert J. Yao was an undergraduate student research trainee assisting with experiments under my direct supervision.

The contents of chapter 4 are modified from the submitted manuscript: "**A.N. Laporte**, N.M. Poulin, A. Lorzadeh, X.Q. Wang, R. Vander Werff, T.M. Underhill, T.O. Nielsen. 2017. Cell death by HDAC inhibition in synovial sarcoma". My contributions

include development of the hypothesis, data analysis, performing the validation experiments and writing of the manuscript. The RNA-seq was performed by Ryan Vander Werff with Michael Underhill. Neal Poulin and Ali Lorzadeh contributed to the RNA-seq data analysis. The animal studies in this thesis were performed by Drs. Jared Barrett and Kevin Jones and Jenny Wang performed the IHC experiments.

This thesis research was performed following the protocols approved by the UBC Research Ethics Board (#H08-0717 and #H06-00013). Mouse synovial sarcoma studies described here were conducted by collaborator Dr. Kevin B. Jones (Huntsman Cancer Institute, University of Utah). The protocol was approved by the Institutional Animal Care and Use Committee of the University of Utah (Permit Number: 14-01016).

TABLE OF CONTENTS

LIST OF TABLES

LIST OF FIGURES

LIST OF ABBREVIATIONS

AKT	Ak strain thymoma (Protein kinase B)
ARF	Alternative reading frame
ATF2	Activating transcription factor 2
BAK	Bcl-2 homologous antagonist killer
BAX	Bcl-2-associated X protein
BCL2	B-cell lymphoma 2
BIM	Bcl-2-like protein 11
BIK	Bcl-2-interacting killer
BMF	Bcl-2-modifying factor
BMI1	B Lymphoma Mo-MLV insertion region 1 homolog
bp	Base pair
BRM	Brahma Homolog
BSA	Bovine serum albumin
CCN	Cyclin
CDK	Cyclin-dependent kinase
CDKN	Cyclin-dependent kinase inhibitor
cDNA	Complementary DNA
ChIP	Chromatin immunoprecipitation
c-kit	tyrosine-protein kinase kit
CRE	cAMP-response element
CtBP	C-terminal binding protein
DCFDA	Dichlorofluorescein diacetate assay

dsDNA	Double-stranded deoxyribonucleic acid
EED	Embryonic ectoderm development
EGR1	Early Growth Response 1
ER	Endoplasmic reticulum
ERK	Extracellular signal-regulated kinases
EZH2	Enhancer of Zeste Homolog 2
FBS	Fetal bovine serum
FFPE	Formalin-fixed paraffin-embedded
FGFR	Fibroblast growth factor receptor
FOXO	Forkhead box protein O
FZD10	Frizzled homologue 10
GEMM	Genetically engineer mouse model
GFP	Green fluorescence protein
GSK3β	Glycogen synthase kinase 3 beta
H3K27me3	Lysine 27 trimethylation on histone H3
H&E	Hematoxylin and eosin
HAT	Histone acetyltransferase
HDAC	Histone deacetylase
HEK293T	Human embryonic kidney 293T
HLA	Human leukocyte antigen
IHC	Immunohistochemistry
IND	Investigational new drug
IP	Immunoprecipitation

IV	Intravenous
JNK	c-Jun N-terminal kinases
KRAB	Kruppel-associated box
MDM2	Mouse Double Minute 2 Homolog
MEK	Mitogen-activated protein kinase kinase
MRI	Magnetic resonance imaging
mRNA	Messenger RNA
mTOR	Mechanistic target of rapamycin
MTD	Maximum tolerated dose
MTS	3-(4,5-dimethylthiazol-2-yl)-5-(3-carboxymethoxyphenyl)-2-(4-sulfophenyl)-2H-tetrazolium
NLS	Nuclear localization signal
NOXA	Phorbol-12-myristate-13-acetate-induced protein
NY-ESO-1	New York esophageal squamous cell carcinoma 1
PcG	Polycomb group
PDGFR	Platelet-derive growth factor receptor
PFS	Progression free survival
PI	Propidium iodide
PI3K	phosphatidylinositol-3-kinase
PLA	Proximity ligation assay
po	Per os (oral)
PORCN	Porcupine homolog – Drosophila

PTEN	Phosphatase and tensin homolog deleted in chromosome 10
PUMA	p53 up-regulated modulator of apoptosis
QPGY	Glycine, proline, glutamine and tyrosine
RAS	Rat sarcoma
Rb	Retinoblastoma protein
RbAp48	Retinoblastoma-associated protein 48
RNA	Ribonucleic acid
RNAi	RNA interference
RNA-seq	RNA-sequencing
ROS	Reactive oxygen species
RT-qPCR	Reverse transcriptase quantitative PCR
SMARCB1	SWI/SNF-related matrix-associated actin-dependent regulator of chromatin subfamily B member 1
SDS-PAGE	Sodium dodecyl sulfate-polyacrylamide gel electrophoresis
SH2	Src homolog 2
SH3	Src homolog 3
shRNA	Small hairpin RNA
siRNA	Small interfering RNA
SQ	Subcutaneous
SSX	Synovial sarcoma X
SS18	Synovial sarcoma 18
SSXRD	SSX repressor domain
SUZ12	Suppressor of zeste 12 homolog

TLE1	Transducin-like enhancer of split 1
TMA	Tissue microarray
Ub	Ubiquitin
VEGFR	Vascular endothelial growth factor receptor
WNT	Wingless-related integration site

ACKNOWLEDGEMENTS

I would foremost like to thank Dr. Torsten Nielsen for allowing me the opportunity to take up this project in his group and for being a great source of support and guidance. I would further like to thank my thesis committee members Drs. Michael Underhill, Christian Steidl and Paul Rogers for great ideas and encouragement, and our collaborators Drs. Kevin Jones, Jared Barrott and Bertha Brodin for their contribution to my studies and making our international team work so well together.

From our group, Jennifer Ji, Jenny Wang, Robert Yao and Angela Goytain for their technical support and assistance in my experimental work, and Dr. Neal Poulin for his bioinformatics and pathway guidance. I would further like to mention rest of the Nielsen lab and GPEC crew for creating such a positive working environment.

Finally, to my parents, siblings, and partner, so much gratitude and love for of all of your continued support throughout my PhD work.

To my parents

CHAPTER 1: INTRODUCTION

1.1 Soft tissue sarcomas

Soft tissue sarcomas are tumours that arise in connective tissue, in cells typically of mesenchymal origin that form muscle, fat, blood vessels, tendons and nerves. This tumour category comprises approximately 2% of all cancer-related deaths and 7.4% of all pediatric malignancies (Ferrari et al., 2011). Soft tissue sarcoma subtypes are highly diverse and are further characterized by cell type and degree of malignancy. Benign soft tissue tumours are common and most resemble normal tissue with almost complete mesenchymal differentiation, presenting limited risk of recurrence. Malignant soft tissue sarcomas are locally aggressive and metastatic, and are further categorized into over 80 different subtypes based on apparent line of differentiation and cell type (M. F. Brennan, Antonescu, Moraco, & Singer, 2014).

The high heterogeneity of this tumour category poses difficulties for diagnosis and management. Proper diagnosis of subtype is important for therapy, as disease progression and response to intervention is variable. Histopathological grading is also required for proper disease classification and treatment planning. Generally, tumours are scored based on differentiation, mitotic count and level of necrosis (Neuville, Chibon, & Coindre, 2014).

Causative pathogenesis of soft tissue sarcoma development remains largely unknown; however certain causative sources of DNA damage have been uncovered. Trauma, environmental carcinogens, radiation, viral infection and familial factors have been implicated as contributory for some soft tissue sarcomas. Approximately half of all sarcomas are associated with apparently oncogenic germline mutations and up to one in six patients are

members of families with hereditary predispositions to cancer development, mostly related to polygenic variations in DNA repair genes (Ballinger et al., 2016). A number of recurrent genetic lesions have been identified as characteristic to specific soft tissue sarcomas, and as many as one-third of all sarcomas are now characterized by specific chromosomal-translocations that result in fusion oncoprotein production (Taylor et al., 2011).

1.2 Translocation-associated soft tissue sarcomas

Chromosomal translocations in soft tissue sarcomas result in gene fusions that produce highly specific chimeric oncoproteins. The specificity and prevalence of these gene fusions make them a defining characteristic of many sarcoma subtypes and are often the only cytogenetic change driving transformation (Taylor et al., 2011). The genomic break underlying these cancers occurs in introns and results in the flanking exons being fused during transcription. Characteristically, the resulting fusion oncogene is detected at the earliest presentation of the tumour, can be detected in all tumour cells, and is not present in benign masses (Mertens et al., 2009).

Contributing factors to these recurrent chromosomal translocation sites are largely unknown, and do not correlate to sequence elements or intron size (Novo & Vizmanos, 2006). The propensity of specific sites to undergo recombination seems largely random, occurring as a result of occurred stress-induced double stranded DNA breaks, incorrect repair and the availability of the gene sites due to the three-dimensional proximity and openness of the chromatin (Mani & Chinnaiyan, 2010).

The resultant chimaeric oncoproteins separate these sarcoma subtypes from the rest as they retain simple karyotypes with a sole mutation generally driving oncogenesis. The fusion

proteins usually disrupt normal transcription and often encode a transcriptional regulator as one of the contributing fusion partners (Aman, 2005; Taylor et al., 2011) (Table 1.1). The FET family of proteins (FUS, EWS, TAF15) have RNA binding functions as well as transcriptional activation domains, and commonly occur as translocation partners (Kovar, 2011). Translocation variants associated with the same specific sarcoma subtype are typically dissimilar only by small exon changes or fusion partners from the same gene family, resulting in consistent transcriptional or signaling changes. Oncoproteins typically retain the DNA or protein binding domain of one partner and the transcriptional regulatory (activating or repressive) domain of the other, ultimately altering transcriptional patterns in the recruitment of new activating or repressive binding partners or in binding and influencing new target gene sites. This leads to the deregulation in expression at a series of target sites, directing multiple oncogenic changes and defining tumour phenotype (Goldblum et al., 2014).

The unique specificity of tumourgenesis from each chimeric oncoprotein is thought to rely heavily on cellular environment. The opportune combination of the translocation occurring within a susceptible cell type at a particular stage of development is likely required for transformation to occur (Goldblum et al., 2014). The aberrant transcriptional changes often redirect differentiation and generally mask the phenotype of the progenitor cells making the distinct cell of origin unclear (Jain, Xu, Prieto, & Lee, 2010).

1.3 Clinical features of synovial sarcoma

1.3.1 Epidemiologic features and clinical presentation

Synovial sarcoma is an aggressive translocation-associated sarcoma subtype, constituting up to 10-20% of all soft tissue sarcomas (Nielsen, Poulin, & Ladanyi, 2015). It primarily occurs in adolescents and young adults between the ages of 15-40, with tumours typically arising in the extremities (majority), head/neck, trunk or viscera (Figure 1.1A) and the most common metastatic pattern occurring to the lungs (Brennan, Antonescu, Alektiar, & Maki, 2016). The proximity of these tumours to the synovium joints coined the misnomer 'synovial' sarcoma; however the synovium is not the cell of origin. Tumours often metastasize late (i.e. after 5 years) (Krieg et al., 2010) and the 10-year survival rate for patients with localized recurrent disease is approximately 50%, with tumour size acting as an important prognostic indicator (Tsang, Chan, Chan, Lai, & Chan, 2016). Patients with tumours of less than 5 cm in diameter have a 10-year survival rate of approximately 88%, while those with tumours of 5-10 cm and 10+ cm are found to have 10-year survival rates of 38% and 8%, respectively (Deshmukh, Mankin, & Singer, 2004).

1.3.2 Pathology and diagnosis

Synovial sarcoma presents with monophasic, biphasic or poorly differentiated histological phenotypes. Monophasic synovial sarcoma consists solely of spindle cells and comprises approximately 75% of cases, while biphasic tumours are made up of spindle and epithelial cells often forming glandular structures, suggestive of a mesenchymal-epithelial transition (Figure 1.1B) (Fisher, 1998; Qi et al., 2013). Less common, poorly differentiated

synovial sarcoma resembles other small round blue cell cancers, but is identified by cytogenetic and immunohistochemical (IHC) features. Synovial sarcoma diagnosis is typically confirmed by fluorescent *in situ* hybridization (FISH) assessment for breakpoints in *SS18* and/or *SSX*, or by RT-PCR for fusion transcripts (Italiano et al., 2016). In the absence of a clinical molecular diagnostic lab, the diagnosis can be confirmed by IHC analysis of synovial sarcoma-associated biomarkers, the most sensitive and specific of which is TLE1 (Jagdis, Rubin, Tubbs, Pacheco, & Nielsen, 2009) (Figure 1.1C).

1.3.3 Current standards of treatment

Synovial sarcoma is typically treated by wide-margin surgical excision and adjuvant or neoadjuvant radiation therapy, but risk of metastasis and local recurrence remains high (Ferrari et al., 2015). Chemotherapy, typically doxorubicin (an anthracycline) and ifosphamide (a DNA-alkylating agent), may be used in attempt to control metastatic disease with high risk tumours (>5 cm) (Table 1.2). Trabectedin, a naturally-derived DNA-alkylating compound, is also approved for use in Europe against soft-tissue sarcomas, including synovial sarcoma (Yasui et al., 2016). Third-line treatments include the anti-angiogenic agent pazopanib, DNA-replication inhibitors etoposide and gemcitabine, and microtubule-binding docetaxel. Despite these best available systemic therapy options, chemotherapeutic intervention in synovial sarcoma generally provides limited benefit (Italiano et al., 2009; Le Cesne et al., 2014). Targeted systemic treatment options against synovial sarcoma are needed; however these would require further biological understanding of targetable fusion oncoprotein effects (given that the SS18-SSX oncoprotein is not directly targeted by currently approved therapies).

1.4 t(X;18) translocation and the SS18-SSX oncoprotein

Synovial sarcoma is characterized by the chromosomal translocation t(X;18)(p11.2;q11.2), resulting in the in-frame fusion of *SS18* to *SSX1*, *SSX2* or rarely *SSX4* (Clark et al., 1994). The translocation fuses the majority of SS18, excluding only its final 8 C-terminal amino acids, to the 78 C-terminal amino acids of the SSX fusion binding partner bringing together various protein domains with different functional interactions (Figure 1.2). *SS18-SSX* is the sole driving cytogenic event in synovial sarcoma and, as mentioned above, is used for diagnosis. Most biphasic tumours contain *SS18-SSX1* fusions, while monophasic tumours have equal likelihood of containing *SS18-SSX1* or *SS18-SSX2* fusions (Brennan et al., 2016).

SS18 (synovial sarcoma chromosome 18 breakpoint) is a ubiquitously expressed nuclear protein that normally functions within the SWI/SNF (SWItch/Sucrose Non-Fermentable) chromatin remodeling complex to regulate transcription (Middeljans et al., 2012). It contains a unique N-terminal homology domain (SNH) that interacts with the BRG1 (SMARCA4) and BRM (SMARCA2) components of the SWI/SNF complex and with activating transcription factor-2 (ATF2) (Su et al., 2012), and a C-terminal QPGY domain that is important for polymerization and resembles the transactivation domain in FET family proteins (Anderson, Denny, Tap, & Federman, 2012) (Figure 1.2). SS18 does not contain a DNA binding domain and is thought to act as a transcriptional regulator by way of protein interactions. It has also been suggested to play role in signal transduction owing to its SH2 (Src homology 2) and SH3 (Src homology 3) binding motifs, which typically interact with tyrosine kinases (Filippakopoulos, Muller, & Knapp, 2009).

The SSX (synovial sarcoma chromosome X breakpoint) family of highly conserved proteins typically exhibits expression restricted to the testes, and at low levels in the thyroid. SSX has now been extensively studied as a tumour-associated cancer-testis antigen due to its uncovered expression in several human tumours of epithelial and mesenchymal origin (D'Arcy, Maruwge, Wolahan, Ma, & Brodin, 2014; Gjerstorff, Andersen, & Ditzel, 2015). SSX proteins also lack a DNA binding domain and are thought to act as transcriptional repressors though the interactions of their incorporated transcriptional repressive domains KRAB (Kruppel-associated box domain) and SSXRD (SSX repression domain) (Haldar, Randall, & Capecchi, 2008). The SSXRD domain directs interactions of SSX with polycomb group (PcG) repression complexes and histones as well as includes a nuclear localization signal (NLS) (dos Santos, de Bruijn, Kater-Baats, Otte, & van Kessel, 2000). SSX has also been found to interact with β-catenin and influence expression of genes important in the regulation of mesenchymal-epithelial transitions (D'Arcy et al., 2014). SS18-SSX has further been shown to interact with transcriptional repressors SNAIL and SLUG resulting in the activation of E-cadherin transcription, which may contribute to mesenchymal-epithelial transition and impact differentiation (Saito, Nagai, & Ladanyi, 2006).

SS18-SSX retains the ability to interact with SWI/SNF components and transcription factors as well as with polycomb repressive complexes, suggesting the fusion drives transformation though epigenetic changes to chromatin status and gene expression. As the central driver in synovial sarcomagenesis, induction of SS18-SSX expression is the sole change required to induce synovial sarcoma-like tumours in conditional mouse models (Haldar, Hancock, Coffin, Lessnick, & Capecchi, 2007) and its inactivation *in vitro* and *in*

vivo results in apoptosis and decreased tumour growth, indicating the oncoprotein to be essential and sufficient for transformation (Takenaka et al., 2010).

1.5 Experimental models of synovial sarcoma

A number of *in vitro* and *in vivo* models have become available in recent years to facilitate the study of synovial sarcoma biology and drug discovery (Table 1.3). At least seven human synovial sarcoma cell lines have been derived for use *in vitro*, encompassing monophasic and biphasic histological, and SS18-SSX1, SS18-SSX2 translocation subtypes. The cell lines are easily grown and manipulated; however, adaptation to culture and secondary mutation accumulation compromise some of their capacity to model human disease *in vivo*. Primary cells derived from patient tumours are available and are less likely to have culture adaptations as well as allow for studies matching cognately-collected normal tissue, but are more difficult to grow than cell lines and are less readily obtainable. *In vivo* xenograft models of synovial sarcoma typically have inconsistent take rates and are often expensive and time consuming to generate and maintain.

The genetically-engineered mouse models (GEMM) of synovial sarcoma, first developed in the Mario Capecchi lab, wherein SS18-SSX is inducibly expressed in Myf5 myogenic precursor cells (Haldar et al., 2007). These models have consistent tumour penetrance, closely represent the human synovial sarcoma phenotype with induced SS18-SSX expression, are easily manipulated and better represent the epigenetic tumour status; however secondary mutations are often utilized to facilitate efficient tumour induction and metastatic disease (Barrott et al., 2015; Barrott et al., 2016; K. B. Jones et al., 2011). These models can provide virtually unlimited sources of tumour material, albeit in a murine genetic

background and with smaller sizes and shorter developmental cycles (from initiation to lethality) than in human tumours. Furthermore, frozen human tumour samples are available for translational studies, though these tumours have often been irradiated prior to excision. Original biopsies are usually formalin fixed and not easily manipulated, but are available at high numbers for biomarker studies, including as tissue microarrays.

1.6 SS18-SSX-mediated epigenetic dysregulation in synovial sarcoma

1.6.1 Nucleosome-mediated epigenetic regulation of transcription

Proper epigenetic regulation of chromatin structure is crucial for maintenance of normal gene expression. DNA is tightly wound around histone proteins to form nucleosome structures, in order to condense and protect chromatin, as well as to regulate transcriptional repression. This highly organized and tightly coiled form is known as heterochromatin and is considered transcriptionally inactive, as its structure prevents transcriptional factors from accessing DNA (Alberts, 2010). Histones are highly basic proteins that form octamers made up of H2A, H2B, H3 and H4 core proteins and recruit an H1 linker protein. The electrostatic interactions between the positively charged histones and negatively charged phosphate groups on DNA promote the coiled chromatin organization. This structure is highly dynamic, and when gene expression is required nucleosomes relax and unwind to allow transcriptional factors access to DNA. This open and transcriptionally activated structure is known as euchromatin. Reversible histone modifications, such as acetylation and methylation, regulate the transition of chromatin states to activate or repress transcriptional expression.

Histone acetylation alters the electrostatic charge required for the tight coiling of nucleosomes. Histone acetyltransferase (HAT) enzymes use acetyl co-enzyme A (co-A) as a donor and transfer the acetyl group to lysine residues on the N-terminal tails of the core histone proteins (Sun et al., 2012) (Figure 1.3). The addition of these acetyl groups neutralizes the histones' positive charges, thereby promoting nucleosome relaxation and allowing the site to be open for transcription. Histone deacetylase (HDAC) enzymes function in reversing this process, removing the acetyl group in order to restore the positive charge and bring about chromatin condensation and transcriptional repression (Grayson, Kundakovic, & Sharma, 2010).

Histone methylation does not alter histone charge, but acts to define recognition sites for proteins that function in chromatin condensation or recruitment of regulatory proteins. The effect of methylation depends on location and number of methyl groups attached as this influences co-factor recruitment. Histone methylation can thereby have activating or repressive effects depending on these features (Alberts, 2010). Specific methylation signatures have been associated with transcriptional repression or activation, including methylation marks on histone H3 lysine 4 (H3K4), H3K36 as activating, and H3K9, H3K27 as repressive (Habibi, Masoudi-Nejad, Abdolmaleky, & Haggarty, 2011; Noh, Allis, & Li, 2016).

PcG proteins form complexes notated as polycomb repressive complexes (PRC) that function in repressing gene expression through epigenetic regulation of histone tail status. PRC1 includes a E3 ubiquitin ligase among its components and in docking to trimethylated H3K27 (H3K27me3) sites, catalyzes monoubiquitination of lysine 119 sites on H2A histones

(H2AK199ub1) for chromatin compaction (Papadopoulou, Kaymak, Sayols, & Richly, 2016).

PRC2 is made up of EZH2 (methyltransferase), SUZ12 (zinc finger), EED (EZH2 and HDAC binding protein) and RbAp48 (histone binding protein) core components, and functions in chromatin compaction by trimethylating H3K27 sites (Figure 1.4). Trimethylation at this site inhibits the ability of the histones to interact with transcriptional regulatory proteins and has been highly associated with silenced gene promotors (Barski et al., 2007; Lu et al., 2016). The catalytic component of PRC2 is EZH2 and is over-expressed in many cancer types, including lymphomas, breast and prostate cancer, and highly correlates with advanced disease and poor prognosis (Wilson et al., 2010). Reduction in EZH2 levels in these tumour models results in growth inhibition, establishing PRC2 function as the driving contributor to oncogenesis (Lu et al., 2016; Varambally et al., 2002).

SWI/SNF nucleosome remodeling complexes are thought to oppose epigenetic silencing by PRC2 (Figure 1.4). SWI/SNF components recognize histone H3 acetylation status and function to remodel nucleosomes by destabilizing the histone-DNA interaction and moving nucleosomes along the DNA strand in an ATP-dependent manner, opening nucleosomes for transcriptional activation (Tang, Nogales, & Ciferri, 2010). Up to 20% of all human tumours have been reported to have some mutation to a component of the SWI/SNF complex, commonly to component SMARCB1 (INI1/BAF47/SNF5) (Kadoch et al., 2013). SMARCB1 has been shown to be an important tumour suppressor, inactivated in several cancers including malignant rhabdoid tumour (Agaimy, 2014; Jackson et al., 2009), undifferentiated soft tissue sarcoma (Kreiger et al., 2009), and epithelioid sarcoma (Jamshidi et al., 2016). SMARCB1 is thought to function in DNA target recognition, and when

inactivated, proper targeting of SWI/SNF to gene promoters is lost, leading to aberrant and non-specific transcriptional regulation (Kuwahara, Wei, Durand, & Weissman, 2013).

It has been proposed that PcG and SWI/SNF complexes function antagonistically and together maintain balance in the regulation of gene expression (Figure 1.5). SMARCB1 inactivation in T-cell lymphoma models results in profound repression of PcG regulated genes dependent on EZH2 activity (Wilson et al., 2010). It is suggested SMARCB1 functions to relieve EZH2 repressive activity and reactivate transcription, and when deleted repressive patterns mediated by PcG are unregulated. EZH2 was shown to be essential for oncogenesis in these SMARCB1-inactivated tumour models and when reduced, cell proliferation accordingly decreased (Wilson et al., 2010). Furthermore, it has been demonstrated that EZH2 structure is required for tumourgenesis in SMARCB1-deleted models, with only partial dependency on its methyltransferase catalytic domain (K. H. Kim et al., 2015). This indicates that a physically intact PRC2 complex is instrumental in oncogenesis in SMARCB1 deactivated tumours. Taken together, this suggests the balance in activity between PRC2 and SWI/SNF is essential for proper gene expression and when disrupted, oncogenic transcription patterns are activated.

In synovial sarcoma, SS18-SSX has been shown to co-localize with PcG proteins (Barco, Garcia, & Eid, 2009; Soulez, Saurin, Freemont, & Knight, 1999) as well as to polycomb-marked nucleosome sites (Garcia, Shaffer, & Eid, 2012), indicating a relationship between polycomb-mediated epigenetic regulation and the oncoprotein. Modifications made by SS18-SSX-protein interactions within the context of PcG activity and nucleosome remodeling and the resultant changes to transcriptional patterns, are thought to be important in synovial sarcoma tumourgenesis.

1.6.2 SS18-SSX/TLE1 interaction and recruitment of PRC2

Transducin-Like Enhancer protein 1 (TLE1) is a transcriptional co-repressor found to be one of the most highly expressed gene products detected in synovial sarcoma (Terry et al., 2007). The consistently elevated expression levels of nuclear TLE1 have made it a distinguishing feature and allow it to function as a synovial sarcoma-specific biomarker (Figure 1.1C) (Valente, Tull, & Zhang, 2013). TLE1 is detectable by IHC in formalin-fixed tissue samples, permitting its use for clinical diagnosis of synovial sarcoma (Jagdis et al., 2009; Valente et al., 2013).

TLE proteins have been found to function in embryogenesis, as co-repressors of WNT (wingless-related integration site) target genes, and pathways important for stem cell self-renewal (Levanon et al., 1998). TLE1 has been shown to interact with the C-terminal portion of SS18-SSX and to function in the recruitment of PRC2 bringing about transcriptional repression though H3K27me3 histone modifications (Su et al., 2012). SS18-SSX acts as a bridge connecting TLE1 to transcription factors with DNA binding domains and in doing so, redirects transcriptional repression (Figure 1.6). These abnormal interactions result in aberrant repression of a number of gene targets, including tumour suppressors *EGR1* and *CDKN2A*, resulting in a proliferative and anti-apoptotic phenotype that promotes tumourgenesis. This SS18-SSX/TLE1/PcG/HDAC driving protein complex has been found to be dissociated with treatment by HDAC inhibitors, resulting in reactivation of repressed gene targets (Lubieniecka et al., 2008; Su et al., 2012).

1.6.3 SS18-SSX incorporation in the SWI/SNF complex

Both wildtype SS18 and chimeric SS18-SSX have been shown to associate with ATPases BRG1 and BRM and to be incorporated into the SWI/SNF complex (Kato et al., 2002; Middeljans et al., 2012; Thaete et al., 1999). It has been further reported that the incorporation of SS18-SSX evicts SMARCB1 from the complex due to aberrant protein interactions with the oncoprotein (Kadoch & Crabtree, 2013). SMARCB1 levels have been reported to be low but not absent, uniquely distinguishing synovial sarcoma from SMARCB1-deleted sarcomas and SMARCB1-intact tumours (Arnold et al., 2013; Rekhi & Vogel, 2015). These low levels are suggested to be due to SMARCB1-degradation following eviction from the SWI/SNF complex (Rekhi & Vogel, 2015). This SS18-SSX-mediated rearrangement of the SWI/SNF complex has been suggested to cause abnormal nucleosome occupancy, altering the availability of DNA for transcription and resulting in dysregulated expression patterns that promote proliferation (Figure 1.6). The eviction of SMARCB1 may therefore promote EZH2 over-activity at SS18-SSX-mediated target sites resulting in an inability to activate transcription, and/or instigate transcriptional activation at non-specific target sites. This EZH2 over-activity is likely to be amplified in the recruitment of PcG by SS18-SSX (Su et al., 2012).

1.7 Characteristic phenotype and targetable pathways of synovial sarcoma

1.7.1 Cyclin D1 and CDK4/6

Cyclin D1 (*CCND1*) is an essential cell cycle regulator responsible for directing progression of G1 to S phase, in binding cyclin dependent kinase co-factors CDK4/6. Over-

activity has been reported in several cancer subtypes, resulting in uncontrolled cell cycle succession and resultant proliferation (Chraybi et al., 2013; Moreno-Bueno et al., 2003; Yu, Geng, & Sicinski, 2001). In synovial sarcoma, it has been suggested that SS18-SSX stabilizes cyclin D1, leading to elevated expression (Y. Xie, Skytting, Nilsson, Gasbarri, et al., 2002; Y. Xie, Skytting, Nilsson, Grimer, et al., 2002) and when the oncoprotein is deactivated, cyclin D1 protein levels decrease (Cai et al., 2011; C. Peng, Guo, Yang, & Zhao, 2008).

Elevation of cyclin D1 levels has been suggested to be regulated by ERK1/2 kinase activity due to highly correlated co-expression levels (Cai et al., 2011) and the observation that sorafenib decreases cyclin D1 levels in synovial sarcoma (C. L. Peng et al., 2009). Elevated cyclin D1 levels have further been associated with loss of cyclin-dependent kinase inhibitor $p16^{INK4A}$ *(CDKN2A*) expression in synovial sarcoma (Sabah, Cummins, Leader, & Kay, 2005; Vlenterie et al., 2016), which has been shown to be directly repressed by SS18-SSX (Su et al., 2012). $p16^{INK4A}$ functions as an important tumour suppressor by inhibiting the interaction of cyclin D1 with CDK4/6, repressing cell cycle progression until appropriate conditions for growth are met. The CDK4/6 inhibitor palbociclib has shown efficacy in blocking proliferation of synovial sarcoma, suggesting it as a potential therapeutic agent (Vlenterie et al., 2016).

1.7.2 *CDKN2A*

The *CDKN2A* gene site has been studied extensively as an important tumour suppressor. It has been shown to be commonly deleted or mutated in familial melanoma (Tsao & Niendorf, 2004), pancreatic cancer (McWilliams et al., 2011) and translocation-

associated acute lymphoblastic leukemia (Sulong et al., 2009), resulting in unchecked cell cycle progression though G1/S phase.

CDKN2A is unusual among eukaryotic genes as it encodes two proteins transcribed from alternative reading frames, $p16^{INK4A}$ and $p14^{ARF}$. While $p16^{INK4A}$ inhibits cell cycle progression, the $p14^{ARF}$ protein inhibits the ubiquitin ligase MDM2, preventing its inactivation of tumour suppressor p53, which regulates expression of cell cycle regulator $p21^{CIP1}$, as well as stress response gene targets and apoptotic pathways (Sharpless & Sherr, 2015).

The *CDKN2A/CDKN2B* locus has been shown to be repressed by PcG activity in proliferating cells, via the recruitment of PRC2 and consequent H3K27me3 implementation along the length of its locus (Bracken et al., 2007). EZH2 is found to be down-regulated in stressed or senescent cell populations, resulting in decreased activity of PRC2 and up-regulation of *CDKN2A/CDKN2B* gene targets, $p16^{INK4A}$, $p14^{ARF}$ and $p15^{INK4B}$, limiting proliferation and favouring apoptotic programs (Bracken et al., 2007).

This locus has been further suggested to be regulated by SWI/SNF activity, evicting PcG proteins, overriding PRC2-mediated repression and activating *CDKN2A/CDKN2B* transcription (Kia, Gorski, Giannakopoulos, & Verrijzer, 2008). SMARCB1 was found to be required for activation of $p16^{INK4A}$ and $p15^{INK4B}$ in malignant rhabdoid tumour models. When re-expressed in these models, as part of SWI/SNF complex SMARCB1 initiates displacement of PcG proteins and HDACs. Following this, histone methyltransferases and acetyltransferases are recruited, activating chromatin marks are created and expression of $p16^{INK4A}$, $p14^{ARF}$ and $p15^{INK4B}$ occurs (Mills, 2010). Together, this suggests a role for SS18-

SSX-mediated PcG recruitment and SMARCB1-deficiency in *CDKN2A* repression in synovial sarcoma.

1.7.3 WNT/β-catenin signaling

WNT signaling been suggested as over-active in synovial sarcoma, with stabilized nuclear β-catenin measured in 30-70% of synovial sarcoma cases. Nuclear β-catenin is associated with poor prognosis (Hasegawa, Yokoyama, Matsuno, Shimoda, & Hirohashi, 2001; Horvai, Kramer, & O'Donnell, 2006; Ng et al., 2005), and correlates with increased cyclin D1 levels (Horvai et al., 2006) in synovial sarcoma. Frizzled homologue 10 (FZD10), a cell surface receptor for WNT pathway signaling, has been shown to be expressed at high levels in synovial sarcoma, and not on normal cells of vital organs apart from the placenta (Tamaki et al., 2015). When activated by WNT ligand signaling, β-catenin translocates to the nucleus where it displaces TLE from repressive complexes and recruits nucleosome remodeling complex components, including SWI/SNF effector BRG1, to activate transcription of cell development and cell cycle effectors, including cyclin D1 (Shtutman et al., 1999). Under non-activating conditions, β-catenin is phosphorylated by GSK3β and ubiquitinated for proteasomal degradation. Deregulated WNT signaling has been associated with mesenchymal-epithelial transitions required for tumour invasion and metastasis (Yao, Dai, & Peng, 2011), and activating mutations to this pathway are common in cancer subtypes, including Ewing sarcoma (Pedersen et al., 2016), colorectal (Clements, Lowy, & Groden, 2003), medulloblastoma (Dahmen et al., 2001) and hepatocellular (Ishizaki et al., 2004).

It has been demonstrated that SS18-SSX induces nuclear β-catenin translocation and when β-catenin is depleted, tumour formation is blocked in synovial sarcoma mouse models (Barham et al., 2013; Trautmann et al., 2014). Stabilization of β-catenin has further been shown to specifically block epithelial differentiation and drive invasion of tumours in a GEMM models of synovial sarcoma (Barrott et al., 2015). In this study, all mouse tumours with stabilized β-catenin presented as monophasic and tumour formation was significantly more aggressive than in SS18-SSX-positive mouse models of wildtype β-catenin. Repression of targets known to be repressed by the oncoprotein were found to be enhanced by this nuclear stabilization, thought to be due to the β-catenin-mediated release of TLE from repressive complexes, liberating it for interaction with the oncoprotein (Barrott et al., 2015) (Figure 1.7). It has also been observed that β-catenin is over-activated in models of SMARCB1 loss, and that SWI/SNF activity is required for proper WNT/β-catenin pathway target expression (Mora-Blanco et al., 2014). The eviction of SMARCB1 by SS18-SSX from SWI/SNF complexes may therefore contribute to β-catenin activation, and its nuclear stabilization may further contribute to transcriptional repression by the oncoprotein in the release of TLE1 (Figure 1.7).

1.7.4 PI3K/AKT/mTOR signaling

The PI3K/AKT/mTOR axis is frequently activated in synovial sarcoma (Bozzi et al., 2008) and is associated with poor prognosis, with mTOR-positive tumours significantly correlating to shorter overall survival (Setsu et al., 2013). The PI3K/AKT/mTOR signaling pathway is required for positive regulation of many aspects of cell cycle progression and cell survival. This pathway has been shown to be aberrantly activated in several cancer subtypes

owing to gain or loss of key regulators, including breast, lung and cervical cancers (Liu, Cheng, Roberts, & Zhao, 2009). Abnormal activation of PI3K/AKT/mTOR signaling provokes cell proliferation and survival, leading to tumour formation, metastasis and resistance to apoptosis (Porta, Paglino, & Mosca, 2014). It has also been reported to activate WNT signaling (Ormanns, Neumann, Horst, Kirchner, & Jung, 2014; Vadlakonda, Pasupuleti, & Pallu, 2013), suggesting a potential relationship between the aberrantly activated AKT and activity of β-catenin/cyclin D1 in synovial sarcoma (Vlenterie et al., 2016).

The SS18-SSX-repressed gene target *EGR1* encodes a positive regulator of PTEN, the functional repressor of PI3K-AKT signal transduction (Su, Cheng, Sampaio, Nielsen, & Underhill, 2010). It has been suggested this repression of *EGR1* leads to activation of the PI3K/AKT/mTOR pathway, contributing to tumourgenesis through promotion of cell proliferation, survival and WNT signal induction. PI3K/AKT signaling has been shown to be essential in synovial sarcoma tumour development and its reduction by PI3K-inhibiting drugs has been found to diminish tumour growth as well as decrease phosphorylation of AKT, mTOR and GSK3β (Friedrichs et al., 2011). Downstream interactions of the PI3K/AKT/mTOR axis with the RAS/MEK/ERK axis, indicate intrinsic resistance mechanisms to monotherapy PI3K-inhibitor strategies in synovial sarcoma, suggesting a requirement for drug combination studies with these agents (Nielsen et al., 2015).

1.7.5 BCL2

Synovial sarcoma presents with an anti-apoptotic phenotype, characterized by relatively slow-growth, long-term risks of late recurrence, and resistance to

chemotherapeutics (Mancuso et al., 2000; Nielsen et al., 2015). This is attributed at least in part to high expression of anti-apoptotic protein BCL2 (B-cell lymphoma 2), found to be consistently up-regulated in synovial sarcoma (Antonescu et al., 2000; Hirakawa, Naka, Yamamoto, Fukuda, & Tsuneyoshi, 1996; Krskova et al., 2009). *BCL2* is abnormally amplified in other cancer subtypes, including non-Hodgkin's lymphomas (Monni et al., 1997) and small cell lung cancers (Ikegaki, Katsumata, Minna, & Tsujimoto, 1994), and was first described as part of a t(14;18) translocation that brings about follicular lymphoma, in which an activating promoter from chromosome 14 fuses to the BCL2 domain on chromosome 18 resulting in significantly amplified expression (Tsujimoto, Cossman, Jaffe, & Croce, 1985).

BCL2 has a family of related proteins that together regulate the mitochondrial apoptosis pathway. BCL2 family proteins are categorized as either pro-apoptotic activators or anti-apoptotic effectors, and are known to contain BCL2 homology (BH) motifs contributing to function. The anti-apoptotic effectors include BCL2, BCL-XL, BCL-W and MCL1, which localize to the outer mitochondrial membrane and act to repress pro-apoptotic effectors BAX/BAK (Wei et al., 2001).

Pro-apoptotic family members are further characterized as activators or effectors. BAX/BAK are effectors which remain associated with the mitochondrial membrane and when induced, function to permeabilize the membrane and release reactive oxygen species (ROS) and cytochrome C, signaling the apoptotic cascade (Hardwick & Soane, 2013). Pro-apoptotic activators function in controlling anti-apoptotic factors, and are characterized as containing a single BH3 domain (Llambi et al., 2011). Triggered by cellular stress and DNA damage, these include proteins BIK, BIM, BMF, NOXA and PUMA, which effectively

inhibit BCL2 anti-apoptotic proteins by way of BH3 binding to allow for BAK/BAX activation, promoting apoptosis induction.

BCL2 silencing in synovial sarcoma has been reported to sensitize cells to chemotherapy-induced apoptosis (Joyner, Albritton, Bastar, & Randall, 2006) and the BCL2 inhibitor navitoclax (ABT-263), a compound that mimics the BH3 domain of apoptosis activators, has been found to decrease tumour burden *in vivo* (K. B. Jones et al., 2013). Resistance to ABT-263 compounds in lymphomas has been suggested to result from activity of MCL1, but in synovial sarcoma this target has been found to be repressed by SS18-SSX (K. B. Jones et al., 2013), suggesting potential for clinical use. However, side effects of BCL2 inhibitors including thrombocytopenia are severe and result in dose-limiting toxicities (Schoenwaelder & Jackson, 2012).

1.8 Drug discovery in cancer therapeutics

A general protocol for drug development is currently employed for drug discovery practices in cancer therapeutics, leading from basic research, to pre-clinical studies and finally clinical development. When studies directly targeting known sensitivities do not lead to successful clinical trials, wider reaching screening studies are often undertaken, beginning with high-throughput primary *in vitro* assays to narrow down efficacious drug classes from large compound libraries (Everett, 2015). Screening read-outs are selected based on the desired modification or target, generally based on their effects in decreasing cell viability.

Following primary analyses, top hits are validated for disease selectivity and class effect, and potent compounds are selected as lead candidates (Hughes, Rees, Kalindjian, & Philpott, 2011). Dose-response studies are undertaken to validate effect and uncover optimal

use concentrations. Validation studies may then further include mechanism of action assessments, and investigation of potential synergy with additional compounds. Drug synergism occurs when two compounds are more highly effective in combination than the sum of the effects of each drug alone, due to combinational augmentation of one or more of the drug-mediated activities. This allows for lower concentrations of use and may therefore decrease adverse side effects (Tallarida, 2011). Drug combinations are commonly used clinically against cancer (Gravitz, 2011).

Pre-clinical studies to determine efficacy *in vivo* are then often initiated in best available disease models, frequently being murine tumour models. *In vivo* studies provide early toxicity data as well as information regarding disease efficacy and pharmacokinetics. In novel compound development, studies may be further undertaken in primate models to effectively investigate toxicology. When proven selective, efficacious and safe in pre-clinical studies, investigational new drug (IND) trials may then be considered. Clinical trials of novel drug protocols typically begin in phase I to assess safety in small groups of patients and may involve dose-escalation studies to uncover the maximum tolerated dose (MTD) (Le Tourneau, Lee, & Siu, 2009). If an acceptable safety profile is observed, these studies will be followed up by phase II trials in larger groups to further evaluate safety and investigate disease efficacy (Hidalgo, Eckhardt, Garrett-Mayer, & Clendeninn, 2010). If some improvement in overall response rate (RR) or progression-free survival (PFS) is observed, phase III clinical trials are conducted in large groups to assess effectiveness, monitor side effects and compare response to current standard treatment protocols. If proven safe, and at least as effective as current treatment standards, new therapeutic platforms may be approved

for general use. Post-approval, phase IV studies may be further initiated to assess the treatment protocol in specific populations or to study effects of long term use.

1.9 Clinical trials in synovial sarcoma

1.9.1 Pazopanib

Pazopanib is a multi-tyrosine kinase inhibitor found to block angiogenesis and inhibit tumour cell growth though blocking activity of c-KIT, PDGFR, VEGFR and FGFR tyrosine kinases (Bramwell, 2012). In a phase III clinical trial (NCT00753688), pazopanib demonstrated activity in patients with advanced soft tissue sarcomas and significantly extended progression free survival versus placebo (van der Graaf et al., 2012). This study included 44 synovial sarcoma patients. Pazopanib is being further investigated in a phase II/III trial (NCT02180867) for its efficacy in soft tissue sarcoma patients previously having received chemotherapy and/or radiation. Pazopanib has now been approved for use in soft tissue sarcomas, and while it can be considered a targeted therapy, it does not target SS18-SSX itself nor other aspects of the synovial sarcoma-specific phenotype, and has not been shown to be cureative.

1.9.2 WNT inhibitors

LGK974 is an inhibitor of WNT signaling in the inactivation of PORCN, an acetyltransferase required for WNT ligand secretion, and is currently under clinical investigation in advanced solid tumours (NCT01351103). If efficacious, LGK974 may present a potential therapeutic option of WNT-activated cancers, including synovial sarcoma.

PRI-724, a compound that blocks activating interactions of β-catenin, has also been investigated in advanced solid tumours (NCT01302405), and demonstrated an acceptable safety profile (Takebe et al., 2015).

A radio-labelled chimeric monoclonal antibody against FZD10 known as OTSA101 has also been investigated in a phase I study against synovial sarcoma (NCT01469975). In addition to tumour uptake, liver and bone marrow non-specific uptake were observed, contributing to toxicity. Absorbed dose in the tumours was low and lacked any measureable response (Sarrut et al., 2017).

1.9.3 NY-ESO-1

New York esophageal squamous cell carcinoma 1 (NY-ESO-1) protein is a highly-immunogenic cancer-testis antigen with unknown function found to be highly expressed in many cancer subtypes, including melanoma, esophageal and ovarian cancers (T. S. Park et al., 2016) and strongly correlates with metastatic disease and poor prognosis (Velazquez et al., 2007). High levels of NY-ESO-1 have been reported in up to 75% of synovial sarcoma cases, suggesting potential benefit from anti-NY-ESO-1 targeted therapies (Endo et al., 2015; Lai et al., 2012). A clinical study was conducted with an adoptive NY-ESO-1-reactive T-cell transfer (NCT00670748) from which 11 of 18 NY-ESO-1 positive synovial sarcoma patients demonstrated an objective response (Robbins et al., 2015). This effect is being further clinically investigated in synovial sarcoma with the use of genetically-engineered NY-ESO-1 reactive T-cells (NCT01343043), however in addition to being expensive compared to standard small molecular or antibody-based systemic therapies, this therapy is restricted to patients with tumours positive for NY-ESO-1 and human leukocyte antigen (HLA) class A2,

and therefore is not likely to present a comprehensive treatment option. Checkpoint inhibitor immunotherapy strategies currently pursued in pleomorphic sarcomas are considered less likely to be of value in synovial sarcoma, as it rarely incorporates prominent inflammatory infiltrates (Dancsok, Asleh-Aburaya, & Nielsen, 2017) ; however these strategies are currently under clinical investigation (NCT02815995).

1.9.4 Tazemetostat

EZH2 inhibitor Tazemetostat (EPZ-6438) has demonstrated efficacy in inducing cytostasis and reactivating normal transcription patterns in synovial sarcoma cell lines and xenograft mouse models (Kawano et al., 2016; Shen et al., 2016). A phase I clinical study demonstrating an acceptable safety profile (NCT02601937), is being followed up by a phase II study in SMARCB1-deficient tumours and relapsed or refractory synovial sarcoma (NCT02601950). The need for non-catalytic EZH2 structural activity in SMARCB1-deficient cancers (K. H. Kim et al., 2015) and residual levels of SMARCB1 (Arnold et al., 2013), which is not typically deleted or mutated in synovial sarcoma may limit the efficacy of this EZH2 inhibitor in synovial sarcoma.

1.9.5 Pracinostat

HDAC inhibition has been shown to dissociate the driving complex in synovial sarcoma as well as reactivate important tumour suppressors (Lubieniecka et al., 2008; Su et al., 2012). A phase-II study of the HDAC inhibitor pracinostat (SB-939) in translocation-associated sarcomas was initiated (NCT01112384), and table disease was achieved in three of three SS18-SSX-positive patients (Chu et al., 2015). This study had to be terminated

prematurely due to prolonged unavailability of pracinostat, however initial results warrant further investigation.

1.10 HDAC inhibitors in cancer

The role of histone post-translational modifications in regulating gene expression has become a known target of deregulation in cancer. In the moderation of histone status, HDACs alter transcription of oncogenic factors and as such have become an attractive target of epigenetic intervention in therapeutic research. HDACs have been shown to be involved at multiple stages of cancer development in the disruption of acetylation homeostasis. Inhibition of HDAC activity may therefore re-establish normal transcriptional activity and in turn block oncogenesis (Y. Li & Seto, 2016).

The HDAC family is made up of 18 proteins and has been subdivided by distribution and activity into four distinct classes (Table 1.4). When over-expressed or deregulated, HDACs are associated with a variety of cancer types with high expression correlating to poor prognosis (Spiegel, Milstien, & Grant, 2012). Class I HDACs are often over-expressed in gastric (Choi et al., 2001), pancreatic (Giaginis et al., 2015) and hepatocellular cancers (Rikimaru et al., 2007). Class IIA HDACs are often mutated in breast cancer and up-regulated in colorectal cancer (Ozdag et al., 2006), while class IIB HDACs are often highly expressed in oral squamous cell cancer (Sakuma et al., 2006). The effect of elevated HDAC activity is widespread and may lead to repression of tumour suppressors, promoting cell growth or inhibiting apoptosis (Y. Li & Seto, 2016).

Knock-out studies have shown class I HDACs to be important for cell cycle regulation and survival (Marks, 2010). Importantly, inhibition of class 1 HDACs has been

found to result in up-regulation of $p21^{CIP1}$ (*CDKN1A*), an important tumour suppressor and regulator of cell cycle progression (Zupkovitz et al., 2010), as well as to induce DNA damage and apoptosis (Bhaskara et al., 2008). Cancer cells have been found to be more highly sensitive to HDAC inhibition-induced cell death than normal cells, suggesting therapeutic potential (Ungerstedt et al., 2005). HDACs have further been found to be important for DNA damage repair, with inhibition causing cells to be more highly susceptible to DNA damaging agents (Bhaskara et al., 2008). Together, functional data suggests HDACs as targets for anti-neoplastic drug intervention and has led to the development of chemical HDAC inhibitors.

To date, four HDAC inhibitors have been approved for clinical use against specific cancer subtypes, with several next-generation compounds under clinical investigation (Table 1.5). Dose-limiting toxicities are observed with IV-administered HDAC inhibiting agents, and long-term exposure often results in potentially dangerous cardiac electrophysiology problems (Spence et al., 2016; S. Subramanian, Bates, Wright, Espinoza-Delgado, & Piekarz, 2010). Newer orally available compounds are expected to be more highly specific for HDAC subclasses, lessening toxicity and off-target effects (Y. Li & Seto, 2016). Efficacy has been most evident with first-generation compounds in hematological malignancies, with little measurable solid tumour activity when used as monotherapies (Arrighetti, Corno, & Gatti, 2015). Because HDAC inhibitor activity targets multiple sites, the compounds have been suggested to work best within rational drug combination strategies targeted to cancer-specific sensitives (Spiegel et al., 2012).

1.11 Thesis rationale and specific objectives

Despite a known driving mutation as the sole cytogenic event in synovial sarcoma, targeted therapeutics for synovial sarcoma are not available. Interactions of the chimeric oncoprotein with nucleosome-regulating complexes are known to be important for aberrant transcriptional regulation, leading to synovial sarcomagenesis. Previous studies have shown disruption of the driving complex by silencing of the oncoprotein or by HDAC inhibition leads to reactivation of normal cellular signaling and apoptosis induction. This led to the hypothesis that compounds able to disrupt SS18-SSX-mediated protein interactions will reverse oncogenesis and present promising clinical candidates against synovial sarcoma.

The goal of this thesis is to uncover novel therapeutic interventions for improved clinical outcome in synovial sarcoma. To this end, the following objectives are outlined:

Chapter 2:

i. To investigate the drug-mediated dissociation of the SS18-SSX driving complex in synovial sarcoma tumourgenesis.
ii. To develop the proximity ligation assay for use in assessing key protein-protein interactions in translocation-associated sarcomas in a high-throughput drug screening format.

Chapter 3:

i. To uncover novel sensitizing agents and targetable pathways in synovial sarcoma.
ii. To investigate drug combination strategies for clinical candidacy in synovial sarcoma.

Chapter 4:

i. To use genome-wide transcriptional analysis to evaluate impact of HDAC inhibition on core transcriptional patterns in synovial sarcoma cell lines
ii. To uncover HDAC inhibitor-induced mechanisms of apoptosis induction by expression profiling of synovial sarcoma cell lines and tumours.

1.12 Thesis overview

Chapter 2 focuses on the development of a newly-emerging technology known as the proximity ligation assay (PLA) for detection of key protein-protein interaction in the driving oncogenic complex in synovial sarcoma. The interaction of SS18-SSX with TLE1 was utilized to show the potential of this technology in a high-throughput drug screening format for targeted drug discovery in translocation-associated sarcomas.

Chapter 3 uses high-throughput drug screening methods and functional validation studies to investigate the treatment potential of HDAC inhibitors in combination with proteasome inhibitors against synovial sarcoma. Both drug classes proved to be among the most highly efficacious and targeted anti-cancer compounds in decreasing synovial sarcoma cell viability. Mechanisms of drug synergy were uncovered and a clinical trial protocol was established.

Chapter 4 focuses on genome-wide transcriptional changes that occur following HDAC inhibition in synovial sarcoma. RNA-seq analyses were utilized to uncover changes in gene and protein expression, and a mouse model of synovial sarcoma was used to validate observations. Class effects and SS18-SSX-specific mechanisms of apoptosis induction were established.

Chapter 5 serves to summarize the main findings in the context of the characteristic synovial sarcoma phenotype and biology, as well as elaborates on the clinical potential of the uncovered therapeutic interventions, including a clinical trial proposal.

Table 1.1: Translocation-associated soft tissue sarcoma subtypes

Soft tissue sarcoma subtype	Translocation	Gene Fusion
Alveolar soft part sarcoma	t(X;17)(p11.2;q25)	ASPSCR1-TFE3
Alveolar rhabdomyosarcoma	t(2;13)(q35;q14)	PAX3-FOXO1
	t(1;13)(P36;Q14)	PAX7-FOXO1
	t(2;X)(q35;q13)	PAX3-FOXO4
	t(2;2)(q35;p23)	PAX3-NCOA1
	t(2;8)(q35;q13)	PAX3-NCOA2
	t(2;2)(q35;q33)	PAX3-INO80D
Angiomatoid fibrous histiocytoma	t(12;16)(q13;p11)	FUS-ATF1
	t(12;22)(q13;q12)	EWSR1-ATF1
	t(2;22)(q33;q12)	EWSR1-CREB1
Clear cell sarcoma	t(12;22)(q13;q12)	EWSR1-ATF1
	t(2;22)(q34;q12)	EWSR1-CREB1
	t(10;16)(p11;p11)	FUS-CREM
Dermatofibrosarcoma protuberans	t(17;22)(q22;q13)	COL1A1-PDGFB
Desmoplastic small round cell tumour	t(11;22)(p13;q12)	EWSR1-WT1
	t(21;22)(q22;q12)	EWSR1/ERG
Endometrial stromal sarcoma	t(7;17)(p15;q21)	JAZF1-SUZ12
	t(6;7)(p21;p15)	JAZF1-PHF1
	t(6;10)(p21;p11)	EPC1-PHF1
	t(10;17)(q22;p13)	YWHEA-FAM22
Epithelioid hemangioendothelioma	t(1;3)(p36;q25)	WWTR1-CAMTA1
	t(X;11)(p11.2;q22.1)	YAP1-TFE3
Ewing sarcoma	t(21;22)(q22;q12)	EWSR1-ERG
	t(11,22)(q24;q12)	EWSR1-FLI1
	t(7,22)(p22;q12)	EWSR1-ETV1
	t(17,22)(q12;q12)	EWSR1-ETV4
	t(2,22)(q33;q12)	EWSR1-FEV
	t(16;21)(p11;q22)	FUS-ERG
	t(2;16)(q33;p11)	FUS-FEV
Ewing sarcoma-like	inv(X)(p11.2p11.4)	BCOR-CCNB3
	t(X;4)(p11;q31)	BCOR-MAML3
	t(20;22)(q13;q12)	EWSR1-NFAT2
	t(4;22)(q31;q12)	EWSR1-SMARCA5
	t(1;22)(p36;q12)	EWSR1-PATZ1
	t(2;22)(q31;q12)	EWSR1-SP3
	t(X;22)(p11;q13)	ZC3H7B-BCOR
Extraskeletal myxoid chondrosarcoma	t(9;22)(q22;q12)	EWSR1-NR4A3
	t(9;17)(q22;q11)	TAF2N-NR4A3
	t(9;15)(q22;q21)	TCF12-NR4A3
	t(9;22)(q22;q15)	TFG-NR4A3
Low Grade fibromyxoid sarcoma	t(7;16)(q33;p11)	FUS-CREB3L2
	t(11;16)(p11;p11)	FUS-CREB3L1
Mesenchymal chondrosarcoma	t(8;8)(q12;q21)	HEY1-PLAG1
	t(12;12)(q15;q21)	NUP107-LGR5
Myxoid liposarcoma	t(12;16)(q13;p11)	FUS-DDIT3
	t(12;22)(q13;q12)	EWSR1-DDIT3
Rhabdomyosarcoma	t(2;13)(q35;q14)	PAX3-FOXO1
	t(1;13)(p36;q14)	PAX7-FOXO1
Sclerosing Epithelioid Fibrosarcoma	t(11;22)(p11;q12)	EWSR1-CREB3L1
Synovial sarcoma	t(X;18)(p11.2;q11.2)	SS18-SSX1 SS18-SSX2 SS18-SSX4
	t(X;20)(p11;q13)	SS18L1/SSX1
Tenosynovial giant cell tumour	t(1;2)(p13;q37)	COL6A3-CSF1

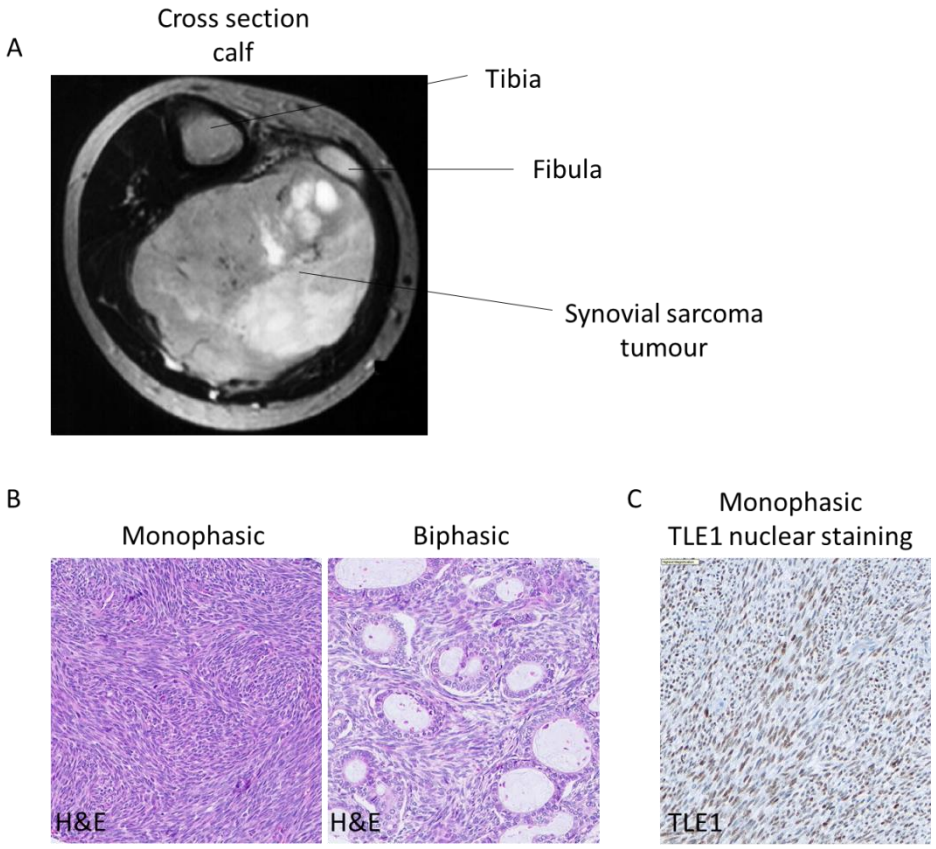

Figure 1.1: Pathological features of synovial sarcoma. A) MRI scan of synovial sarcoma of the calf. B) Histological subtypes of synovial sarcoma include monophasic (spindle cells) and biphasic (spindle and epithelial cells). C) TLE1 is highly expressed in synovial sarcoma nuclei. *Images taken by T.O. Nielsen.*

Table 1.2: **Current standard of chemotherapeutic intervention against synovial sarcoma**

Condition	Line	Treatment
Neo/adjuvant chemotherapy		doxorubicin + ifosphamide for high-risk tumours
Metastatic disease	1st	doxorubicin + ifosphamide (if not previously administered)
	2nd	anthracycline (if not previously administered) trabectedin (in countries where available)
	3rd +	pazopanib etoposide gemcitabine-docetaxel

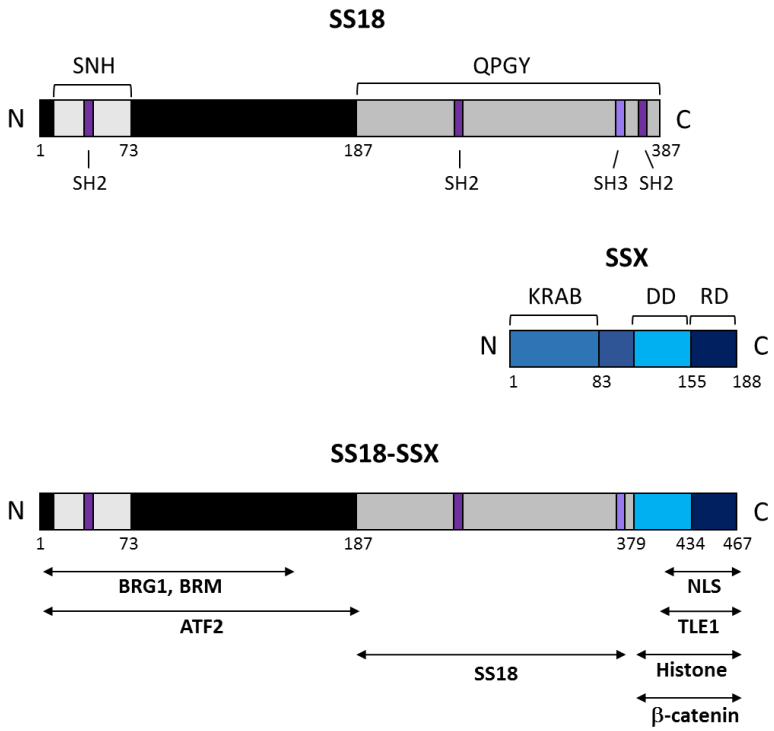

Figure 1.2: SS18-SSX fusion site and relevant protein binding domains. The translocation breakpoint results in the fusion of the majority of SS18 to the C-terminal of SSX. Protein domains on SS18: SNH (SS18 N-terminal homology); QPGY (glutamine/proline/glycine/tyrosine-enriched domain); SH2 (Src homology 2 binding motif); SH3 (Src Homology 3 binding motif). Protein domains on SSX: KRAB (Kruppel-associated box domain); DD (SSX divergent domain); RD (SSX repression domain); NLS (nuclear localization signal).

Table 1.3: **Experimental models of synovial sarcoma**

Type	ID	Fusion	Subtype	Reference	Advantages	Disadvantages
Human cell lines	SYO-1	SS18-SSX2	biphasic	Kawai *et al*., 2004	- Easily grown and manipulated	- Likely to adapt in culture and take on secondary mutations
	FUJI	SS18-SSX2	monophasic	Nojima *et al*., 1990		
	Yamato-SS	SS18-SSX1	biphasic	Naka *et al*., 2010		
	ASKA-SS	SS18-SSX1	biphasic	Naka *et al*., 2010		
	MoJo	SS18-SSX1	biphasic	Jones *et al*., 2016		
	HS-SY-II	SS18-SSX1	monophasic	Sonobe *et al*., 1992		
	YaFuss	SS18-SSX1	monophasic	Ishibe *et al*., 2005		
Primary human cells	83-SS	SS18-SSX1	monophasic	Brodin *et al*., 2017	- Less likely to take on secondary mutations and should better represent disease condition - Enables comparison of results to matched normal muscle cells from same patient	- Difficult to grow and passage
Mouse models			Cell line xenograft	Yasui *et al*., 2014	- Cell lines are readily available and easy to grow at high numbers for xenograft	- Xenograft take is inconsistent - Expensive
			Patient-derived xenograft	Kawano *et al*., 2016	- PD Xenografts are closer to human tumour biology	- Material is not readily available, xenograft take is inconsistent - Expensive
		SS18-SSX2	Genetically engineered	Haldar *et al*., 2007	- Tumours are easily induced and grown - Facilitates drug intervention studies	- Genetic background is murine and may not be translatable to human models - Expensive
Tissue Microarray (FFPE)				Horvai *et al*., 2006 Jardis *et al*., 2009	- Facilitates biomaker study of multiple samples concurrently	- Not easily manipulated
Primary tumour tissue (frozen)					- Enables study of human tumour biology	- Not readily available - Tumours are often irradiated before excision

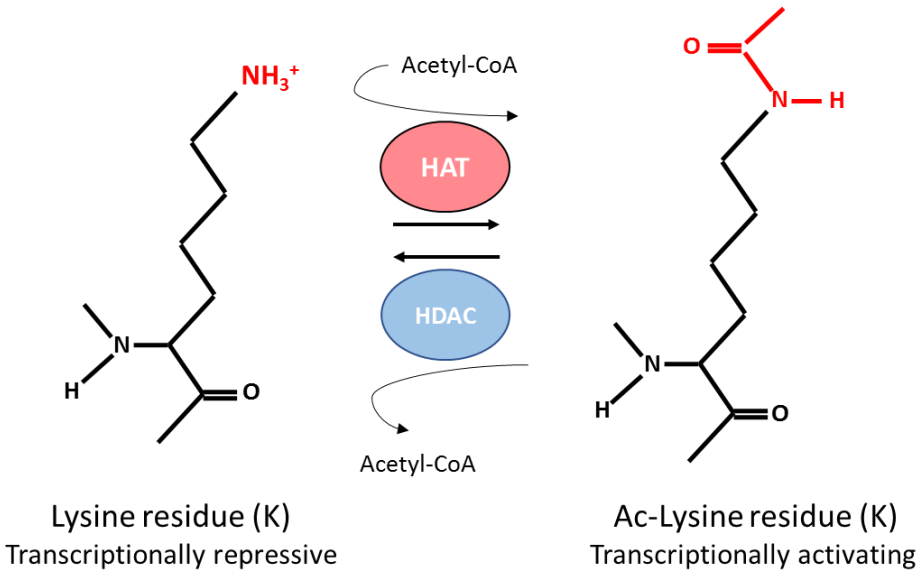

Figure 1.3: Dynamic histone acetylation status mediation. Acetylation of histone lysine residues by histone acetyltransferases (HAT) neutralizes the R group charge, leading to decreased interaction with negatively charged phosphate group on the DNA backbone and allowing transcriptional activation. Co-enzyme acetyl coenzyme-A (CoA) is used as an acetyl-group donor. Deacetylation of histone lysine residue by histone deacetylases (HDAC) restores the positively charged R group, repressing transcription through chromatic compaction.

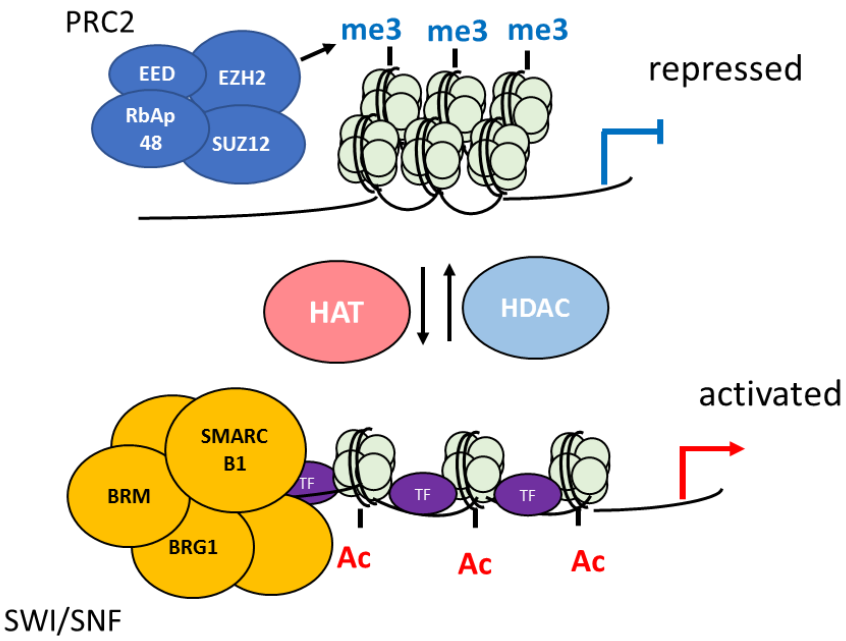

Figure 1.4: Polycomb repressor complex 2 (PRC2) and the SWItch/Sucrose Non-Fermentable (SWI/SNF) complex work in opposition in regulation of transcriptional patterns. PRC2 functions to trimethylate H3 histones at lysine reside 27 (H3K27me3) leading to transcriptional repression. Histone deacetylases (HDAC) remove acetyl groups from histones, further contributing to transcriptional repression by restoring lysine-residue positive charges, creating an electrostatic interaction between histones and DNA. The SWI/SNF complex rearranges nucleosomes to destabilize this interaction and allow transcription factors access to DNA. Histone acetyl transferase (HAT) acetylate lysine resides, neutralizing the positive charge and further functioning to disrupt the nucleosome interactions, allowing for transcriptional activation.

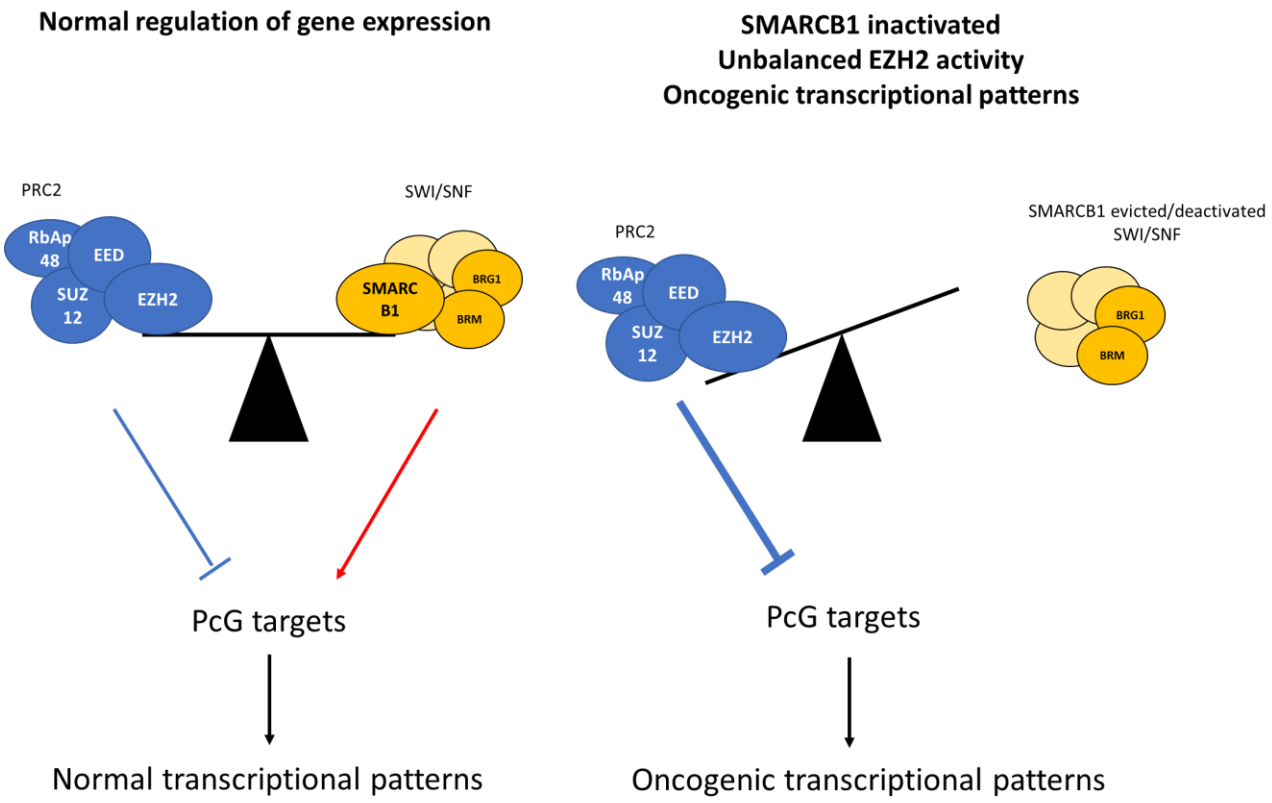

Figure 1.5: Polycomb repressor complex 2 (PRC2) and the SWItch/Sucrose Non-Fermentable (SWI/SNF) complex are proposed to antagonistically balance for proper transcriptional regulation. When components are under normal regulation, PRC2 and SWI/SNF activities balance to activate and repress transcription polycomb group (PcG) targets as needed. When SMARCB1 is deactivated PRC2 is no longer constrained, resulting in unbalanced, over-activation of EZH2 and oncogenic transcriptional repression patterns.

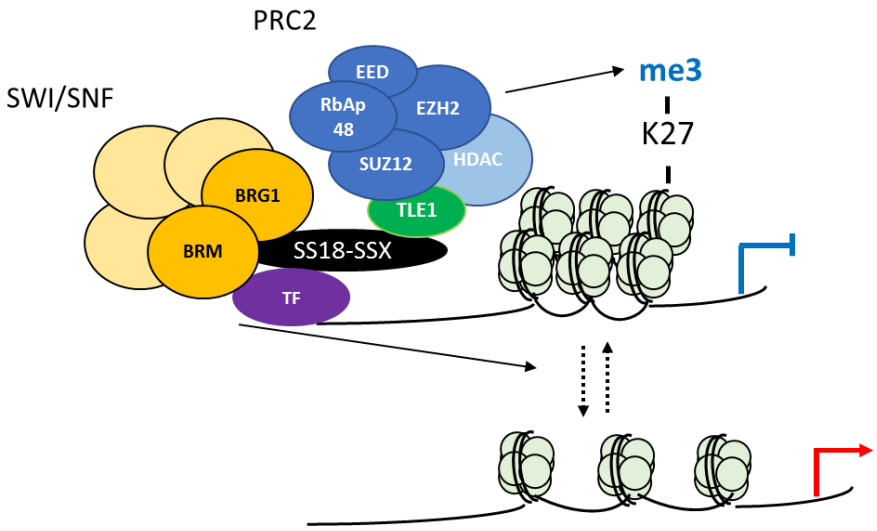

Figure 1.6: Model of transcriptional deregulation in synovial sarcoma. SS18-SSX recruits TLE1 and promotes aberrant assembly of polycomb repressor complex 2 at oncoprotein-mediated binding sites. This leads to abnormal transcriptional repression by EZH2-mediated trimethylation of lysine 27 residues on H3 histones (H3K27me3). SS18-SSX further interacts within the SWItch/Sucrose Non-Fermentable (SWI/SNF) complex evicting SMARCB1, further promoting EZH2 activity and leading to abnormal nucleosome rearrangement that may result in non-specific transcriptional activation and/or failure to activate transcription at SS18-SSX-mediated target sites.

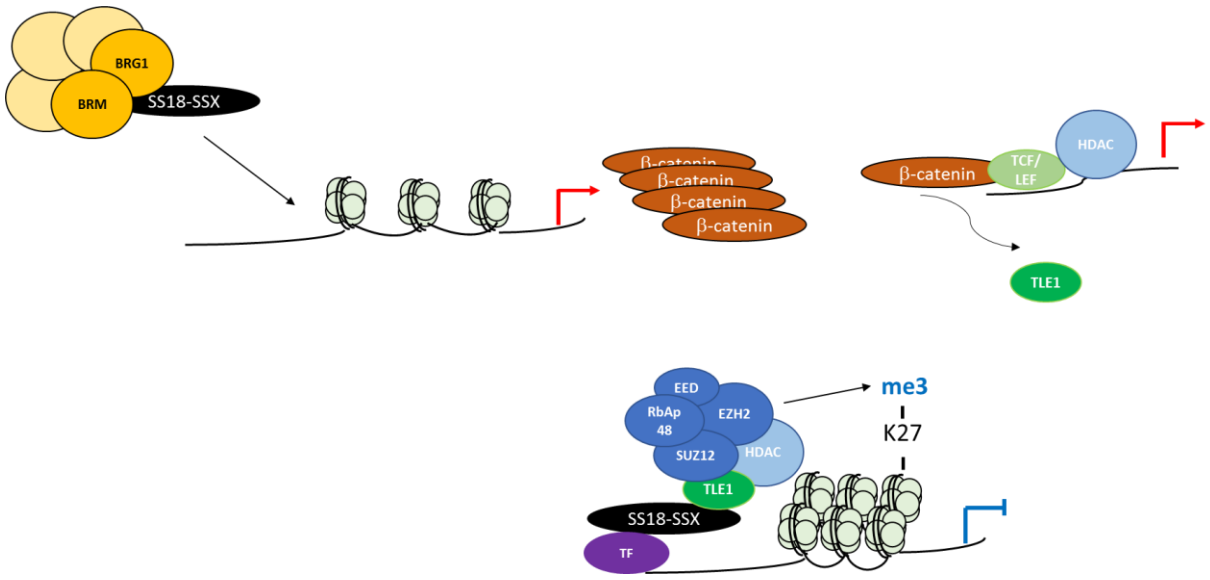

Figure 1.7: Proposed model of contributors to WNT pathway deregulation in synovial sarcoma. SMARCB1-deactivated SWItch/Sucrose Non-Fermentable (SWI/SNF) complex activity may result in over-activation of β-catenin due to SS18-SSX occupancy. β-catenin functions in displacing TLE1 from repressive complexes to activate transcription of cell cycle effectors. TLE is then available at higher concentrations to interact within the SS18-SSX/Polycomb group mediated repressive complex and decrease expression of oncoprotein target genes.

Table 1.4: Summary of cellular histone deacetylases

Class	Member	Location	Distribution	Deacetylase Domains
I	HDAC1	Nucleus	Ubiquitous	(1) N-terminal
	HDAC2	Nucleus		
	HDAC3	Nucleus/Cytoplasm		
	HDAC8	Nucleus		
IIA	HDAC4	Nucleus/Cytoplasm	Heart, skeletal muscle, brain	(1) C-terminal with N terminal serine phosphorylation sites
	HDAC5		Heart, skeletal muscle, brain	
	HDAC7		Heart, skeletal muscle, pancreas, placenta	
	HDAC9		Brain, skeletal muscle	
IIB	HDAC6	Cytoplasm	Heart, liver, kidney, placenta	(2) N-terminal and C-terminal
	HDAC10		Liver, spleen, kidney	(1) N-terminal and (incomplete) C-terminal
III	SIRT1-7	Nucleus/Cytoplasm/ Mitochondria	Ubiquitous	(1) Require NAD+ as a co-factor
IV	HDAC11	Nucleus/Cytoplasm	Brain, heart, skeletal muscle, kidney	(1) N-terminal

Table 1.5: Summary of selected HDAC inhibitors in clinical development

Name	Target	Phase	Use
Panobinostat	Pan-HDAC	Approved 2015	Multiple myeloma
Belinostat	Pan-HDAC	Approved 2014	Peripheral T cell lymphoma
Romidepsin	HDAC1, HDAC2	Approved 2009	Cutaneous T cell lymphoma
Vorinostat	HDAC1, HDAC3	Approved 2006	Cutaneous T cell lymphoma
Pracinostat	HDAC1-5, HDAC7-11	III	Acute myeloid leukemia
Entinostat	HDAC1, HDAC3	III	ER+ Breast cancer, Hodgkin lymphoma
Quisinostat	Pan-HDAC	II	Multiple myeloma, ovarian, advanced solid tumours
Givinostat	HDAC1-5, HDAC7-9	II	Refractory leukemia
Abexinostat	HDAC1-3, HDAC6, HDAC10	II	Sarcoma, lymphoma

CHAPTER 2: IDENTIFICATION OF CYTOTOXIC AGENTS DISRUPTING SYNOVIAL SARCOMA ONCOPROTEIN INTERACTIONS BY PROXIMITY LIGATION ASSAY

2.1 Introduction

The chromosomal translocation t(X;18)(p11.2;q11.2) is the main cytogenetic event in synovial sarcoma and results in the fusion of the BAF complex member *SS18* with one of three highly homologous transcriptional repressor genes, *SSX1, SSX2* or *SSX4* (Clark et al., 1994; Skytting et al., 1999). The resulting *SS18-SSX* fusion oncogene can be detected in nearly all synovial sarcomas and is used clinically to confirm the diagnosis. Importantly, the expression of *SS18-SSX* is necessary and sufficient for the development of synovial sarcoma, as demonstrated in transgenic mice wherein the conditional expression of *SS18-SSX* in early myoblasts leads to tumour development without the requirement of any cooperative transgenic changes (K. B. Jones et al., 2011).

The SS18-SSX fusion protein has been proposed to displace native SS18, leading to aberrant SWI/SNF-mediated gene transcription (Kadoch & Crabtree, 2013). The fusion of SSX to SS18 also recruits interacting proteins involved in epigenetic regulation, including transducin-like enhancer of split 1 (TLE1), activating transcription factor 2 (ATF2), members of the polycomb group and histone deacetylases (HDAC) (Cironi et al., 2016; Su et al., 2012). Together, this is thought to bring about the abnormal transcriptional pattern that drives malignant transformation in synovial sarcoma (Kadoch & Crabtree, 2013; Su et al., 2012).

Polycomb recruitment by TLE1 and the fusion oncoprotein triggers the repression of genes targeted by the SS18-SSX/ATF2/SWI-SNF core through trimethylation at lysine 27

H3 histones (Su et al., 2012). We have previously shown that the association of TLE1 with the SSX domain of the fusion oncoprotein results in the repression of ATF2 target genes, including early growth response-1 (*EGR1*), a key positive regulator of the PTEN tumour suppressor (Lubieniecka et al., 2008; Su et al., 2012). This permits up-regulation of PI3K/AKT/mTOR signaling, resulting in a proliferative, anti-apoptotic phenotype (Su et al., 2010). When this association is disrupted by specific knockdown of TLE1, ATF2 or SS18-SSX synovial sarcoma cell lines are observed to undergo apoptosis, indicating this complex association is important for tumour cell survival (Su et al., 2012).

The SS18-SSX/TLE1/ATF2 protein complex has been shown to be disrupted following treatment with HDAC inhibitors (Su et al., 2012), providing an explanation for the sensitivity of synovial sarcoma cells to HDAC inhibition (Ito et al., 2005). Based on the finding that the SS18-SSX fusion oncoprotein is unique to synovial sarcoma and is necessary and sufficient for tumour initiation (Haldar et al., 2007), small molecules able to disrupt the SS18-SSX protein complex may have selective anti-tumour activity in synovial sarcoma. As SSX is not expressed in somatic tissues, an attractive drug target in this system is the SSX/TLE1 interface.

In the present investigation, a proximity ligation assay (PLA) was used to screen for drugs that disrupt the interaction between SS18-SSX and TLE1. The method was developed to visualize protein associations and modifications *in situ* with very high specificity, at interaction distances within 30 nm (Olink Bioscience) (Fredriksson et al., 2002; Schweitzer et al., 2000). This assay methodology allows for the direct identification of proteins in such close proximity by utilizing protein-specific antibodies conjugated with oligonucleotides that are ligated and amplified using fluorophore-labelled primer sequences (Bagchi, Fredriksson,

& Wallen-Mackenzie, 2015). The resulting fluorescent signal can be detected by fluorescent microscopy. PLA has been used to detect protein complexes and post-translational modifications *in situ*, as well as for high-throughput screening practices, demonstrating potential for use in pre-clinical drug screening models (Jarvius et al., 2007; Leuchowius et al., 2010; Soderberg et al., 2006; Soderberg et al., 2008). PLA technology has further been used in excised tissues from *in vivo* studies to monitor disease state and therapy responses (Falkenberg et al., 2015; Flanders et al., 2014; Kaitu'u-Lino et al., 2012).

In this study, we apply the proximity ligation assay to show that the interaction of SS18-SSX with TLE1 is detectable only in synovial sarcoma, confirm that this interaction is disrupted by HDAC inhibitors, and identify novel molecules capable of disrupting this interaction using high-throughput drug screens. This work instantiates the value of the proximity ligation technique in uncovering compounds that disrupt oncogenic protein associations, applicable to important oncogenic mechanisms among the growing collection of neoplasms driven by translocation-associated fusion oncoproteins.

2.2 Materials and methods

2.2.1 Cell culture and chemicals

Six human synovial sarcoma cell lines were kindly provided: SYO-1 (Dr. Akira Kawai, National Cancer Centre Hospital, Tokyo, Japan), FUJI (Dr. Kazuo Nagashima, Hokkaido University School of Medicine, Sapporo, Japan), YaFuss, HS-SY-II (Dr. Scott Lowe, Memorial Sloan Kettering Cancer Centre, New York, USA), MoJo (Dr. K. Jones, University of Utah, Salt Lake City, UT) CME-1 (Dr. J.C. Knight, UMDS, London), Yamato-

SS and ASKA-SS (Dr. K. Itoh, Osaka Medical Center for Cancer and Cardiovascular Diseases, Japan). For use as controls, A673 (Ewing sarcoma) and SU-CCS-1 (clear cell sarcoma) lines were purchased from the ATCC, while 402-91 (myxoid liposarcoma) was received from Dr. Pierre Aman, University of Gothenburg, Sweden. Sarcoma cell lines were maintained in RPMI-1640 medium with 10% fetal bovine serum (FBS) (Life Technologies). As additional human non-sarcoma controls, breast cancer cell line MCF7 and cervical cancer cell line HeLa were purchased from the ATCC and cultured in DMEM medium with 10% FBS. All cells were grown at 37°C, 95% humidity, and 5% CO_2.

Pharmacologic compounds were purchased from Selleck Chemicals (Houston, TX, USA). Small molecule inhibitor library compounds were purchased from Maybridge Chemicals (Waltham, MA, USA).

2.2.2 Tissue sections

Paraffin embedded tissue from a synovial sarcoma lung metastasis was obtained from the Vancouver General Hospital. Synovial sarcoma and control cell lines were fixed overnight in 10% NBF and embedded in paraffin as previously described (Anglesio et al., 2013). FFPE tissue and embedded cell line pellets were sectioned at 4 µm onto micro-slides for use in both conventional immunohistochemistry and proximity ligation assay procedures. Immunohistochemistry staining was carried out using the Ventana automated staining platform, with primary antibody at a 1/150 dilution for both SS18 (Santa-Cruz Biotechnologies, Dallas, TX, USA sc-28698) and TLE1 (Origene, Rockville, MD, USA TA800301).

2.2.3 Proximity ligation assay

Cells were seeded in culture treated chamber slides or in 96 well plates. The following day, wells were treated with pharmacologic agents for 0, 4, 8, or 12 hours. Cells were washed twice with PBS, fixed with 3% formaldehyde and permeabilized with 0.1% Triton X-100. Wells were blocked with blocking buffer and incubated overnight at 4°C with primary antibodies at a 1/1000 dilution: SS18 (rabbit polyclonal, Santa-Cruz Biotechnologies, sc-28698) or TLE1 (mouse monoclonal, Origene, TA800301). Proximity ligation was performed utilizing the Duolink® *In Situ* Red Starter Kit Mouse/Rabbit (Sigma-Aldrich, Oakville, ON, Canada) according to the manufacturer's protocol. The oligonucleotides and antibody-nucleic acid conjugates used were those provided in the Sigma-Aldrich PLA kit (DUO92101). Alexa Fluor 488 secondary antibody (Life Technologies) was added during signal amplification to confirm the presence of nuclear proteins. Fluorescence was detected using a Zeiss Axioplan2 microscope at 40x. Images were quantified in triplicate using ImageJ software (NIH) as foci per nucleus, defined as the number of interaction points counted per nucleus. High-throughput co-localization fluorescence signal staining intensity was detected using the automated Cellomics ArrayScan VTI compartmentalization analysis software (Thermo Scientific, Waltham, MA, USA). With this automated method, twenty images per well were quantified. Relative PLA stain signal was normalized to the vehicle (0.1% DMSO) treated control as well as to TLE1 antibody-only control, to account for background signal. Both ImageJ and Cellomics ArrayScan view fields were counted with 15-35 nuclei per image; from this data, average number of foci per nucleus was calculated. Counts per individual nucleus were not captured by the software; the

average per nucleus was defined using the total foci per field (red channel) over the total nuclei per field (DAPI channel).

Proximity ligation in FFPE samples was performed according to the manufacturer's brightfield protocol. Sections were heated at 60°C for one hour, then de-paraffinized in Citrisolv (Fisher Scientific) and rehydrated using an ethanol gradient. Antigen retrieval was performed with Borg Decloaker (Biocare. Pacheco, CA, USA) in a water bath heated at 95°C for 20 minutes. The slides were cooled to room temperature in antigen retrieval solution for 10 minutes and in a cold-water bath for an additional 10 minutes. Endogenous peroxidase activity was blocked with 2% hydrogen peroxide for 10 minutes at room temperature, and cell membranes permeabilized with 0.1% Triton X-100 in PBS for 5 minutes. Slides were incubated with Dako protein block for 30 minutes at room temperature to eliminate nonspecific protein background. The antibody pair was diluted using Dako antibody diluent and incubated on the slides overnight. The proximity ligation procedure was carried out the following day. Images were captured using an Olympus BX46 brightfield microscope with a WHN10x-h/22 eyepiece and an Olympus DP21 camera.

2.2.4 Cell viability assays

Cells were seeded in 96 well plates and treated in triplicate at IC_{50} doses of the tested pharmacological agents. IC_{50} doses were determined in synovial sarcoma cell lines by dose curve studies. Cell viability was assessed as compared with the vehicle 0.1% DMSO condition at 24 hours post treatment using MTS reagent (Promega, Madison, WI, USA). Cell confluency and apoptosis induction was assessed over a 48-hour timeframe utilizing the

IncuCyte Zoom® live cell imaging software (Essen BioScience). Apoptosis was assessed by IncuCyte™ Kinetic Caspase-3/7 Apoptosis Assay Reagent (Essen BioScience, 4440).

2.2.5 Co-immunoprecipitation and western blots

According to the manufacturers protocol, 6 μg of antibody (TLE1: Abcam, ab125183; normal rabbit IgG: Santa-Cruz Biotechnologies, sc-2027) in PBST was added to 50 μL of Dynabeads® Protein G magnetic beads (Life Technologies) for 30 minutes with rotation at room temperature. Antibody was then crosslinked to the beads with the addition of 5 mM BS^3 (ThermoScientific, 21580) in conjugation buffer for 30 minutes with rotation at room temperature. Crosslinking was quenched with Tris-HCl pH 7.5 for 15 minutes at room temperature. Beads were then washed 3 times with conjugation buffer and once with PBST. Following drug treatment, cells were washed with ice-cold PBS and incubated with Triton X-100 (Sigma-Aldrich) lysis buffer for 30 min on ice, with inversion every 10 minutes. Whole cell lysates were centrifuged at 4°C, 10 000 rpm for 15 minutes. Supernatants were quantified and 1000 μg of protein was mixed with the antibody-crosslinked beads. The immunoprecipitation was incubated overnight at 4°C with rotation. The supernatant was then removed and the beads were washed 3 times in lysis buffer and 3 times in PBST, and then boiled in 2X loading dye for 5 minutes.

Samples were separated by 10% SDS-PAGE and transferred to PVDF membranes (Bio-Rad Laboratories, Hercules, CA, USA). Blots were incubated with indicated antibodies (TLE: Origene TA800301; SS18: Santa Cruz Biotechnologies, sc-28698; EGR1: Cell Signaling, 4153S; GAPDH: Santa Cruz Biotechnologies sc-25778). Signals were visualized using the Odyssey Infrared System (LI-COR Biosciences, Lincoln, NE, USA).

2.2.6 RNA interference

Duplex oligo (sense, CAAGAAGCCAGCAGAGGAATT; antisense, UUCCUCUGCUGGCUUCUUGTT) *SS18-SSX2* siRNAs were designed to target the *SSX* portion of *SS18-SSX* using the Integrated DNA Technologies RNA interference (RNAi) design tool, and synthesized by Integrated DNA Technologies (IDT, Coralville, IA, USA) as previously described (Lubieniecka et al., 2008). SYO-1 cells were seeded in 6 well plates. At 60% confluence, cells were transfected with 30-50 pmol si*SS18-SSX2* and 9 μL Lipofectamine RNAiMax transfection reagent (Invitrogen) in Opti-MEM serum free media (Life Technologies), according to the manufacturer's protocol. Protein was harvested 48 hours post transfection, and knock-down confirmed by western blot with SS18 antibody (Santa Cruz Biotechnologies).

The synovial sarcoma CME-1 cell line was stably transfected with a doxycycline-inducible shRNA targeting *SS18-SSX*. CME-1 cells were used for these experiments because they are more easily transfected than other available synovial sarcoma cell lines. The inducible line was generated with the use of a pcDNA6 TR and subsequently with the pSuperior shRNA vector encoding a target oligonucleotide specific for the 3' UTR region of *SS18-SSX* (1, 2 and 4), as previously described (D'Arcy, Maruwge, Ryan, & Brodin, 2008; D'Arcy et al., 2014). shRNA-mediated knockdown of SS18-SSX was induced by the addition of doxycycline (Clontech). Protein was harvested 24 hours post transfection and knock-down was confirmed by western blot with SS18 antibody (Santa Cruz Biotechnologies).

2.2.7 High-throughput drug screen assay

The 16 000 compound Maybridge Chemicals library drug screen was undertaken in SYO-1 cells. Cells were seeded in 96 well plates at 1e4 cells/well. The following day, compounds from the Maybridge library were transferred from stock plates (5 mM in DMSO) using a Biorobotics Biogrid II pinning robot with a 96-pin tool diameter of 0.4-mm, to bring about a final concentration of approximately 5 μM per well. Plates were developed with MTS reagent 24 hours post treatment to select for direct effects at this dose. Hits bringing about a decrease in viability of greater than 50% were validated in a dose-response curve and in additional synovial sarcoma cell lines. IC_{50} doses of the small molecules were used for PLA validation studies.

2.2.8 Chromatin immunoprecipitation

ChIP experiments were performed following the Active Motif ChIP-IT Express Enzymatic kit protocol. Cells were cross-linked with 1% formaldehyde prior to lysis and homogenization. Cross-linked DNA was sheared by enzymatic digestion. After centrifugation, the supernatants were incubated with the indicated antibody at 4°C overnight. Precipitates were washed, eluted with 1% SDS and incubated at 65°C to reverse crosslinking. ChIP-enriched DNA was purified by phenol-chloroform (Invitrogen) and ethanol precipitation, and was subjected to SYBR Green qPCR analysis (Roche) using an ABI ViiA7 qPCR system and an *EGR1* promoter primer set (hEGR1 -0.1 kb/CRE sense: TAGGGTGCAGGATGGAGGT, antisense: AAGCAGGAAGCCCTAATATGGCAG) [5].

2.2.9 Reverse transcriptase quantitative PCR

Total RNA was isolated from treated cells using the RNeasy Mini kit (Qiagen) and was then reverse transcribed to cDNA using Oligo(dT) (Invitrogen) and Superscript III (Invitrogen). SYBR Green (Roche) reagent was used for qPCR expression analysis, using an ABI ViiA7 qPCR system. The following primers for *EGR1* expression were used; sense: AGCCCTACGAGCACCTG, antisense: CGGTGGGTTGGTCATG. All transcript levels were normalized to *GAPDH* RNA expression.

2.3 Results

2.3.1 The proximity ligation assay detected SS18-SSX/TLE1 co-localization *in situ*

In order to visualize SS18-SSX/TLE1 co-localization in synovial sarcoma *in situ*, we set-up a proximity ligation assay (PLA) using antibodies specifically recognizing SS18 and TLE1. Nuclear proximity ligation signal was detectable between SS18 and TLE1 in all six-tested synovial sarcoma patient derived cell lines: SYO-1 (SS18-SSX2), FUJI (SS18-SSX2), MoJo (SS18-SSX1) (Figure 2.1A); Yamato-SS (SS18-SSX1), and ASKA-SS (SS18-SSX1) (Figure I.1A); and CME-1 (SS18-SSX2) (Figure 2.2B). Weak or non-specific PLA signals were detectable in cells lines of other cancer subtypes (including three sarcomas bearing different fusion oncoproteins): MCF7 (breast carcinoma), HeLa (cervical carcinoma), A673 (Ewing sarcoma, EWS-FLI1) (Figure 2.1A), 402-91 (myxoid liposarcoma, FUS-DDIT3), SU-CCS-1 (clear cell sarcoma, EWS-ATF1), as well as single antibody, no antibody and non-specific antibody conditions (Figure I.1B).

Quantification of SS18/TLE1 PLA signals in synovial sarcoma cell line nuclei was more than 10-fold higher than the level seen in control cell lines (Figure 1B, I.1C). Co-

immunoprecipitation analyses further demonstrated that the interaction of SS18-SSX with TLE1 was specific to synovial sarcoma, as SS18-SSX was pulled down with TLE1 exclusively in synovial sarcoma cell lines (Figure 2.1C). All cell lines used in this study express some level of SS18 and of TLE1; the lack of SS18 and TLE1 co-localization in SS18-SSX negative cell lines therefore indicated the nuclear proximity ligation signal was a result of the SS18-SSX/TLE1 interaction and not of wild-type SS18/TLE1 protein interactions (Figure I.1D).

2.3.2 TLE1 co-localized with SS18 only in the context of SS18-SSX

Reliable antibodies to detect SSX, suitable for co-IP or PLA assays, are currently not available. To determine whether SS18-SSX/TLE1 co-localization was specific for the fusion oncoprotein, knockdown of SS18-SSX was achieved with siRNA molecules (Figure 2.2A-C) as well as shRNA vectors (Figure 2.2D-F). When *SS18-SSX* expression was silenced, co-localization of SS18-SSX with TLE1 was lost and quantification of foci per nucleus was significantly decreased (Figure 2.2C, 2.2F). Both siRNA systems target *SSX* mRNA regions of the fusion transcript, and result in the specific silencing of SS18-SSX but not of endogenous SS18, bringing about a loss of SS18-SSX/TLE1 proximity ligation signals. This verified previous results (Su et al., 2012) which demonstrated that the interaction of SS18 with TLE1 occurs only in the context of the SS18-SSX fusion oncoprotein.

2.3.3 Proximity ligation signals could be detected in FFPE synovial sarcoma tumour tissue samples

Formalin-fixed paraffin embedded (FFPE) patient-derived synovial sarcoma tumour samples were used to detect SS18-SSX/TLE1 co-localization in human tumour tissue samples. Immunohistochemical staining in synovial sarcoma patient surgical specimens demonstrated the presence of SS18-SSX and TLE1 as well as the specificity of TLE1 for synovial sarcoma cells (Figure 2.3A, 2.3B). In an excised pulmonary metastasis, SS18-SSX/TLE1 complex co-localization signal was detected exclusively in synovial sarcoma tissue nuclei (Figure 2.3C, 2.3D) while the adjacent normal lung tissues were negative (Figure 2.3E). The specificity of the proximity ligation signal in FFPE samples was additionally validated in embedded synovial sarcoma cell pellets in comparison to control sarcoma cell lines bearing different translocations (Figure I.2). SS18-SSX/TLE1 proximity ligation signal was detected only in synovial sarcoma samples.

2.3.4 PLA enabled *in situ* visualization of HDAC inhibitors-induced dissociation of SS18-SSX from TLE1

Previous studies have demonstrated that HDAC inhibitors disrupt the fusion oncoprotein complex in synovial sarcoma, re-establishing expression of tumour suppressor gene and apoptotic response (Lubieniecka et al., 2008; Su et al., 2010; Su et al., 2012). To investigate if the SS18-SSX/TLE1 complex disruption induced by HDAC inhibitors can be detected *in situ* using the PLA method, SYO-1 synovial sarcoma cells were treated at IC_{50} doses with the class I HDAC inhibitors FK288 (romidepsin), MS275 (entinostat), SAHA (vorinostat) or the pan-HDAC inhibitor SB939 (pracinostat) as well as nexturastat A (a

cytoplasmic class IIb HDAC6 inhibitor). SS18-SSX/TLE1 complex assembly following HDAC inhibition was assessed by proximity ligation signal in five synovial sarcoma cell lines (Figure 2.4B and I.3A-F) and was confirmed by co-immunoprecipitation (Figure 2.4C).

Class I HDAC inhibitor-induced dissociation of SS18-SSX/TLE1 interactions was visualized as a significant decrease in PLA nuclear signal as well as a loss of SS18-SSX pulled down with TLE1 (Figure 2.4C). HDAC6 inhibition had minimal effect on SS18-SSX/TLE1 co-localization (Figure 2.4A-C), supporting class I HDAC inhibition as being required for disruption of this complex. Dissociation of the SS18-SSX/TLE1 complex following HDAC inhibition correlated with apoptotic induction in synovial sarcoma cell lines (Figure 2.4D). The addition of proteasome inhibitor MG-132 did not prevent complex disruption, demonstrating that the observed dissociation of the SS18-SSX/TLE1 complex induced by class I HDAC inhibitors was not due to protein degradation (Figure I.3A-B).

To demonstrate specificity of this drug-mediated protein complex dissociation, a panel of drug classes was tested concurrently in a 96-well high-throughput format, and the relative signal intensity of SS18-SSX/TLE1 co-localization was quantified (Figure 2.4E). SYO-1 cells were exposed to IC_{50} doses of the HDAC inhibitors FK228, MS-275, SAHA, SB939, ITF2357 (givinostat), JNJ-26481585 (quisinostat), LAQ824 (dacinostat), PCI-24781 (abexinostat), as well as doxorubicin (DNA intercalator) and PI-103 (PI3K inhibitor). Only class I HDAC inhibitors consistently disrupted SS18-SSX/TLE1 co-localization and decreased cell viability. By comparison, drugs primarily acting via DNA intercalation or PI3K inhibition significantly decreased cell viability without concomitant effects on the relative co-localization signal staining intensity of the fusion oncoprotein with its partner.

2.3.5 PLA detection of oncoprotein interactions could be used in high-throughput drug screens to identify molecules that disrupt the SS18-SSX oncoprotein complex

A high-throughput drug screen consisting of 16 000 small molecule inhibitors (Maybridge Chemicals) was completed in synovial sarcoma cell lines expressing the SS18-SSX oncoprotein. Compounds eliciting a decrease in cell viability of greater than 50% were assessed for disruptions to SS18-SSX/TLE1 co-localization in a high-throughput 96-well PLA format. At IC_{50} doses, the top 20 hits from the viability assessment had different degrees of concurrent effect on the protein co-localization measures (Figure 2.5A). The top three available compounds capable of disrupting the SS18-SSX/TLE1 proximity ligation signal were validated in multiple synovial sarcoma cell lines. One compound (designated SXT1596) demonstrated particular efficacy in decreasing cell viability selectively in synovial sarcoma cell lines (Figure 2.5B-C). Compound SXT1596 effectively disrupted interaction between SS18-SSX and TLE1, as confirmed by PLA and immunoprecipitation (Figure 2.5D-F).

2.3.6 Novel compound SXT1596 re-established normal cell signaling in synovial sarcoma

Treatment of SYO-1 cells with SXT1596 resulted in significantly decreased cell viability (Figure 2.6A) and increased apoptosis (Figure 2.6B) that correlated with the decrease in SS18-SSX/TLE1 co-localization signal (Figure 2.6C-D). Chromatin immunoprecipitation revealed a decrease in HDAC1 and H3K23me3 at the *EGR1* promoter, a known target for repression by the SS18-SSX/TLE1/ATF2 complex consistent with a disruption of the biologic effects on SS18-SSX target genes in synovial sarcoma (Figure

2.6E) (Lubieniecka et al., 2008; Su et al., 2010; Su et al., 2012). Similar to class I HDAC inhibitors, the compound SXT1596 reactivated EGR1 transcription and protein expression (Figure 2.6F-G). SS18-SSX protein levels remained relatively constant following SXT1596 treatment, whereas the HDAC inhibitor FK228 led to oncoprotein loss (Figure 2.6G).

2.4 Discussion

In this study, the proximity ligation assay was applied to a neoplasm driven by a fusion oncoprotein, in this case confirming the key SS18-SSX interaction with TLE1 in synovial sarcoma cells and patient samples. This method can assess the capacity for drugs to disrupt the relevant functional interactions of a mutant oncoprotein, and can be used in high-throughput drug screens. As t(X;18) is the sole driving cytogenic event in synovial sarcoma, inhibiting the interactions of the resulting SS18-SSX chimeric oncoprotein with its effector partners can prevent aberrant transcriptional repression, potentially reverse oncogenic effects and initiate apoptosis. PLA allows for quantification of the loss of protein interactions, which can be used to assess drug action and select the most potent agents in this model.

In a high-throughput PLA format, inhibitors capable of disrupting the driving complex can be revealed quickly, *in situ*. This is an efficient means to screen large compound libraries for their capacity to disrupt the relevant oncogenic interactions. In addition, in contrast to fluorescence resonance energy transfer (FRET) methodology, in which fluorescent probes must be engineered onto proteins of interest (Song, Madahar, & Liao, 2011), PLA requires no synthetic protein modifications (that may obstruct normal protein complex interactions). Physical interactions among proteins are time and cell context

dependent, and the detection of a particular protein-protein interaction in a generic experimental condition or in cell culture models may not accurately represent the situation in patients.

PLA is performed in the context of the cell's naturally occurring biology, reducing the likelihood of artifactual alterations to SS18-SSX interactions (which are likely to occur, for example, when SS18-SSX is forcibly overexpressed in vector-based systems, as opposed to being expressed under its endogenous promoter at physiological levels in its original cellular background). This methodology therefore anticipates a streamlined approach to screen for effective therapeutics targeting the driving complex in synovial sarcoma, and will be similarly applicable in other cancers driven by fusion transcription factors. These include other sarcomas and hematopoietic neoplasms typically afflicting young patients, as well as an increasing number of other tumours wherein recurrent fusions are being identified by RNA-Seq technologies (Maher et al., 2009).

The compound designated SXT1596 (5-(2-Nitro-1-propenyl)-1,3-benzodioxole) identified in the PLA drug screen to decrease SS18-SSX/TLE1 co-localization is a biologically active chemical. A number of similar 1,3-benzodioxole derivatives have demonstrated anti-tumour activity by various mechanisms, including binding to tubulin and heat-shock protein inhibition (Jurd, Narayanan, & Paull, 1987; Micale, Zappala, & Grasso, 2002; Yokota, Kitahara, & Nagata, 2000). In addition, the trans-β-Nitrostyrene domain possessed by SXT1596 has been observed in related compounds to inhibit protein phosphatases (J. Park & Pei, 2004) and telomerase (J. H. Kim, Kim, Lee, Lee, & Chung, 2003), resulting in anti-tumour action in several cancer subtypes (Kaap et al., 2003; Messerschmitt et al., 2012; Mohan, Rastogi, Namboothiri, Mobin, & Panda, 2006). Whether

the compound directly inhibits the SS18-SSX/TLE1 interaction domain or disrupts the complex by a secondary mechanism is currently unknown, but the structure of SXT1596 indicates that it is likely a covalent protein inhibitor, not expected to be well tolerated until further pharmacologic optimization steps are carried out (Pifl et al., 2005).

Driving protein complexes are often recruited and deregulated in translocation-associated sarcomas (Anderson et al., 2012). Uncovering new methods of study and utilizing emerging technologies such as the proximity ligation assay may allow better means to identify therapeutic strategies. In synovial sarcoma, this technique can be used in a high-throughput format to screen targeting compounds as a means of identifying novel agents with disease-specific activity. This methodology should also be applicable in other types of translocation-associated cancers.

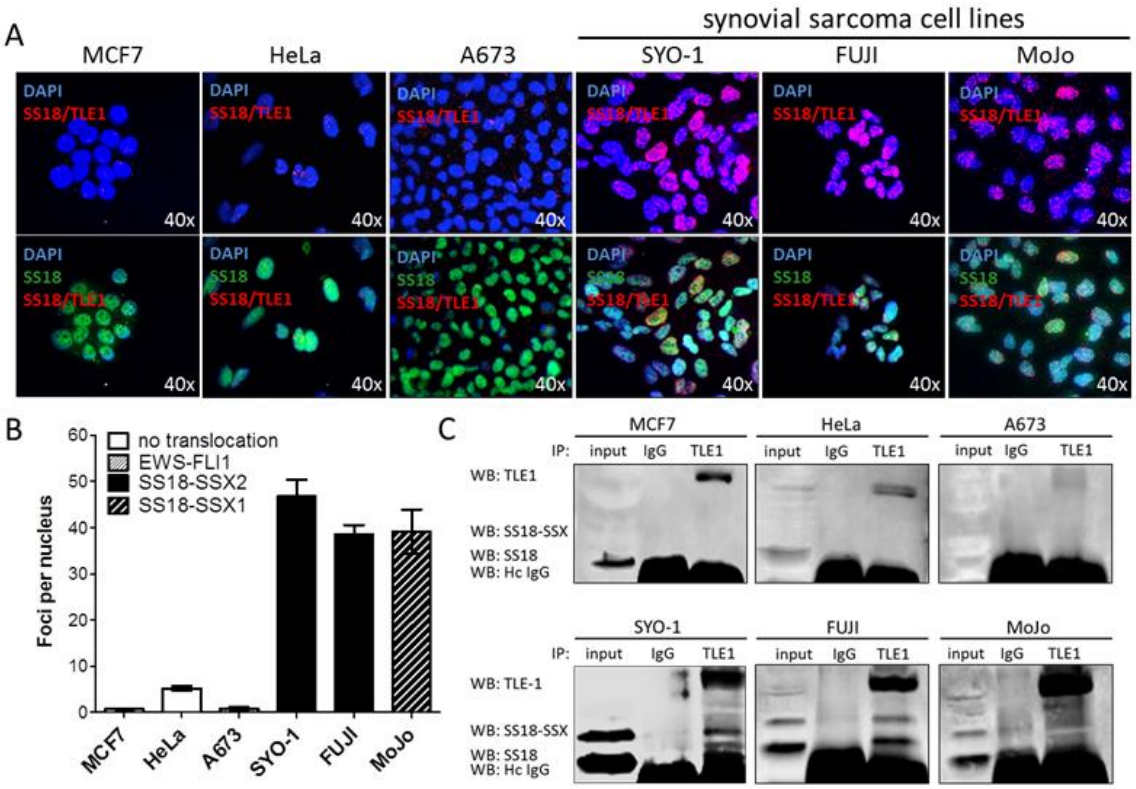

Figure 2.1: The proximity ligation assay demonstrated SS18-SSX/TLE1 co-localization selectively in synovial sarcoma cell lines. (A) SS18-SSX positive cell lines (SYO-1, FUJI, MoJo) demonstrated SS18-SSX/TLE1 proximity by visualization of fluorescent nuclear foci while control cell lines (MCF7, HeLa, A673) showed little nuclear staining. (B) The intensity of the nuclear signal was quantified and shown to be significantly greater in SS18-SSX confirmed-positive cell lines. (C) The SS18-SSX/TLE1 protein-protein interaction was confirmed to be specific for synovial sarcoma cell lines by co-immunoprecipitation. Scale bars represent 20 μm. Error bars represent standard error of mean from three independent studies. Figure reprinted with permission from Laporte *et al.*, 2016 Oncotarget.

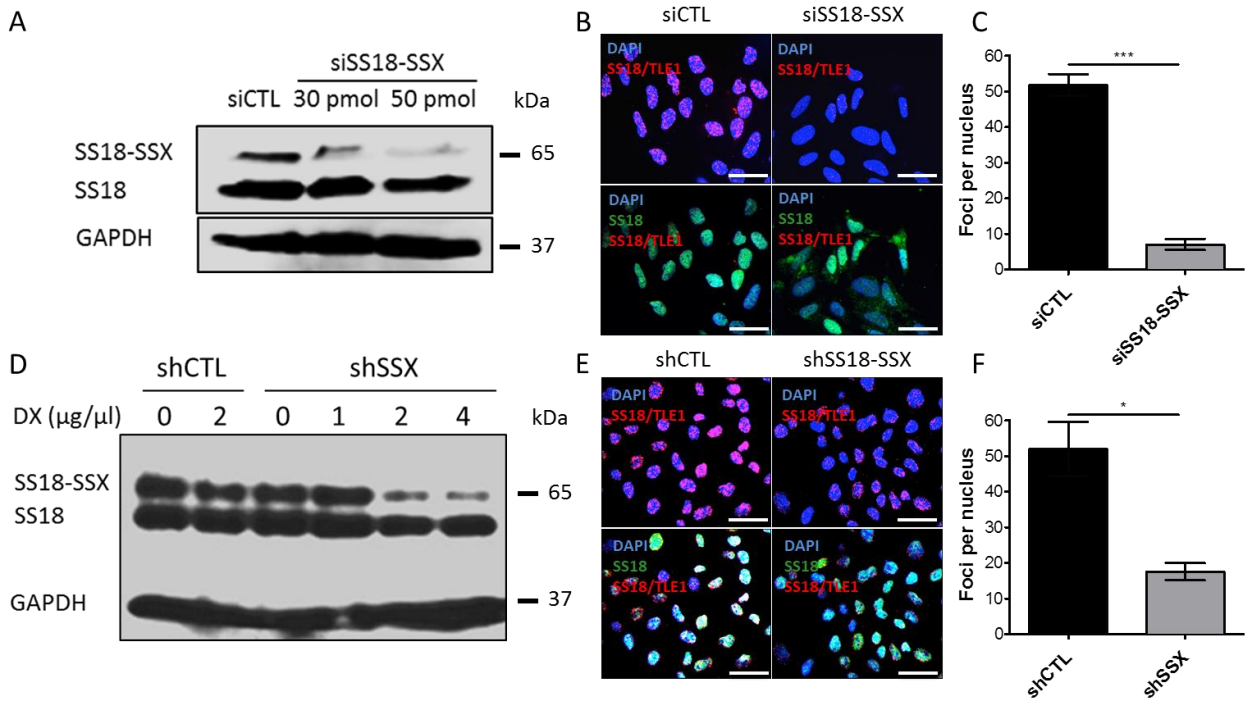

Figure 2.2: Knockdown of SS18-SSX resulted in a loss of SS18-SSX/TLE1 co-localization and a significant decrease in PLA nuclear signals. To demonstrate specificity of PLA signal, 50 pmol of siRNA was used to knockdown SS18-SSX in SYO-1 cells, as demonstrated by a loss of protein expression. (A) Protein levels and (B, C) PLA signals were analyzed 48 hours post siRNA treatment. CME-1 cells were stably transfected with a doxycycline-inducible shRNA against SS18-SSX. (D) Protein level and (E, F) PLA signals were assessed at 24 hours post 4 µg/µL doxycycline (DX) treatment. Scale bars represent 20 µm. Statistical significance compared to RNA interference controls was determined by Student t test: * denotes $p < 0.05$; ** denotes $p < 0.01$. Error bars represent standard error of mean from three images. Figure reprinted with permission from Laporte *et al.*, 2016 Oncotarget.

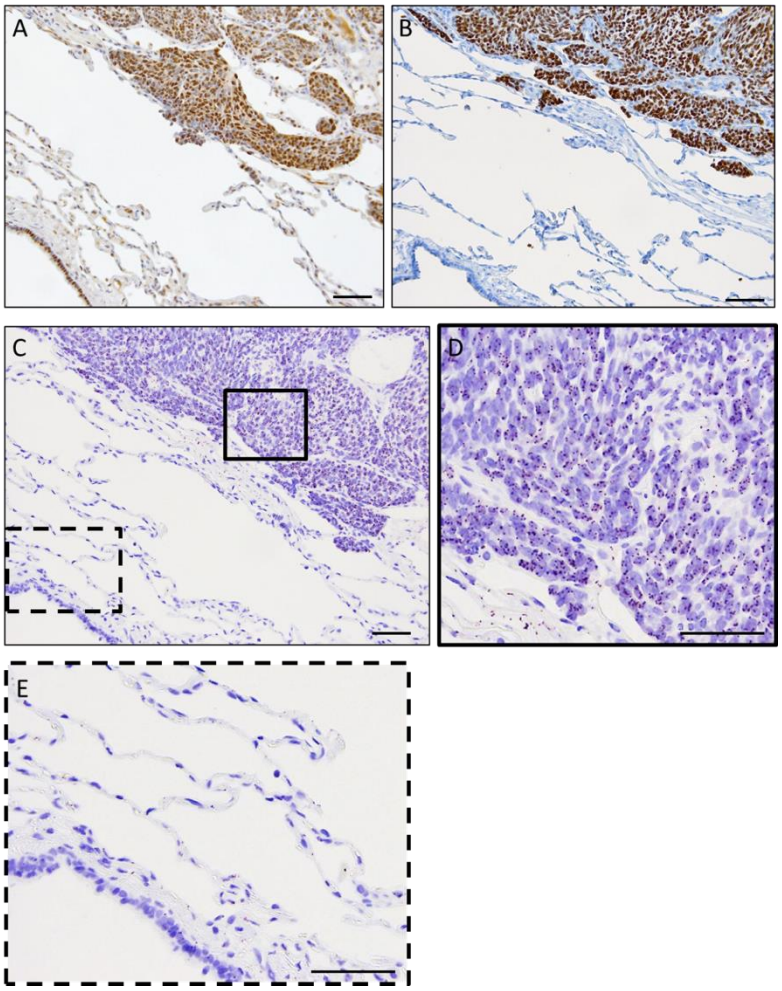

Figure 2.3: The PLA assay could be used to detect SS18-SSX/TLE1 co-localization in FFPE human synovial sarcoma tumour samples. IHC staining of (A) SS18 and (B) TLE1 was strongly positive in synovial sarcoma tumour tissue from the metastasectomy specimen. The PLA nuclear signal was detected in the fixed (C, D) human synovial sarcoma tumour tissue but not in the immediately adjacent (C, E) normal lung tissue. Scale bars represent 100 μm. Figure reprinted with permission from Laporte *et al.*, 2016 Oncotarget.

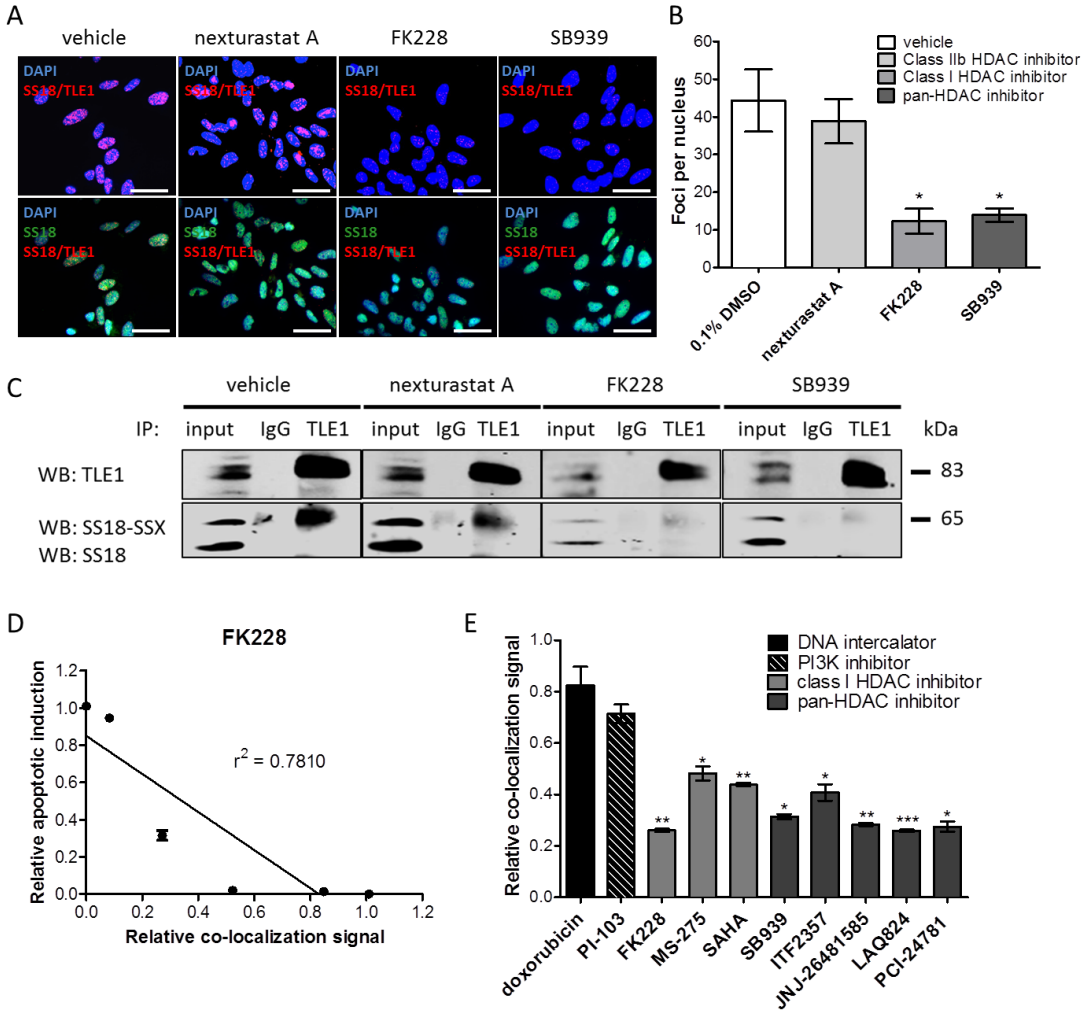

Figure 2.4: HDAC inhibitors disrupted SS18-SSX/TLE1 co-localization. (A, B) A significant decrease in detectable PLA signal following HDAC inhibition in SYO-1 cells (C) was also confirmed by immunoprecipitation. (D) The decrease in PLA co-localization signal correlated with apoptosis induction by HDAC inhibitor FK228 in SYO-1 cells. (E) A panel of cytotoxic compounds and HDAC1/3 inhibitors was screened on SYO-1 cell at IC50 doses for 12 hours. While all compounds were effective in decreasing cell viability, only compounds inhibiting class I HDACs were found to decrease the PLA nuclear signal, as a result of disrupting SS18-SSX/TLE1 co-localization. Scale bars represent 20 μm. Statistical significance compared to vehicle treatment controls was determined by Student t test: * denotes $p < 0.05$; ** denotes $p < 0.01$; *** denotes $p < 0.001$. Error bars represent standard error of mean from conditions performed in triplicate. Linear regression was measured by goodness of fit calculations in Prism Graphpad. Figure reprinted with permission from Laporte *et al.*, 2016 Oncotarget.

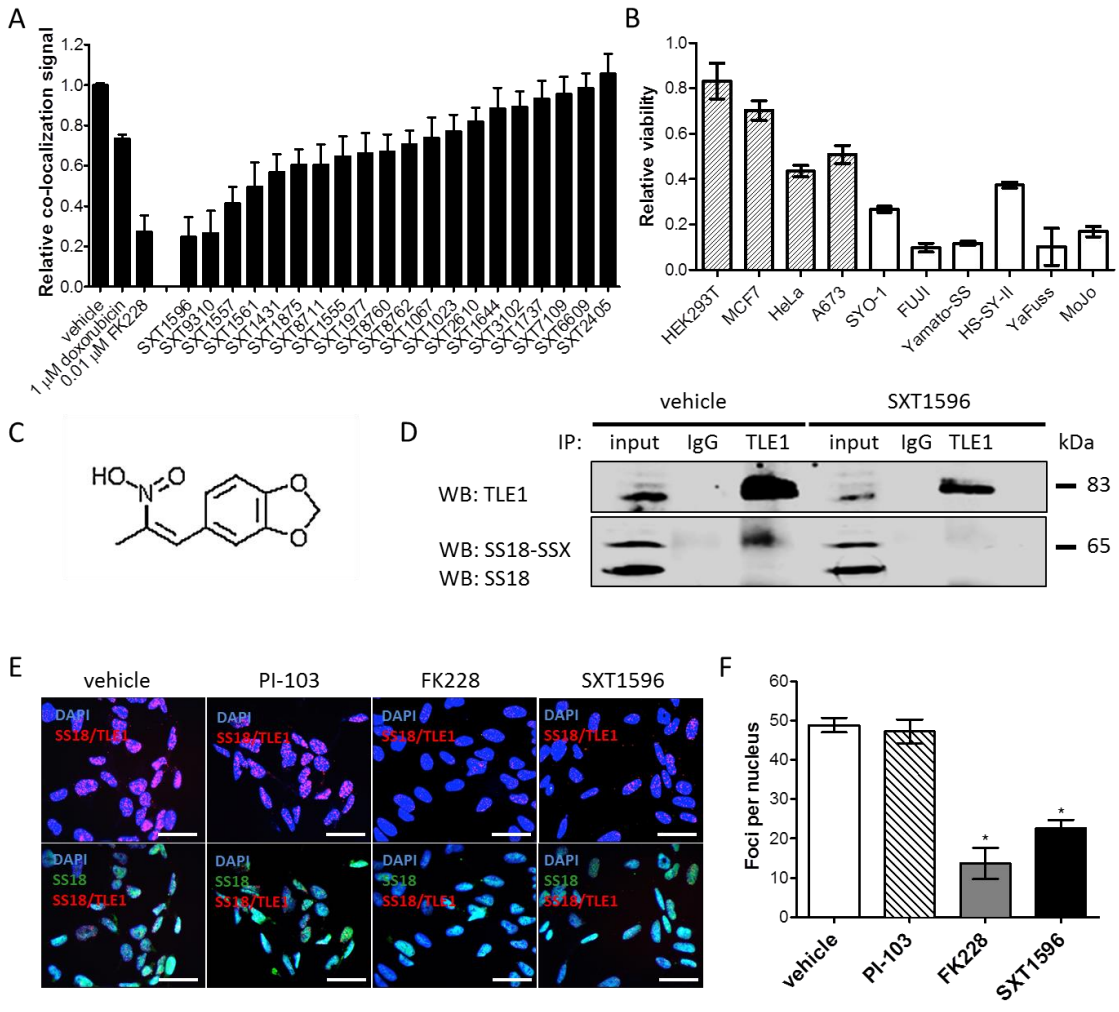

Figure 2.5: The PLA assay could be used for high-throughput drug screening for targeted compounds in synovial sarcoma. (A) From a 16 000 compound small molecule drug library, a compound designated SXT1596 was recognized to significantly decrease relative co-localization of SS18-SSX/TLE1 in human synovial sarcoma cells. (B) SXT1596 selectively decreased cell viability in synovial sarcoma cell lines, SYO-1, FUJI, Yamato-SS, HS-SY-II, YaFuss and MoJo (white bars), when compared to negative control cell lines HEK293T, MCF7, HeLa and A673 (shaded bars) at a concentration of 5 µM. Negative control cell lines HeLa and A673 were sensitive to SXT1596 at higher doses. (C) SXT1596 (5-(2-Nitro-1-propenyl)-1,3-benzodioxole) mediated (D) disruption of the SS18-SSX/TLE1 association was confirmed by immunoprecipitation. (E, F) Nuclear SS18-SSX/TLE1 PLA signal in SYO-1 cells decreased following SXT1596 treatment to a degree similar to that obtained with the HDAC inhibitor FK228. Statistical significance compared to vehicle treatment controls was determined by Student t test: * denotes $p < 0.05$. Error bars represent standard error of mean from conditions performed in triplicate. Small molecule C. was drawn using iChem Labs ChemDoodle software. Scale bars represent 20 µm. Figure reprinted with permission from Laporte *et al.*, 2016 Oncotarget.

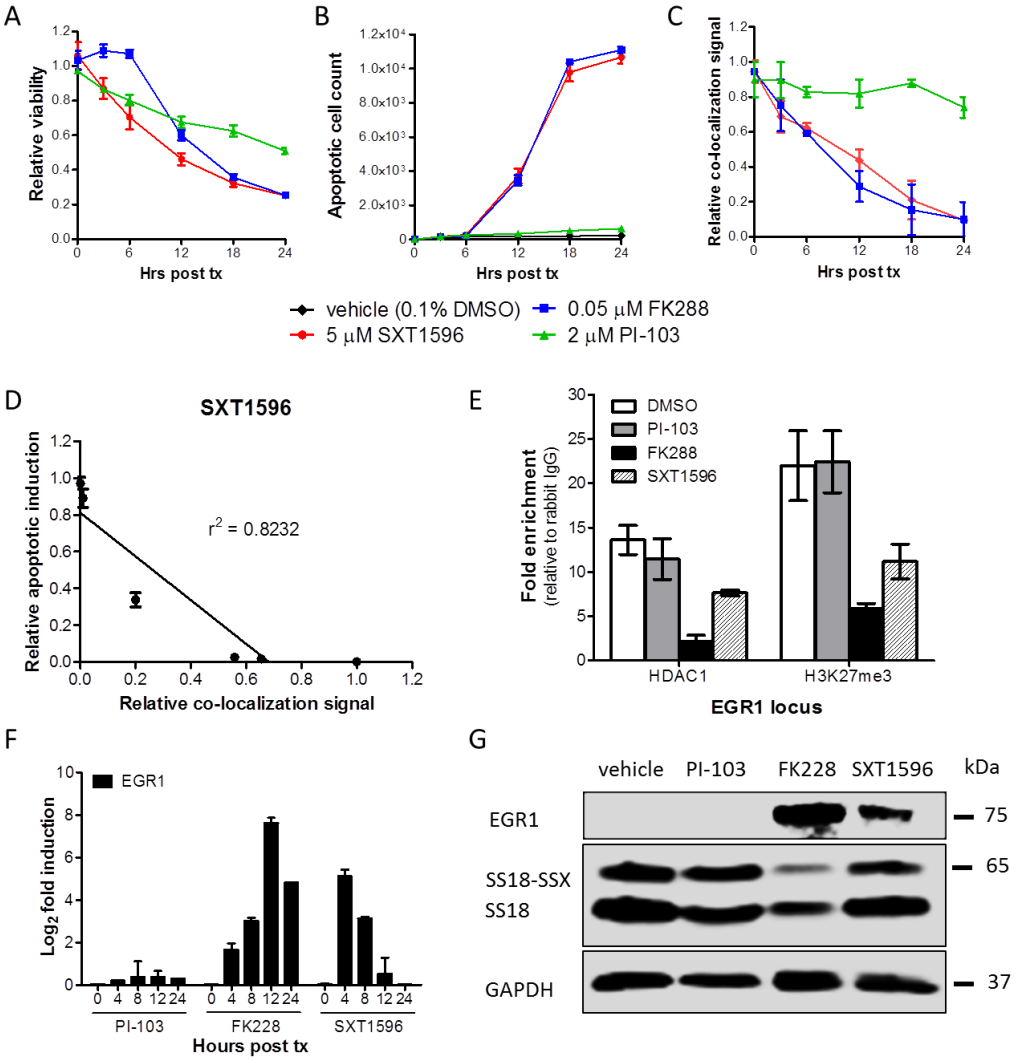

Figure 2.6: SXT1596 decreased cell viability and reactivated EGR1 expression in synovial sarcoma. (A, B) The small molecule SXT1596 induced apoptosis at a similar rate to that of HDAC inhibitor FK228 in SYO-1 cells, and (C) brought about a consistent decrease in SS18-SSX/TLE1 PLA co-localization signal in SYO-1 cells. (D) The induction of apoptosis correlated with the decrease in PLA co-localization signal. (E) Chromatin immunoprecipitation at the EGR1 promoter revealed a decrease in H3K27me3 enrichment following SXT1596 treatment. SXT1596 reactivated EGR1 expression, at the (F) RNA and (G) protein level. Error bars represent standard error of mean from conditions performed in triplicate. Linear regression was measured by goodness of fit calculations in Prism Graphpad. Figure reprinted with permission from Laporte *et al.*, 2016 Oncotarget.

CHAPTER 3: HDAC AND PROTEASOME INHIBITORS SYNERGIZE TO ACTIVATE PRO-APOPTOTIC FACTORS IN SYNOVIAL SARCOMA

3.1 Introduction

Synovial sarcoma is an aggressive, high-grade soft tissue tumour arising most frequently in the extremities of adolescents and young adults (Okcu et al., 2001). Conventional cytotoxic therapy, including doxorubicin and ifosphamide, provides limited benefit. Following surgery and radiation, patients remain at high risk for both early and late metastases, and despite best available therapies the mortality rate remains approximately 50% within 10 years of diagnosis (Krieg et al., 2010).

Synovial sarcoma is characterized by a fusion oncogene derived from the chromosomal translocation t(X;18)(p11.2;q11.2) (Sandberg & Bridge, 2002). This translocation results in the fusion of the N-terminus of *SS18* to the C-terminus of *SSX1, SSX2* or *SSX4*, resulting in the chimaeric oncoprotein SS18-SSX. SS18 has been described as a member of the SWI/SNF complex involved in nucleosome remodeling, while SSX proteins (normally expressed only in adult testes and at low levels in the thyroid) can act as transcriptional corepressors (Brett et al., 1997; Ladanyi, 2001; Middeljans et al., 2012).

Although neither SS18 nor SSX possesses DNA binding domains, interactions with transcriptional and epigenetic regulators allow SS18-SSX to elicit significant deregulation of gene expression (de Bruijn et al., 2006). The fusion protein has been proposed to interact in place of native SS18, leading to aberrant SWI/SNF-mediated gene transcription (Kadoch & Crabtree, 2013). We have shown that SS18-SSX acts as a bridge connecting activating

transcription factor 2 (ATF2) to transducin-like enhancer of split 1 (TLE1), proteins which otherwise do not associate (Su et al., 2012). ATF2 binds DNA at CRE/ATF sites, where under normal conditions it functions as a histone acetyltransferase (HAT) to increase gene transcription in response to cellular stress signals (Kawasaki et al., 2000). TLE1 has been observed to interact with polycomb-repressor complex 2 (PRC2) and histone deacetylases (HDAC), and has been shown to mediate formation of a complex in which PRC2/HDAC1 represses gene expression at SS18-SSX targeted loci (Laporte, Ji, Ma, Nielsen, & Brodin, 2016; Su et al., 2012). When this association is disrupted by specific knockdown of TLE1, ATF2 or SS18-SSX, synovial sarcoma cell lines undergo apoptosis, indicating this complex association is important for tumour cell survival (Su et al., 2012).

Observed targets for SS18-SSX-mediated repression include early-growth factor 1 (*EGR1*), a key positive regulator of tumour suppressor PTEN, and *CDKN2A*, important for normal cell cycle regulation (Lubieniecka et al., 2008; Su et al., 2010; Su et al., 2012). In addition, up-regulation of the PI3K/AKT/mTOR growth signaling pathway as well as increased expression of the pro-apoptotic protein BCL-2 (B-cell lymphoma-2) are hallmarks of synovial sarcoma biology, together eliciting a proliferative and apoptosis-resistant phenotype (Hirakawa et al., 1996; Su et al., 2010).

HDAC inhibitors have been shown to disrupt the SS18-SSX/TLE1/ATF2 protein complex (Laporte et al., 2016; Su et al., 2012), providing an explanation for the sensitivity of synovial sarcoma cells to HDAC inhibition (Ito et al., 2005). Though no drugs able to specifically target the SS18-SSX fusion oncoprotein are currently available, compounds able to disrupt its partnering interactions might be expected to reactivate normal gene transcription and elicit anti-tumour effects and clinical response. In this study, we undertook

a high-throughput drug screen of over 900 compounds representing 100 drug classes, in an effort to identify sensitizing agents and targetable pathways in synovial sarcoma that might expand treatment options. From this, the potency of HDAC inhibition in synovial sarcoma was reinforced, with specific effects on the oncoprotein and consequent gene reactivation demonstrated in a panel SS18-SSX-containing cell lines. In addition, an effective combination treatment with proteasome inhibitors was uncovered. The combination of HDAC and proteasome inhibition synergizes to activate pro-apoptotic factors and bring about cell death and suppresses tumour growth in a murine model of synovial sarcoma, presenting a strong candidate strategy for clinical benefit in synovial sarcoma.

3.2 Materials and methods

3.2.1 Cell culture and chemicals

The following human synovial sarcoma cell lines were kindly provided: SYO-1 (Kawai et al., 2004) (Dr. Akira Kawai, National Cancer Centre Hospital, Tokyo, Japan), FUJI (Nojima et al., 1990) (Dr. Kazuo Nagashima, Hokkaido University School of Medicine, Sapporo, Japan), YaFuss (Ishibe et al., 2005), and HS-SY-II (Sonobe et al., 1992) (Dr. Scott Lowe, Memorial Sloan Kettering Cancer Centre, New York, USA), SSR3A1 (murine), and MoJo (K. B. Jones et al., 2016) (Dr. K. Jones, University of Utah, Salt Lake City, UT), Yamato-SS (Naka et al., 2010), and ASKA-SS (Naka et al., 2010) (Dr. K. Itoh, Osaka Medical Center for Cancer and Cardiovascular Diseases, Japan). Sarcoma cell lines were maintained in RPMI-1640 medium supplemented with 10% fetal bovine serum (FBS) (Life Technologies, Waltham, MA, USA) and the presence of a disease-defining *SS18-SSX* fusion

oncogene was confirmed by PCR analysis. As additional human non-sarcoma controls, breast cancer cell line MCF7 (ATCC HTB22) and human embryonic kidney HEK293T (ATCC CRL3216) were purchased from the ATCC (Manassas, VA, USA) and cultured in DMEM medium with 10% FBS. Patient-derived primary synovial sarcoma (83-SS) and matched muscle cells (83-muscle) were obtained from a surgical specimen in accordance with ethics guidelines and approval from Regionala Etikprovningsnämden, Stockholm (No. 2013/1979-31/3). The cells were dissociated by enzymatic digestion using 0.01% collagenase (Sigma-Aldrich, St. Louis, MI, USA). The dispersed cells were grown in DMEM/F12 media containing 10% FBS. Muscle cells were grown in muscle-specific growth media (PromoCell, Heidelberg, Germany). The outgrowing synovial sarcoma primary cells were confirmed for *SS18-SSX* expression by PCR analysis. All cells were grown at 37°C, 95% humidity, and 5% CO_2. Pharmacologic compounds were purchased from Selleck Chemicals (Houston, TX, USA).

3.2.2 High-throughput drug screen assay

A 900 compound library composed of over 100 different classes of tool compounds and epigenetic modifiers from the Ontario Institute of Cancer Research (OICR, Toronto, ON, Canada) together with epigenetic modifiers (Cayman Biochemical, Ann Arbor, MI, USA, Item 11076) were screened on six synovial sarcoma cell lines and two unrelated control cell lines (MCF7 and HEK293T). Cells were seeded in 96-well plates at 1e4 cells/well. The following day, compounds from the drug library were transferred from stock plates (1 mM in DMSO) using a 96-pin tool with a diameter of 0.4-mm, to bring about a final concentration of ~1 μM per well. Plates were developed with MTS reagent 48 hours post treatment and

viability assessed relative to vehicle-only controls (0.1% DMSO). For each synovial sarcoma cell line, compounds bringing about a decrease in relative viability of greater than 90% were scored as 1 (+++), 75.1-90% as 0.5 (++), 50-75% as 0.25 (+), and less than 50% as 0 (-). The total score across the six cell lines was calculated as a sum to a maximum score of 6. Control cell lines MCF7 and HEK293T were screened concurrently to demonstrate potential drug specificity against synovial sarcoma. A viability heatmap was created using the Gene-E software program (Broad Institute, Cambridge, MA, USA). Top hits were validated in a dose-response curve and IC_{50} values were calculated.

3.2.3 Western blots

Protein was collected following 24-hour treatments with indicated compounds. Samples were separated by 10% SDS-PAGE and transferred to PVDF membranes (Bio-Rad Laboratories, Hercules, CA, USA). Blots were incubated with indicated antibodies; Santa-Cruz Biotechnology (Dallas, TX, USA): SS18 sc-28698 1:200, GAPDH sc-25778 1:1500, BIK (NBK) sc-305625 1:500, BIM sc-374358 1:500, BCL-2 sc-492 1:250, p-BCL-2 sc-101762 1:250, HDAC6 sc-11420 1:250, vinculin sc-5573 1:5000, α-tubulin sc-8035 1:200; Cell Signaling (Danvers, MA, USA): EGR1 4153S 1:1000, Ac-α-tubulin 5335 1:1000, HDAC1 5356 1:1000, LC3B 2775 1:1000, p-PERK 3179S 1:1000, ER stress antibody kit 9956 (PERK, IRE1α, BiP, CHOP) 1:1000; Abcam (Cambridge, MA, USA): p16INK4a ab108349 1:500, p14ARF ab124282 1:500. Signals were visualized using the Odyssey Infrared System (LI-COR Biosciences, Lincoln, NE, USA).

3.2.4 Proximity ligation assay

Cells were seeded in culture-treated chamber slides at 3e4 cells/well. The following day, wells were treated with indicated compounds for 12 hours. Cells were then washed twice with PBS, fixed with 4% formaldehyde and permeabilized with 0.1% Triton X-100. Wells were blocked with blocking buffer and incubated overnight at 4°C with primary antibodies at a 1:1000 dilution: SS18 (Santa-Cruz Biotechnology, Dallas, TX, USA, sc-28698), TLE1 (Origene Technologies, Rockville, MD, USA, TA800301). Proximity ligation was performed utilizing the Duolink® *In Situ* Red Starter Kit Mouse/Rabbit (Sigma-Aldrich, Oakville, ON, Canada) according to the manufacturer's protocol. The oligonucleotides and antibody-nucleic acid conjugates used were those provided in the Sigma-Aldrich PLA kit (DUO92101). Alexa Fluor 488 secondary antibody (Life Technologies, Waltham, MA, USA) was included during the final incubation of the PLA protocol. Fluorescence was detected using a Zeiss Axioplan 2 microscope at 40x. PLA images were quantified in triplicate using ImageJ software (NIH, Bethesda, MD, USA) as foci per nucleus, defined as the number of interaction points counted per nucleus.

3.2.5 Reverse transcriptase quantitative PCR

Total RNA was isolated from treated cells using the RNeasy Mini kit (Qiagen, Valencia, CA, USA) and was then reverse transcribed to cDNA using Oligo(dT) (Invitrogen, Waltham, MA, USA) and Superscript III (Invitrogen, Waltham, MA, USA). SYBR Green (Roche, Mississauga, ON, Canada) reagent was used for qPCR expression analysis, using an ABI ViiA7 qPCR system. The following primers for expression were used; *EGR1*: sense: AGCCCTACGAGCACCTG, antisense: GGTGGGTTGGTCATG; *CDKN2A*: sense:

CAACGCACCGAATAGTTACGG, antisense: AACTTCGTCCTCCAGAGTCGC. All transcript levels were normalized to *GAPDH* RNA expression as well as to DMSO treated conditions to calculate relative fold induction of expression using the comparative Ct (ΔΔCt) method.

3.2.6 Cell viability assays

Cells were seeded in 96-well plates at 1e4 cells/well and treated in triplicate at indicated doses of the tested compounds. IC_{50} doses were determined in synovial sarcoma cell lines by dose curve studies. Cell viability was assessed in the cell lines as compared with the vehicle condition (0.1% DMSO) at 48 hours post treatment using MTS reagent (Promega, Madison, WI, USA). The primary cells were seeded in 384-well plates at 1e3 cells/well, and viability was assessed by quantifying ATP levels using the CellTitre-Glo luminescence-based assay (Promega, Madison, WI, USA), as compared with the vehicle condition (0.1% DMSO) at 48 hours post treatment. Cell confluency and apoptosis induction was assessed over a 48-hour timeframe utilizing the IncuCyte Zoom® live cell imaging software (Essen BioScience, Ann Arbor, MI, USA). Apoptosis was assessed by IncuCyte™ Kinetic Caspase-3/7 Apoptosis Assay Reagent (Essen BioScience, Ann Arbor, MI, USA, 4440).

3.2.7 Flow cytometry

Apoptosis was assessed by Annexin V/propidium iodide (PI) flow cytometry assay following an incubation of 16 hours with indicated drugs. Cells were then trypsinized and collected, washed with PBS and resuspended in binding buffer. Cells were stained with Annexin-V-FITC and propidium iodide (BD Biosciences, San Jose, CA, USA, 556547) and

flow cytometry was undertaken on a BD FACSCanto II flow cytometer (BD Biosciences, San Jose, CA, USA).

The PROTEOSTAT® aggresome detection kit (Enzo Lifesciences, Farmingdale, NY, USA, ENZ-51035-0025) was used to detect aggresome formation following drug treatment at 4 and 18 hours. Following indicated treatment, cells were trypsinized, washed twice with PBS, fixed with 4% formaldehyde and permeabilized with 0.1% Triton X-100. Cells were then stained with the PROTEOSTAT® Aggresome Red Detection Reagent and analyzed by flow cytometry on the FL3 channel of the FACSCanto II.

3.2.8 Dichlorofluorescein diacetate assay (DCFDA)

ROS levels were assessed by DCFDA assay (Abcam, Cambridge, MA, USA, ab113851). Cells were seeded in a 96-well plate at 1e4 cells/well. The following day cells were treated with indicated compounds in indicator-free media. At 24 hours post treatment, wells were over-layed with 2x diluted DCFDA reagent, as suggested by the manufacturer's protocol. Fluorescence was read by microplate reader at Ex/Em = 485/535 nm. A ratio of untreated to treated wells was calculated to determine relative response. Wells were normalized to media only wells to account for background signal.

3.2.9 Mice

Pten$^{fl/fl}$*;hSS2* mice (as previously described (Haldar et al., 2007)) received a 10 µL injection of 42 µM TATCre in the hindlimb at 4 weeks of age, to induce expression of SS18-SSX2. A cohort of 7 mice with tumour volumes ranging from 600-1500 mm^3 were randomly assigned treatment of quisinostat (750 µg/kg) + bortezomib (60 µg/kg) (n=4) or vehicle

control (10% hydroxyl-propyl-β-cyclodextrin/25 mg/mL mannitol/H_2O) (n=3). Mice received daily intraperitoneal injections and tumour volumes were measured three times weekly for 21 days. Tumour volumes (mm^3) were measured using digital calipers and calculated with the formula ($length \times width^2)/2$ (Faustino-Rocha et al., 2013). Tumour volumes at the end of treatment ranged from 900 to 2800 mm^3.

Mice were monitored daily and tumours monitored at least three times weekly during treatment. No toxicity was observed in the treatment regimens of these mice. Mice demonstrating poor mobility, poor feeding/watering behaviors or poor interactions with cage mates, suggestive of ill-health or discomfort, were humanely euthanized. Any tumour burden greater than 10% body mass, that impeded mobility, feeding, or watering or that caused apparent discomfort, or any ulcerated mass or weight loss of more than 20% was also managed by humane euthanasia. Mice were euthanized by exposure to compressed CO^2 followed by a bilateral thoracotomy. No analgesics or anesthetics were administered during this study. To minimize suffering and distress cages were cleaned regularly, fresh food and water were provided, and mice were housed with siblings for social interaction. Attention was given to routine animal husbandry, and close and frequent observations of mice with tumours or undergoing treatment. This study was carried out in strict accordance with the recommendations in the Guide for the Care and Use of Laboratory Animals of the National Institutes of Health. The protocol was approved by the Institutional Animal Care and Use Committee of the University of Utah (Permit Number: 14-01016).

3.3 Results

3.3.1 High-throughput drug screen revealed HDAC inhibitors and proteasome inhibitors as potent cytotoxic agents in a panel of synovial sarcoma cell lines

In order to identify drugs effectively targeting synovial sarcoma, a 900 compound high-throughput drug screen representing over 100 drug classes at a concentration of ~1 μM was undertaken in six synovial sarcoma cell lines: SYO-1 (SS18-SSX2), FUJI (SS18-SSX2), Yamato-SS (SS18-SSX1), ASKA-SS (SS18-SSX1), MoJo (SS18-SSX1) and SSR3A1 (murine, SS18-SSX2), as well as negative control cell lines HEK293T (human embryonic kidney) and MCF7 (breast carcinoma). Compounds were scored based on impact on cell viability in and specificity for synovial sarcoma (complete screen data set available: PMC5215898).

There were 84 scored hits out of the 900 library compounds. Of the top 40 scored compounds, 15 (37.5%) of the most potent drugs were HDAC inhibitors (Figure 3.1A, 3.1B). Both of the proteasome inhibitors in the drug library scored in the top ten (Figure 3.1C). Also of note, PI3K inhibitors comprised five (12.5%) of the top hits. The most potent drugs were further validated in dose-response studies, and IC_{50} values in all cell lines were calculated (Figure 3.1D). The novel second generation pan-HDAC inhibitor quisinostat (JNJ-26481585) was the most potent and specific of the studied HDAC inhibiting compounds in synovial sarcoma cell lines. Proteasome inhibitors bortezomib and carfilzomib were similarly potent in decreasing cell viability in synovial sarcoma. Drug classes that have little effect on synovial sarcoma at the studied doses included modulators of the Wnt pathway and MDM2 inhibitors (Figure 3.1A).

3.3.2 HDAC inhibition by quisinostat derepressed tumour suppressor gene targets of SS18-SSX in synovial sarcoma

To demonstrate the effects of HDAC inhibition on gene expression in synovial sarcoma, RNA and protein analyses were undertaken following treatment with quisinostat in six SS18-SSX-containing cell lines. In accordance with previous reports (Laporte et al., 2016), the key association of SS18-SSX with TLE1 was lost following treatment with quisinostat, with or without the addition of proteasome inhibitor bortezomib (Figure 3.2A, 3.2B). To assess whether there are any super-additive effects in this model, an interaction term between quisinostat and bortezomib was added in a linear regression model (foci per nuclei as the dependent variable, and quisinostat/bortezomib treatment as independent variables). The disruption of the SS18-SSX/TLE1 proximity interaction was additive but not significantly synergistic in the combination treatment arm, as demonstrated by the synergy interaction statistical analysis ($p=0.66$). RNA expression at gene targets previously shown to be directly repressed by SS18-SSX activity (Su et al., 2012) was reactivated by quisinostat treatment in six synovial sarcoma cell lines (Figure 3.2C). Following quisinostat treatment, tumour suppressors EGR1 and p16INK4a/ p14ARF (*CDKN2A)* were reactivated at the protein level, whereas SS18-SSX oncoprotein levels were reduced (Figure 3.2D).

3.3.3 HDAC inhibition synergized with proteasome inhibition to decrease synovial sarcoma cell viability

To investigate the potential of drug combinations building on an HDAC inhibitor backbone, we tested quisinostat in combination with proteasome inhibitors, the next most potent drug class revealed from the drug screen. Synovial sarcoma cells were assayed for

relative cell viability, in comparison with the vehicle control (0.1% DMSO) by way of a dose curve of quisinostat, with and without the addition of 0.005 μM of bortezomib. With bortezomib, a significant increase in normalized response was observed: in the presence of low-dose proteasome inhibition, quisinostat dosage could be reduced by an order of magnitude yet achieve the same effect (Figure 3.3A). This combinatorial benefit was not observed in control cell line HEK293T at the studied doses. Similar studies were also undertaken with HDAC and PI3K inhibitor combinations, but with this combination no synergy was observed in the synovial sarcoma cell lines at the studied doses.

Synergy was assessed by isobologram analysis (Figure 3.3B), in which the combination isoboles at a constant ratio and at six increasing concentrations fall below the additive isobole, indicating synergism of the effects of the two compounds. Combination index (CI) values were calculated using the Chou-Talalay methodology and found to be less than 1, demonstrating synergy of the combination in all six tested synovial sarcoma cell lines (Figure 3.3C). The combination of bortezomib and quisinostat brought about significantly stronger anti-proliferative effects than either drug alone, at low nanomolar doses across the panel of SS18-SSX-containing cell lines. This synergistic effect was consistently observed with additional compounds of each drug class, including the pan-HDAC inhibitor panobinostat, and proteasome inhibitors carfilzomib and ixazomib (Figure 3.4A, 3.4B). CI values with combinations of these agents were consistently found to be less than 1 in synovial sarcoma cell lines.

3.3.4 HDAC inhibition disrupts aggresome formation in response to proteasome inhibition

To investigate potential mechanisms of synergy, the effect of HDAC inhibition on aggresome formation was assessed. Proteasome inhibition is known to bring about aggresome formation as a response to accumulating misfolded proteins, a mechanism facilitated by HDAC6 activity (Johnston, Ward, & Kopito, 1998; Kawaguchi et al., 2003). Silencing of HDAC6 by siRNA brought about a decrease in LC3B protein levels, a marker of aggresome formation (Figure 3.5A). When treated with quisinostat, LC3B protein levels were similarly decreased, whereas the pure class I HDAC inhibitor romidepsin (which does not inhibit HDAC6) enhanced LC3B expression (Figure 3.5B). When treated with proteasome inhibitors bortezomib, carfilzomib, or a combination of proteasome inhibition and romidepsin, LC3B levels were increased. When used in combination with proteasome inhibition, treatment with quisinostat remained able to elicit a decrease in LC3B levels, suggesting that inhibition of aggresome formation was attributable to its impact on HDAC 6 activity (Figure 3.5B).

By flow cytometry, aggresome formation was demonstrated to be induced by proteasome inhibition (Figure 3.5C). HDAC inhibition by quisinostat was consistently found to inhibit the aggresome response. Aggresome propensity factors (APF) were calculated using the Enzo Life Sciences Aggresome detection assay, wherein an APF of greater than 25 is indicative of aggresome formation in response to proteasome inhibition. With the addition of quisinostat, the APF was significantly decreased when compared with bortezomib alone in SYO-1 synovial sarcoma cells at 4 and 18 hours post treatment (Figure 3.5C).

3.3.5 HDAC and proteasome inhibitor combination treatment led to ER stress and increased ROS levels

In order to further examine the role of the HDAC/proteasome inhibitor drug combination in augmenting stress in synovial sarcoma, the unfolded protein response was investigated. Bortezomib has been shown previously to bring about endoplasmic reticulum (ER) stress in cells due to misfolded protein accumulation leading to high levels of reactive oxygen species (ROS) (Bush, Goldberg, & Nigam, 1997; Santos, Tanaka, Wosniak, & Laurindo, 2009). The combination of quisinostat and bortezomib elicited high expression of ER stress markers in synovial sarcoma cell lines, as demonstrated by the activation of: phosphorylated-PERK (slows translation (Kaufman et al., 2002)), IRE1α (unfolded protein response element involved in ER chaperone up-regulation and stress recovery (Lee et al., 2002)), BiP (molecular chaperone (Kohno, Normington, Sambrook, Gething, & Mori, 1993)), phosphorylated-JNK (c-Jun N-terminal kinases, activated in response to cellular stress (Leppa & Bohmann, 1999)) and CHOP (DDIT3, pro-apoptotic protein (Zinszner et al., 1998)) (Figure 3.5D). ROS accumulation was also significantly increased in response to the combination of HDAC and proteasome inhibition (Figure 3.5E). ROS levels could be experimentally abrogated by the addition of antioxidant N-acetylcysteine (N-AC) during drug treatment. Addition of N-AC rescued SYO-1 cells from HDAC inhibitor/proteasome inhibitor-mediated cell death by approximately 50% (Figure 3.5F).

3.3.6 The combination of HDAC and proteasome inhibition led to apoptosis in synovial sarcoma cells and inhibition of tumour growth in a synovial sarcoma conditional mouse model

Pro-apoptotic proteins BIM and BIK were up-regulated by both quisinostat and bortezomib treatments, and combination treatment elicited phosphorylation of anti-apoptotic protein BCL-2 (Figure 3.7A). Cleaved caspase 3/7 induction was significantly increased over time in synovial sarcoma cell lines SYO-1 and MoJo following low dose treatment of the quisinostat/bortezomib combination, while only doxorubicin had a significant effect on the HEK293T cells as measured by IncuCyte™ Kinetic Caspase-3/7 Apoptosis Assay Reagent (Figure 3.7B). A significant increase in Annexin-V staining was observed when the drugs were used in combination, to an extent greater than that of either drug alone (Figure 3.7C). Cell viability was also significantly decreased by the low-dose quisinostat/bortezomib combination in primary patient synovial sarcoma cells (83-SS) as compared with their matched normal muscle cells (83-muscle) (Figure 3.7D).

To demonstrate the efficacy of the drug combination *in vivo*, quisinostat and bortezomib were tested for their effect on tumours in a murine model of synovial sarcoma harboring the SS18-SSX2 translocation. Doses used were similar or less than that of previous animal studies of this drug combination in multiple myeloma, in which single drug arms showed little to no efficacy, while the combination decreased tumour burden (Deleu et al., 2009). Due to the large number of drug dose combinations and replicates required, synergy is more practically assessed in cell line experiments. The mouse model of synovial sarcoma was used in this study to confirm the activity of the best drug combination. Tumour growth

was significantly reduced by treatment with the combination of quisinostat and bortezomib, as compared with vehicle treated mice over a period of 21 days (Figure 3.7E).

3.4 Discussion

Current cytotoxic therapies offer limited benefit in synovial sarcoma; improved, more targeted therapeutics are needed. As the sole driving cytogenic event, t(X;18) generates the SS18-SSX protein complex that leads to the distinct phenotype of this cancer and provides an attractive target for drug intervention. In this study, we show that HDAC inhibition by quisinostat is able to dissociate the driving complex in synovial sarcoma, resulting in reactivated expression of tumour suppressors otherwise repressed by SS18-SSX. Furthermore, we demonstrate that apoptosis is enhanced following HDAC inhibition when used in combination with a proteasome inhibitor. This combination triggers ER stress, phosphorylation of the overexpressed anti-apoptotic protein BCL-2, and activation of pro-apoptotic proteins BIM and BIK. Together these drug classes synergize at low nanomolar doses to induce synovial sarcoma cell death.

We have previously shown that SS18-SSX interacts with its partners at promoters recognized by ATF2, repressing transcription at critical tumour suppressor loci including *EGR1* and *CDKN2A* (Su et al., 2012). HDAC inhibitors dissociate the driving complex and reactivate *EGR1* and p16INK4a/p14ARF *(CDKN2A)* expression in synovial sarcoma; we confirm this occurs with treatment by quisinostat, a newer HDAC inhibitor that was the top hit in our compound screen. EGR1 is an important regulator of several tumour suppressors including PTEN (Virolle et al., 2001) and p53 (Nair et al., 1997), and reports have shown

EGR1 directly transactivates expression of BIM (B. Xie et al., 2011) and mediates c-MYC-induced apoptosis in cooperation with p14ARF (Boone, Qi, Li, & Hann, 2011). In addition, regulation by p16INK4a and p14ARF is important for cell cycle arrest via inhibition of CDK4/6 (Quelle, Zindy, Ashmun, & Sherr, 1995), as well as for apoptosis induction via up-regulation of BIK (Kovi, Paliwal, Pande, & Grossman, 2010) and p53-dependent signaling (Pomerantz et al., 1998). HDAC inhibition may therefore impede SS18-SSX-mediated deregulation at these loci, allowing for reactivation of normal cell cycle regulation and apoptotic pathways.

Proteasome inhibition has been shown to induce ER stress due to misfolded protein accumulation; aggresome formation functions as a cytoprotective mechanism in this system by packaging misfolded protein aggregates for lysosomal degradation (Johnston et al., 1998; Nawrocki et al., 2006). With the addition of HDAC6 inhibition by quisinostat, shuttling of misfolded proteins to aggresomes is blocked, circumventing this resistance mechanism (Kawaguchi et al., 2003). Excessive ER stress resulting from misfolded protein accumulation leads to elevated ROS levels and initiation of apoptosis (Fribley, Zeng, & Wang, 2004).

Proteasome inhibition has also been established as a specific vulnerability of Ewing sarcoma (*EWS-FLI1*) (Shukla et al., 2016), suggesting a particular susceptibility of this related translocation-associated sarcoma to proteasome inhibitor drug intervention, and SMARCB1 deleted-cells have been shown to be specifically sensitive to proteasome inhibitors when compared to their SMARCB1-intact counterparts (Genovese et al., 2017). Additional reports have characterized BIM and BIK activation as key components of proteasome inhibitor induced apoptosis, as they are found to be significantly up-regulated and stabilized following bortezomib treatment (C. Li, Li, Grandis, & Johnson, 2008; Zhu et

al., 2005). Phosphorylation of BCL-2, deactivating this important anti-apoptotic regulator (Deng et al., 2001; Yamamoto, Ichijo, & Korsmeyer, 1999), is also found to occur following the quisinostat/proteasome inhibitor combination treatment, resulting in a pro-apoptotic shift not seen with doxorubicin treatment in synovial sarcoma (Mancuso et al., 2000).

HDAC inhibitor-treated tumour cells have further been shown to be deregulated in protein folding, making them highly susceptible to proteasome inhibitors (Dupere-Richer et al., 2017). Recent studies have demonstrated a compensatory role for proteasome activity in response to HDAC inhibition. A genome-wide screen revealed RAD23B, a protein that shuttles ubiquitinated proteins to the proteasome, is a biomarker for sensitivity to HDAC inhibition in cutaneous T-cell lymphoma (Fotheringham et al., 2009; Khan et al., 2010), and this relationship has been further demonstrated to also apply in sarcomas (IHle et al., 2016). These studies suggest RAD23B is regulated by HDAC activity, and upon HDAC inhibition the shuttling function is over-activated and may sensitize cells to proteasome inhibition, providing further support for a combinatorial treatment strategy combining these drug classes.

The combination of quisinostat and bortezomib has been evaluated in a phase-Ib clinical trial in multiple myeloma, from which an acceptable safety profile was observed, and partial response or better was achieved in 15 out of 17 patients (Moreau et al., 2016). The combination of the pan-HDAC inhibitor vorinostat with bortezomib has also been shown to be active in refractory multiple myeloma, offering a third-line treatment modality in difficult and relapsed cases (Siegel et al., 2016). Our study shows that in synovial sarcoma models, the combination of HDAC and proteasome inhibition functionally dissociates the oncogenic driving complex, reactivates tumour suppressor gene expression, and elicits ER stress, ROS

accumulation, and pro-apoptotic factor induction, resulting in significant cell death even at very low drug concentrations. The present study demonstrates the potential value of the combining HDAC and proteasome inhibitors as a treatment for synovial sarcoma (Appendix II).

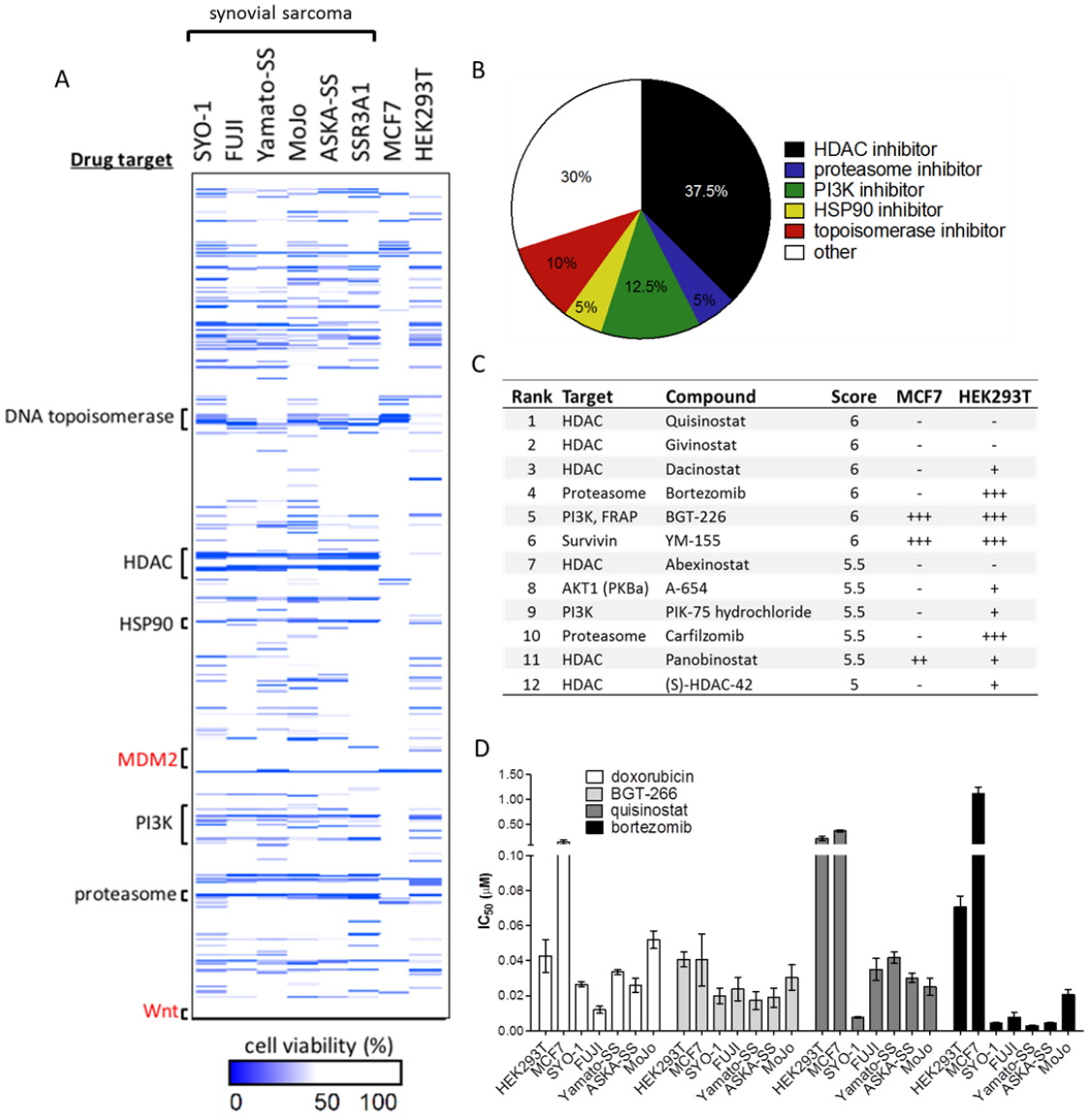

Rank	Target	Compound	Score	MCF7	HEK293T
1	HDAC	Quisinostat	6	-	-
2	HDAC	Givinostat	6	-	-
3	HDAC	Dacinostat	6	-	+
4	Proteasome	Bortezomib	6	-	+++
5	PI3K, FRAP	BGT-226	6	+++	+++
6	Survivin	YM-155	6	+++	+++
7	HDAC	Abexinostat	5.5	-	-
8	AKT1 (PKBa)	A-654	5.5	-	+
9	PI3K	PIK-75 hydrochloride	5.5	-	+
10	Proteasome	Carfilzomib	5.5	-	+++
11	HDAC	Panobinostat	5.5	++	+
12	HDAC	(S)-HDAC-42	5	-	+

Figure 3.1: High-throughput drug screen revealed HDAC and proteasome inhibitors as potent drug classes against synovial sarcoma. (A) Compounds resulting in measured relative cell viability of less than 50% are annotated as hits (blue). Y-axis denotes drug target classes arranged in alphabetical order. (B) The top 40 drug screen hits out of the 900 compound screen represented by drug target class, demonstrated HDAC inhibitors as the most abundant hits in the screen. (C) Compounds that brought about greater than 90% decreased relative cell viability were scored as 1 (+++), 75.1-90% as 0.5 (++), 50-75% as 0.25 (+) and less than 50% as 0 (-). Total score across the six cell lines was calculated out of 6. (D) IC_{50} measurements were calculated for drug screen hits quisinostat (HDAC inhibitor), BGT-226 (PI3K/mTOR inhibitor), bortezomib (proteasome inhibitor) as compared with the current standard for synovial sarcoma treatment doxorubicin (cytotoxic DNA/RNA intercalating agent and topoisomerase inhibitor), in a panel of six human SS18-SSX positive cell lines and two control cell lines (HEK293T, MCF7). Error bars signify standard error of mean from conditions performed in triplicate. Figure reprinted with permission from Laporte *et al.*, 2017 PLoS ONE.

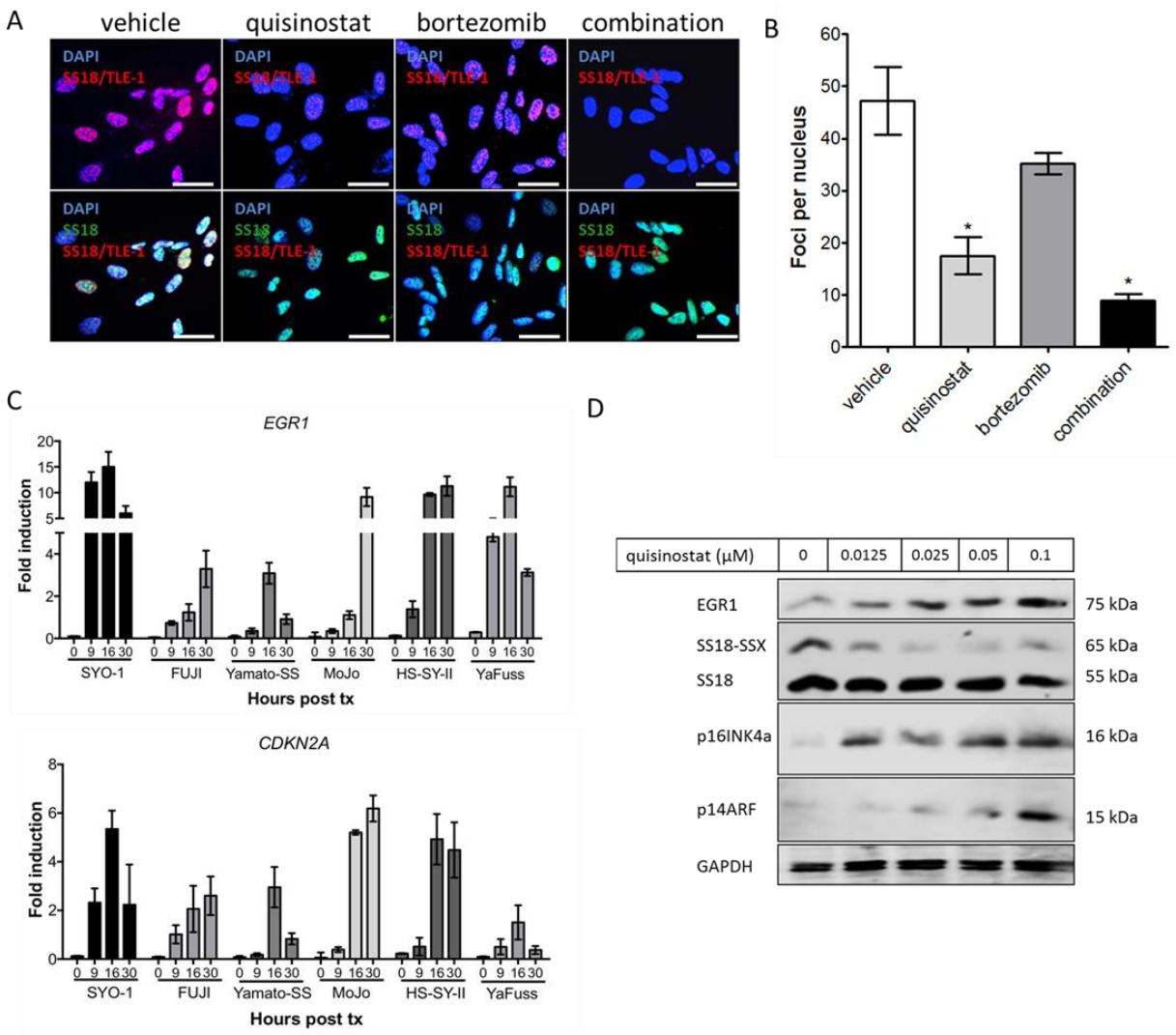

Figure 3.2: Quisinostat-mediated HDAC inhibition resulted in a dissociation of the driving complex in synovial sarcoma. (A, B) Proximity ligation assay of SS18-SSX/TLE1 nuclear signal demonstrated a significant decrease in detectable protein co-localization following HDAC inhibition in SYO-1 synovial sarcoma cells. (C) Quisinostat treatment at 0.025 μM reactivated targets of SS18-SSX-mediated gene repression, *EGR1* and *CDKN2A*, in six human synovial sarcoma cell lines. (D) Expression of EGR1, p16INKa and p14ARF (*CDKN2A*) protein levels increased with increasing concentrations of quisinostat, concomitant with a decrease in SS18-SSX protein levels. GAPDH was used as a loading control. Scale bars in panel A represent 20 μm. Statistical significance compared to vehicle treatment controls was determined by Student t test: * denotes $p < 0.05$. Error bars represent standard error of mean from conditions performed in triplicate. Figure reprinted with permission from Laporte *et al.*, 2017 PLoS ONE.

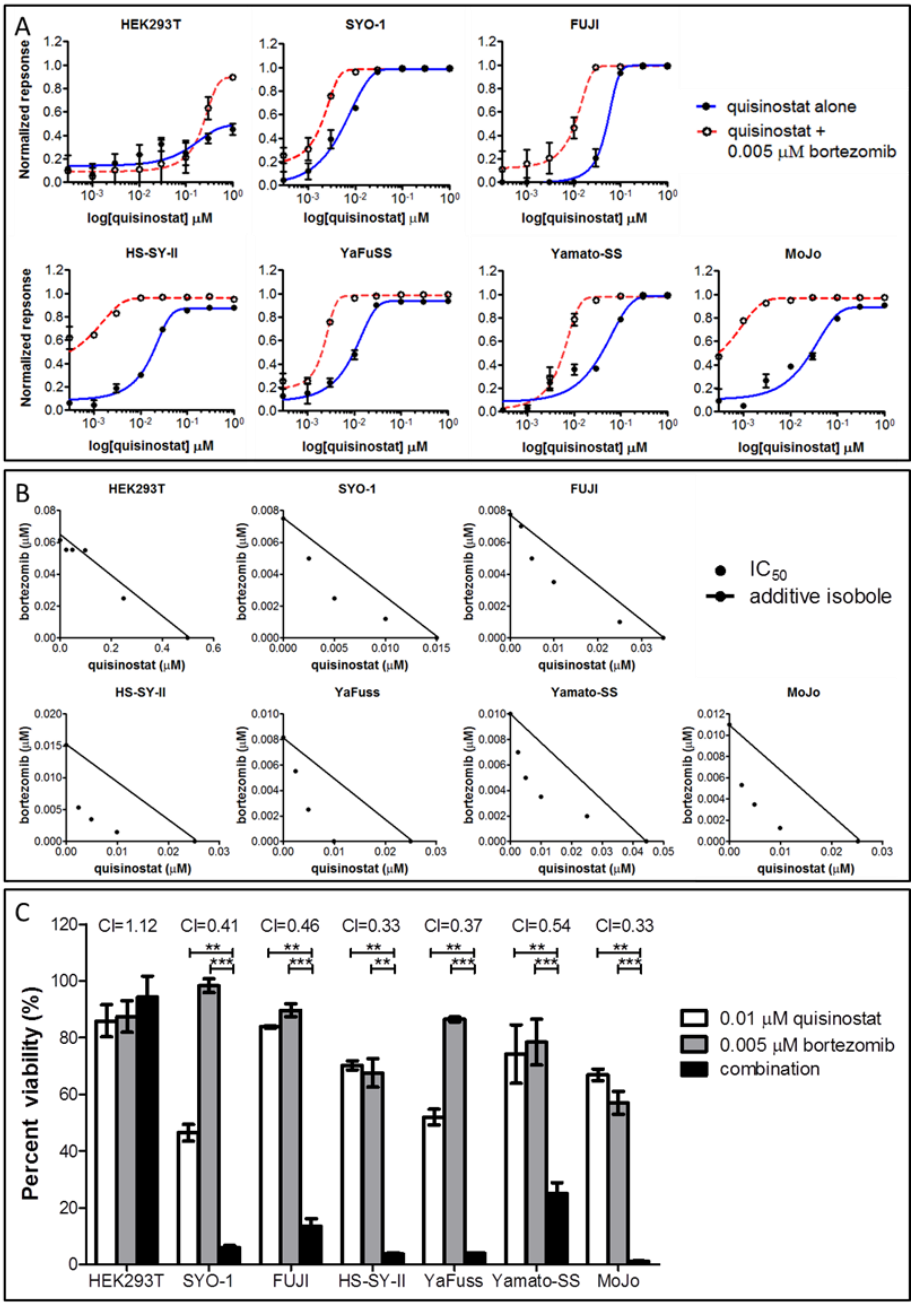

Figure 3.3: **HDAC inhibition by quisinostat synergizes with proteasome inhibition to decrease synovial sarcoma cell viability.** (A) In all synovial sarcoma cell lines, but not HEK293T controls, the addition of 0.005 μM of bortezomib resulted in a downshift of approximately a full log of quisinostat, decreasing the amount of drug required to achieve the same effect as the HDAC inhibitor alone. (B) Isobologram analysis demonstrated synergy of these drug classes in synovial sarcoma cell lines (but not HEK293T controls), as increasing concentration combinations fell below the additive isoboles. (C) Combination index (CI) values calculated for the combination of bortezomib and quisinostat in synovial sarcoma were significantly less than 1, indicating synergy of the compounds is occurring in all six synovial sarcoma cell lines (but not HEK293T controls). Isobolograms and CI values were calculated using the Chou-Talalay-designed program CompuSyn. Statistical significance compared to vehicle treatment controls was determined by Student t test: * denotes $p < 0.05$; ** denotes $p < 0.01$; *** denotes $p < 0.001$. Error bars represent standard error of mean from conditions performed in triplicate. Figure reprinted with permission from Laporte *et al.*, 2017 PLoS ONE.

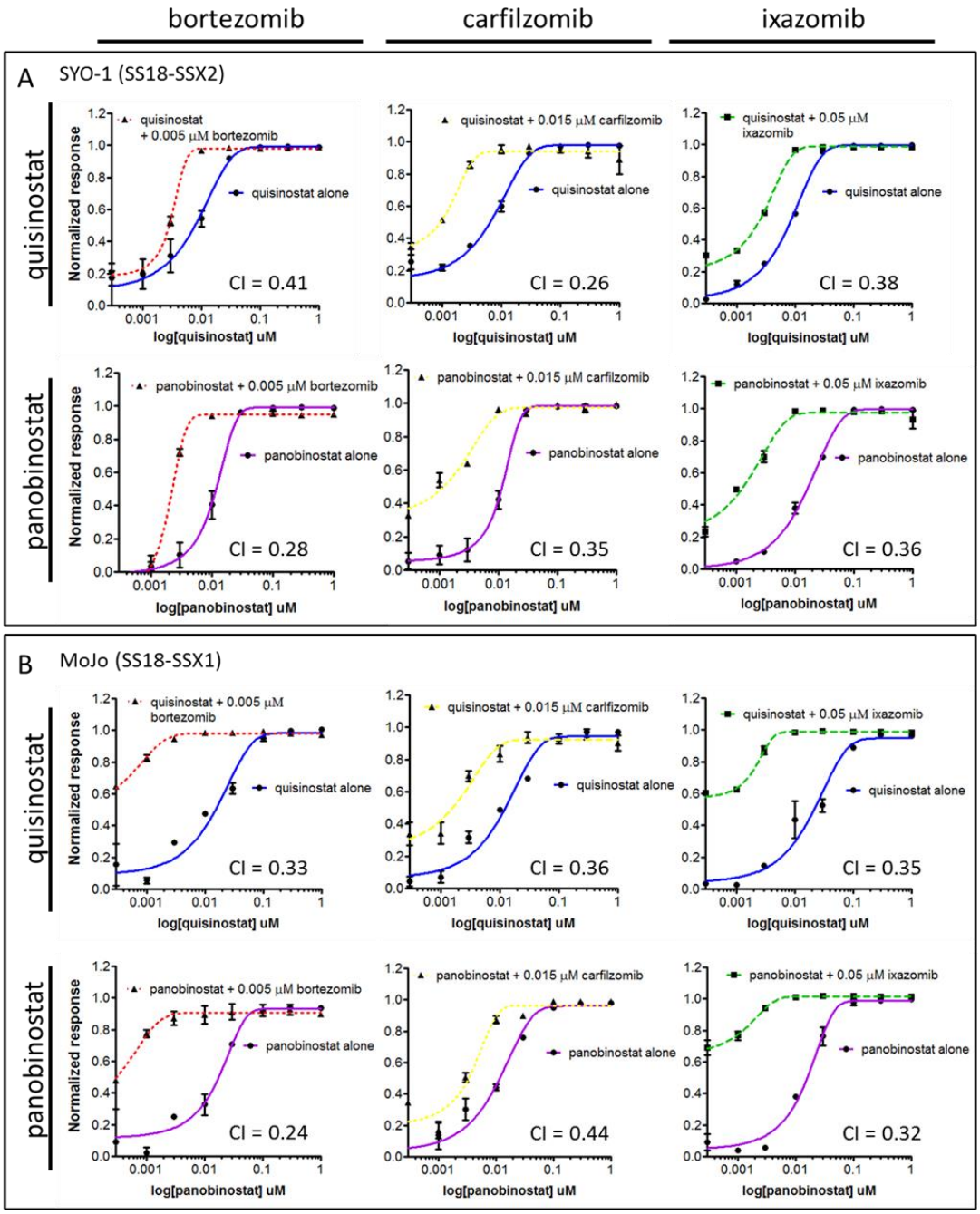

Figure 3.4: The synergistic effect of HDAC and proteasome inhibition was consistent within each drug class. Additional compounds of each drug class were tested in combinational synergy studies. Quisinostat, panobinostat (pan-HDAC inhibitors), and bortezomib, carfilzomib and ixazomib (proteasome inhibitors) were studied in all combinations in the SYO-1 (A) and MoJo (B) SS18-SSX containing cell lines. CI values were less than 1 in these synovial sarcoma cell lines. CI values were calculated using the Chou-Talalay-designed program CompuSyn. Error bars represent standard error of mean from conditions performed in triplicate. Figure reprinted with permission from Laporte *et al.*, 2017 PLoS ONE.

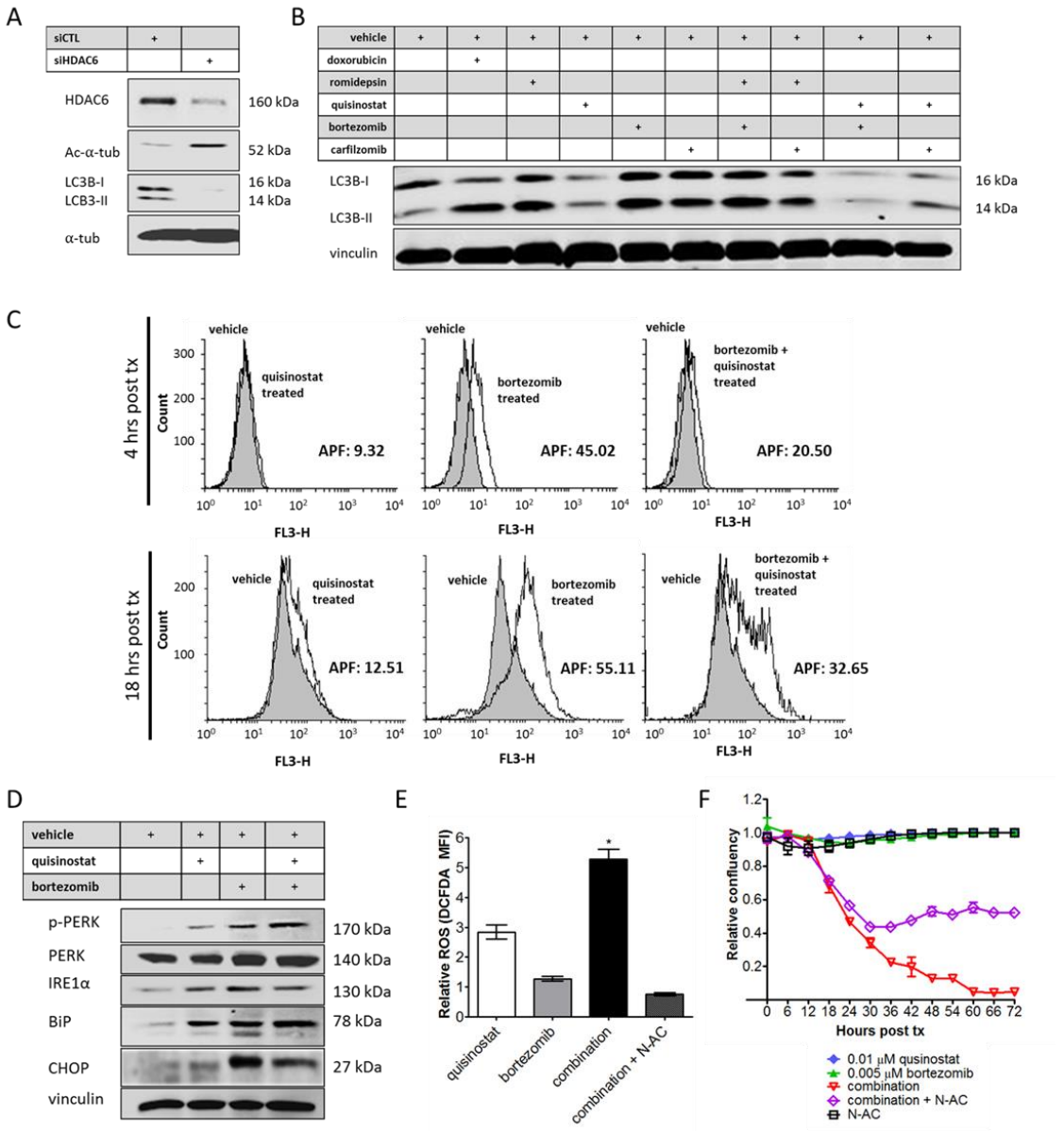

Figure 3.5: HDAC inhibition prevented aggresome formation in response to proteasome inhibitors, and combination treatment led to endoplasmic reticulum stress. (A) Knockdown of HDAC6 resulted in decreased levels of LC3B in the SYO-1 synovial sarcoma cell line. (B) Proteasome inhibition as well as treatment with class I HDAC inhibitor romidepsin increased in LC3B levels, whereas quisinostat treatment decreased protein levels following treatment with proteasome inhibitors bortezomib or carfilzomib. (C) Aggresome formation was induced by bortezomib at 4-hours post treatment by PROTEOSTAT® staining analyzed by flow cytometry, an effect that was abrogated by quisinostat. The aggresome propensity factor (APF) was significantly decreased with the addition of quisinostat in the context of proteasome inhibition. (D) Endoplasmic reticulum stress markers were expressed following combination treatment and (E) a significant increase in ROS accumulation was measured by mean fluorescence intensity (MFI) of DCFDA, as compared with vehicle treated cells. ROS accumulation was abrogated by N-acetylcysteine (N-AC) treatment at 10 mM. (F) Cell death was rescued with N-AC by ~50%. Statistical significance compared to vehicle treatment controls was determined by Student t test: * denotes $p < 0.05$. Error bars represent standard error of mean from conditions performed in triplicate. Vinculin or α-tubulin was used as a loading control for protein analysis. Figure reprinted with permission from Laporte *et al.*, 2017 PLoS ONE.

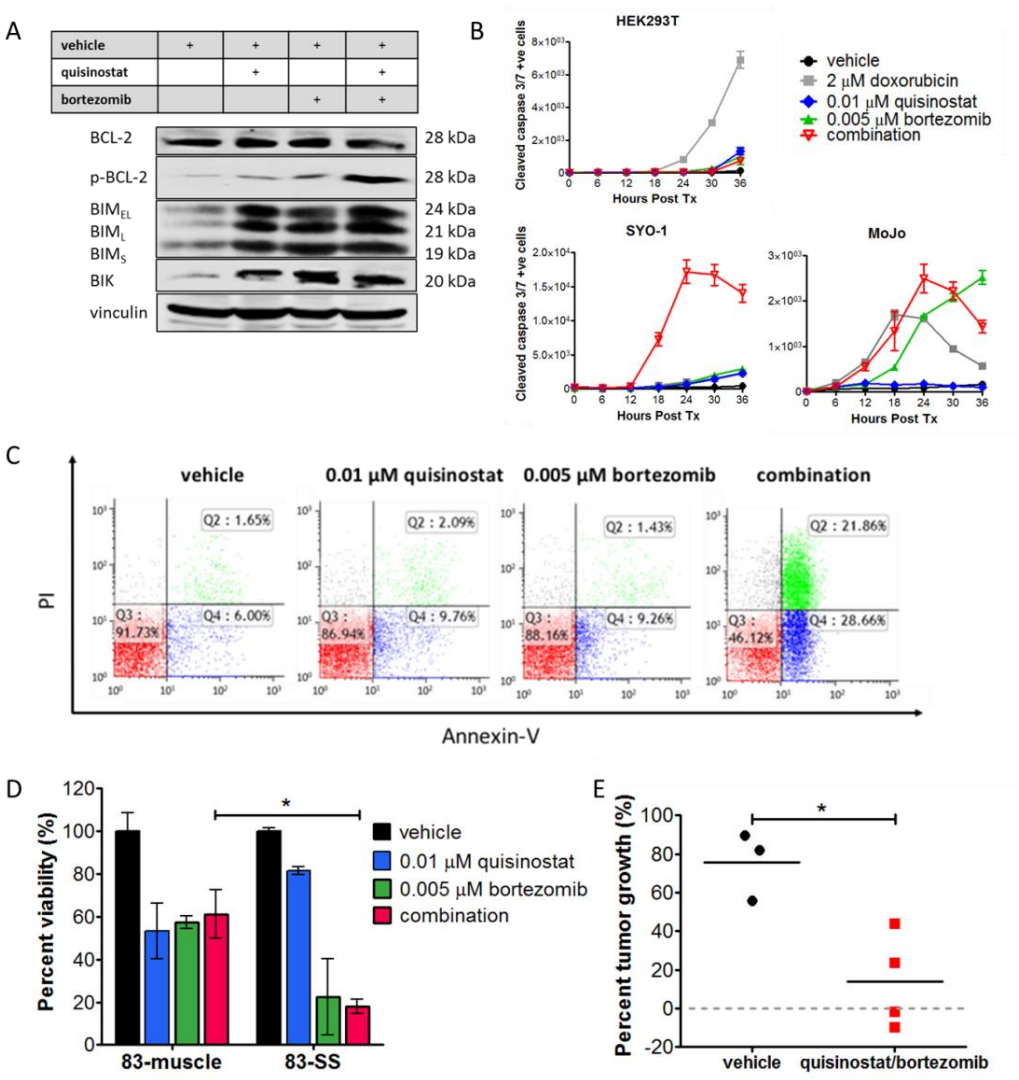

Figure 3.6: HDAC and proteasome inhibition led to apoptosis via pro-apoptosis protein activation, ROS production and caspase activation. (A) Pro-apoptotic proteins BIM and BIK were up-regulated by both quisinostat and bortezomib, and the drug combination elicited phosphorylation of anti-apoptotic protein BCL-2 in SYO-1 cells. (B) Cleavage of caspase 3 occurred following treatment with the drug combination in synovial sarcoma cell lines, demonstrated by staining with IncuCyte™ Kinetic Caspase-3/7 Apoptosis Assay Reagent, (C) inducing significant apoptosis as confirmed by Annexin-V/PI staining in the SYO-1 cell line (Q3: live, Q2: necrotic/late apoptotic, Q4: early apoptotic). (D) The low-dose quisinostat/bortezomib drug combination brought about a significant decrease in the viability of primary synovial sarcoma cells (83-SS) as compared to matched normal muscle cells derived from the same patient (83-muscle). Two-way ANOVA indicated a significant interaction between cell type and response to the drug combination ($p < 0.05$). (E) Tumour growth in a murine model of synovial sarcoma was significantly reduced by day 21 with the quisinostat/bortezomib combination treatment, as compared to the vehicle only control. Statistical significance compared to vehicle treatment controls was determined by Student t test or two-way ANOVA where indicated: * denotes $p < 0.05$. Error bars represent standard error of mean from conditions performed in triplicate. Vinculin was used as a loading control for protein analysis. Figure reprinted with permission from Laporte *et al.*, 2017 PLoS ONE.

CHAPTER 4: CELL DEATH BY HDAC INHIBITION IN SYNOVIAL SARCOMA

4.1 Introduction

Synovial sarcoma is an aggressive, translocation-associated soft tissue cancer that primarily affects adolescents and young adults (Okcu et al., 2001). It is characterized by the driving chimeric oncoprotein SS18-SSX, derived from the t(X;18)(p11.2;q11.2) translocation (Sandberg & Bridge, 2002). The SS18-SSX fusion protein has been proposed to interact in place of native SS18, leading to aberrant SWI/SNF-mediated transcription (Kadoch & Crabtree, 2013), and the abnormal assembly of polycomb group members (PcG) and transcription factors that leads to transcriptional repression by EZH2-mediated H3K27me3 (Su et al., 2012). Expression of tumour suppressor genes *EGR1* and *CDKN2A* have been shown to be directly repressed by SS18-SSX, while the anti-apoptotic protein BCL2 is characteristically up-regulated (Hirakawa et al., 1996) leading to a proliferative and anti-apoptotic phenotype.

Current cytotoxic therapies, including doxorubicin and ifosphamide, provide limited benefit for synovial sarcoma patients. Following surgery and radiation, patients remain at high risk for both early and late metastases, and despite best available therapies the mortality rate remains approximately 50% within 10 years of diagnosis (Krieg et al., 2010). Thus, there is a significant need for targeted therapies against synovial sarcoma.

Histone deacetylase (HDAC) inhibition has been shown to elicit apoptosis in synovial sarcoma models, as well as disrupt SS18-SSX-mediated repressive complexes (Laporte et al., 2016; Su et al., 2012). This inhibition was observed to elicit reactivation of repressed gene targets, including *CDKN2A* (Laporte et al., 2016; Su et al., 2010; Su et al., 2012). As a result,

a phase II study of pan-HDAC inhibitor pracinostat in translocation-associated sarcomas was initiated, and progression-free survival was observed in three of three SS18-SSX-positive patients over 12 months (Chu et al., 2015). This study had to be terminated prematurely due to unexpected interruptions in the supply of the studied compound; however initial results did warrant further investigation.

Histone acetylation status is an important element in the regulation of gene expression. HDAC inhibition has been shown to induce cell cycle arrest (Y. B. Kim, Ki, Yoshida, & Horinouchi, 2000), senescence (X. N. Li et al., 2005), differentiation (Marks, Richon, & Rifkind, 2000), and/or apoptosis (Bolden, Peart, & Johnstone, 2006) among cancer cell subtypes, generally leading to a decrease in tumour burden (West & Johnstone, 2014). While maintaining some pathway commonalities, the distinct mechanism of HDAC inhibitor-induced cell death may be specific to the underlying oncogenic lesion. With efficacy observed in reversing the abnormal epigenetic status of several cancer subtypes, a variety of HDAC inhibitors are currently under clinical investigation. Since 2006, five clinical drugs have been approved as treatments for advanced T-cell lymphoma or multiple myeloma, while several additional HDAC-inhibiting compounds are currently under investigation in solid tumour clinical trials (West & Johnstone, 2014). Used in this study, quisinostat is a second-generation pan-HDAC inhibitor showing promising efficacy against synovial sarcoma in preclinical studies (Laporte et al., 2017).

Although strong and specific responses to HDAC inhibition have been consistently observed in synovial sarcoma, the mechanism of apoptosis induction remains unclear. Advancing understanding of this relationship may lead to improved targeted therapy development and improved trial design, as well as aid in further elucidating the important

pathways implicated in synovial sarcoma oncogenesis. In this study, we used next-generation sequencing of six human synovial sarcoma cell lines to investigate the mechanisms of induced cell cycle arrest and cell death in synovial sarcoma following HDAC inhibition by quisinostat, a relatively new, orally available HDAC inhibitor that was the top hit in a synovial sarcoma drug screen (Laporte et al., 2017)

.

4.2 Materials and methods

4.2.1 Cell culture and chemicals

The following human synovial sarcoma cell lines were kindly provided: SYO-1 (Kawai et al., 2004) (Dr. Akira Kawai, National Cancer Centre Hospital, Tokyo, Japan), FUJI (Nojima et al., 1990) (Dr. Kazuo Nagashima, Hokkaido University School of Medicine, Sapporo, Japan), YaFuss (Ishibe et al., 2005), and HS-SY-II (Sonobe et al., 1992) (Dr. Marc Ladanyi, Memorial Sloan Kettering Cancer Centre, New York, USA), MoJo (K. B. Jones et al., 2016) (Dr. K. Jones, University of Utah, Salt Lake City, UT), and Yamato-SS (Naka et al., 2010) (Dr. K. Itoh, Osaka Medical Center for Cancer and Cardiovascular Diseases, Japan). Sarcoma cell lines were maintained in RPMI-1640 medium supplemented with 10% fetal bovine serum (FBS) (Life Technologies, Waltham, MA, USA) and the presence of a disease-defining *SS18-SSX* fusion oncogene was confirmed by PCR analysis. All cells were grown at 37°C, 95% humidity, and 5% CO_2. Pharmacologic compounds were purchased from Selleck Chemicals (Houston, TX, USA).

4.2.2 Cell line RNA-seq

Using the RNeasy Mini kit (Qiagen, Valencia, CA, USA), total RNA was isolated from six human synovial sarcoma cell lines treated for 16 hours with the HDAC inhibitor quisinostat at 0.025 μM or with vehicle (0.1% DMSO) control. Quality control was performed using the Agilent 2100 Bioanalyzer to confirm RNA Integrity Numbers over 8. Qualifying samples were further prepared using the TruSeq stranded mRNA library kit (Illumina) on the Neoprep Library System (Illumina). Paired end sequencing was performed on a NextSeq 500 sequencer to a read length of 81, with a median of 26.3 million reads per sample. Sequence quality metrics were evaluated using FastQC (http://www.bioinformatics.babraham.ac.uk/projects/fastqc/): across cell line specimens (N=12), the average quality of sequenced reads at any position was 33.6, and 90% of base calls were of quality 30 or greater. Alignment statistics were assessed using Picard tools (http://broadinstitute.github.io/picard/): across 12 specimens, the average value of median insert size was 226 bp, and the average percentage of high quality alignments was 95% (map quality of 20 or greater). Paired reads were aligned to the human genome version hg38 (v24) using STAR (Trapnell et al., 2012) with default parameter settings.

Reads of quality 10 or greater were enumerated on the sense strand for the exonic regions of each gene. FPKM (Fragments Per Kilobase of exon per Million mapped reads) values were calculated using the robust normalization method of DESeq2, and variance stabilized log fold- changes were calculated using the regularized log transformation of DESeq2 (Love, Huber, & Anders, 2014). DESeq2 was used to determine significance values for differential expression between treated and untreated cells, specifying pairwise comparison of drug effects across cell lines. A significance threshold of 0.01 was selected for

adjusted *p* values. Gene enrichment analyses were performed for gene ontologies using PANTHER with Bonferroni correction (Mi, Muruganujan, Casagrande, & Thomas, 2013), and for the MsigDB (molecular signatures database) v5.2 (A. Subramanian et al., 2005) using the hypergeometric test.

Raw count data for the TCGA sarcoma dataset were obtained from Genomic Data Commons (https://gdc.cancer.gov/node/31). FPKM, log2 fold-changes, and significance values were determined using DESeq2, comparing synovial sarcoma to all other sarcoma types.

4.2.3 Public microarray studies

The gene expression ominibus was surveyed for studies of HDAC inhibition at lethal doses in cancer cell lines, and five studies on more recent microarray platforms were selected for comparison (prostatic adenocarcinoma: GSE74418, neuroblastoma: GSE49158, NUT midline carcinoma: GSE18668, ovarian carcinoma GSE53603, atypical teratoid rhabdoid tumour (AT/RT): GSE37373). Expression data was downloaded from the processed data files supplied to GEO (series matrix files), and differential expression was determined using uniform criteria for each study using Limma (Ritchie et al., 2015). Gene IDs were mapped to the RNA-seq dataset using the supplied platform specifications. Expression data for GEO studies was ranked according to log2 fold change of treatment vs control, and Gene Set Enrichment Analysis (GSEA version 2.2.3) was used to gage the extent of over-representation of significant fold changes from RNA-seq data.

4.2.4 Western blots

Protein was collected from indicated cell lines grown in 10 cm dishes or following 24-hour treatments with indicated compounds. Samples were separated by 10% SDS-PAGE and transferred to PVDF membranes (Bio-Rad Laboratories, Hercules, CA, USA). Blots were incubated with indicated antibodies; Santa-Cruz Biotechnology (Dallas, TX, USA): SS18 sc-28698 1:200, GAPDH sc-25778 1:1500, BIK (NBK) sc-305625 1:500, BIM sc-374358 1:500, BCL2 sc-492 1:250, p-BCL2 sc-101762 1:250; Abcam (Cambridge, MA, USA): $p16^{INK4a}$ ab108349 1:500, $p14^{ARF}$ ab124282 1:500. Signals were visualized using the Odyssey Infrared System (LI-COR Biosciences, Lincoln, NE, USA).

4.3.5 Reverse transcriptase quantitative PCR

Total RNA was isolated from treated samples using the RNeasy Mini kit (Qiagen, Valencia, CA, USA) and was then reverse transcribed to cDNA using Oligo(dT) (Invitrogen, Waltham, MA, USA) and Superscript III (Invitrogen, Waltham, MA, USA). SYBR Green (Roche, Mississauga, ON, Canada) reagent was used for qPCR expression analysis, using an ABI ViiA7 qPCR system. All transcript levels were normalized to *GAPDH* RNA expression as well as to DMSO treated conditions to calculate relative fold induction of expression using the comparative Ct ($\Delta\Delta$Ct) method.

4.2.6 Cell viability assays

Cells were seeded in 96-well plates at 1e4 cells/well and treated in triplicate at indicated doses of the tested compounds. IC_{50} doses were determined in synovial sarcoma cell lines by dose curve studies. Cell viability was assessed in the cell lines as compared with

the vehicle condition (0.1% DMSO) at 48 hours post treatment using MTS reagent (Promega, Madison, WI, USA). Cell confluency and apoptosis induction were assessed over a 48-hour timeframe utilizing the IncuCyte Zoom® live cell imaging software (Essen BioScience, Ann Arbor, MI, USA). Apoptosis was assessed using the IncuCyte™ Kinetic Caspase-3/7 Apoptosis Assay Reagent (Essen BioScience, Ann Arbor, MI, USA, 4440).

4.2.7 Dichlorofluorescein diacetate assay (DCFDA)

ROS levels were assessed by DCFDA assay (Abcam, Cambridge, MA, USA, ab113851). Cells were seeded in a 96-well plate at 1e4 cells/well. The following day cells were treated with indicated compounds. At 24 hours post treatment, wells were over-layed with 2x diluted DCFDA reagent, as suggested by the manufacturer's protocol. Fluorescence was read by microplate reader at Ex/Em = 485/535 nm. A ratio of untreated to treated wells was calculated to determine relative response. Wells were normalized to media-only wells to account for background signal.

4.2.8 Mice

Mice harbouring the *Pten*$^{fl/fl}$*;hSS2* genotype (as previously described (Haldar et al., 2007)) received a 10 μL injection of 42 μM TATCre in the hindlimb at 4 weeks of age, to induce expression of SS18-SSX2 and deletion of *Pten*. A cohort of 8 mice with tumour volumes ranging from 600-1500 mm^3 were randomly assigned treatment of quisinostat (2 mg/kg) (n=4) or vehicle control (10% hydroxyl-propyl-β-cyclodextrin/25 mg/mL mannitol/H_2O) (n=4). Mice received daily intraperitoneal injections and tumour volumes were measured three times weekly for 7 days. Tumour volumes (mm^3) were measured using

digital calipers and calculated with the formula (*length* × *width*^{2}*)/2*. Mice were monitored daily and tumours monitored at least three times weekly during treatment. Tumours were excised and RNA was isolated with the RNeasy Mini kit (Qiagen, Valencia, CA, USA). This study was carried out in strict accordance with the recommendations in the Guide for the Care and Use of Laboratory Animals of the National Institutes of Health. The protocol was approved by the Institutional Animal Care and Use Committee of the University of Utah (Permit Number: 14-01016).

4.2.9 RNA interference

Duplex oligo (sense, CAAGAAGCCAGCAGAGGAATT; antisense, UUCCUCUGCUGGCUUCUUGTT) siRNAs were designed to target the *SSX* portion of *SS18-SSX* using the Integrated DNA Technologies RNA interference (RNAi) design tool, and synthesized by Integrated DNA Technologies as previously described (Lubieniecka et al., 2008). *siFOXO1* (sc-35382), *siFOXO3* (sc-37887) and *siFOXO4* (sc-29650) were purchased from Santa-Cruz Biotechnology (Dallas, TX, USA). *siBIK* (L-004388-00-0005), *siBIM* (L-004383-00-0005), and *siBMF* (L-004393-00-0005) were purchased from GE Healthcare Dharmacon (Lafayette, CO, USA). *siFOXO1* (sc-35382), *siFOXO3* (sc-37887), and *siFOXO4* (sc-29650) were purchased from Santa-Cruz Biotechnologies (Dallas, TX, US). SYO-1 cells were seeded in 6 well plates. At 60% confluence, cells were transfected with 30 pmol siRNA and 9 μL Lipofectamine RNAiMax transfection reagent (Invitrogen) in Opti-MEM serum free media (Life Technologies), according to the manufacturer's protocol. Protein was harvested at 48 hours post transfection, and knock-down was confirmed by western blot.

4.2.10 Immunofluorescence

Cells were seeded in culture-treated chamber slides at 3e4 cells/well. The following day, wells were treated with indicated compounds. Following indicated incubation times, cells were then washed twice with PBS, fixed with methanol at -20°C and permeabilized with 0.1% Triton X-100. Wells were blocked with blocking buffer and incubated overnight at 4°C with primary antibodies at a 1:250 dilution: FOXO1 (sc-374427), FOXO3 (sc-11351), FOXO4 (sc-5221), Ac-FOXO1 (sc-49437) (Santa-Cruz Biotechnology, Dallas, TX, USA),), P-FOXO1 (Cell Signaling 9464S). Wells were washed 3x with PBST then incubated for 45 minutes with AlexaFluor secondary antibody (Life Technologies, Waltham, MA, USA). Fluorescence was detected using a Zeiss Axioplan 2 microscope at 40x.

4.2.11 Immunohistochemical (IHC) staining

All IHC analysis was performed on 4 µm FFPE whole sections. Unstained slides were processed with the Ventana Discovery XT automated system (Ventana Medical Systems, Tucson, AZ, USA), according to the manufacturer's protocol with proprietary reagents. The heat-induced antigen retrieval method was used in Cell Conditioning solution (CC1-Tris-based EDTA buffer, pH 8.0; Ventana Medical Systems). Rabbit monoclonal Ki-67 (clone SP6, CRM 325 A, Biocare Medical, Concord, CA, USA) was used for primary incubation, for 60 min (37°C) at a 1:50 dilution. Biotinylated Goat Anti-Rabbit IgG Antibody (BA-1000, Vector Laboratories, Burlingame, CA, USA) was incubated for 32 min at 37°C. The detection systems used was the DABMap kit (760-124, Ventana Medical Systems, Tucson, AZ, USA).

4.2.12 Proximity ligation assay

Cells were seeded in culture-treated chamber slides at 3e4 cells/well. The following day, wells were treated with 25 nM quisinostat or vehicle (0.1% DMSO) for 16 hours. Cells were washed twice with PBS, fixed with 4% formaldehyde and permeabilized with 0.1% Triton X-100. Wells were blocked with blocking buffer and incubated overnight at 4°C with primary antibodies at a 1:1000 dilution: MDM2 (Santa-Cruz Biotechnology, Dallas, TX, USA, sc-965), p53 (Abcam, Cambridge, MA, USA, ab32389), $p14^{ARF}$ (Abcam ab124282). Proximity ligation was performed utilizing the Duolink® *In Situ* Red Starter Kit Mouse/Rabbit (Sigma-Aldrich, Oakville, ON, Canada) according to the manufacturer's protocol. The oligonucleotides and antibody-nucleic Fluorescence was detected using a Zeiss Axioplan 2 microscope at 40x. PLA images were quantified in triplicate using ImageJ software (NIH, Bethesda, MD, USA) as foci per cell, defined as the number of interaction points counted per number of cells as counted by DAPI nuclear staining.

4.3 RESULTS

4.3.1 HDAC inhibition modulated common transcriptional programs across synovial sarcoma cell lines

The complete expression profiles from six synovial sarcoma cell lines following 16-hour treatment with the HDAC inhibitor quisinostat or vehicle control (DMSO) was assembled by RNA-seq. In order to focus on larger transcriptional changes, genes showing significant differential expression in paired comparisons of treatment to control were analyzed, as defined by an adjusted *p*-value of less than 0.01 and a log2-fold change greater

than 1, in combination with expression above the 25th percentile observed in quisinostat-treated conditions across a minimum of 4 of the 6 cell lines (Figure 4.1A). In this manner, lists of 1967 up-regulated genes and 609 downregulated protein-coding genes were compiled. Analysis of expression patterns with gene ontology (GO) revealed at least six highly-enriched categories when using the genes observed to be up and down-regulated revealing core effects of HDAC inhibitors in synovial sarcoma, summarized with representative genes in Figure 4.1B.

Neural differentiation. A number of the highly-enriched GO categories relate to neuron differentiation, including pronounced up-regulation of genes encoding a spectrum of synapse components, neurotransmitter systems, and BDNF/NGFR/NTRK1 signaling. Expression levels of homeodomain transcription factors characteristic of neural differentiation were also observed to be up-regulated upon treatment with quisinostat, including *PAX6, SOX2, POU3F1, POU3F2, POU4F1, POU4F2* (Figure 4.1B, 4.1C).

Antigen presentation. HDAC inhibition in synovial sarcoma cells was associated with up-regulation of several components of MHC class I and class II antigen presentation, the immunoproteasome component *PSMB9*, and natural killer ligands *MICA, MICB, ULBP1-3* (Figure 4.1B, 4.1C).

Response to reactive oxygen species (ROS). Up-regulation of factors important for response to oxygen-containing species occurred as a result of HDAC inhibition (Figure 4.1B, 4.1C), including *FOXO1*, *FOXO4, JAK3* and *SESN3*.

Polycomb Targets. Significant enrichments in the MSigDB data set included up-regulation to targets of polycomb components SUZ12, EZH2, and EED in hESC, which are known to regulate proximal promoters with high CpG content (Ben-Porath et al., 2008;

Meissner et al., 2008; Mikkelsen et al., 2007) (Figure 4.1D). Significant overlap with gene targets down-regulated with EZH2 knockdown was also observed (Nuytten et al., 2008) (Figure 4.1F).

Apoptosis induction. The primary therapeutic goal of HDAC inhibition is the induction of cell death in cancer cells, and this was reflected in the increased expression of apoptosis genes in the synovial sarcoma cell lines treated with 16-hour quisinostat, including the classic activated inducers *CDKN2A* ($p14^{ARF}$), *BIK* and *BMF* (Figure 4.1B, 4.1F).

Cytostasis. A major class effect of HDAC inhibition was the negative regulation of proliferation, as evident in the down-regulation of E2F target genes including *MCM*, *PCNA* and up-regulation of several cyclin-dependent kinase inhibitors. Cell cycle progression GO terms were significantly decreased with HDAC inhibition (Figure 4.1E, 4.1F). This observation was confirmed by cell cycle analysis using flow cytometry, where arrest at G2 following HDAC inhibition by low dose quisinostat was observed (Figure 4.2A). Expression of cell cycle effectors and macromolecule biogenesis globally decreased following HDAC inhibition in synovial sarcoma, further suggesting the cells were coming out of cycle (Figure 4.2B).

4.3.2 Transcriptome analysis revealed class effects of HDAC inhibition in synovial sarcoma and five additional cancer subtypes

The derived average transcript expression values from the six synovial sarcoma cell lines were compared to five available HDAC inhibitor treatment microarray human tumour studies: neuroblastoma (GSE49158), NUT midline carcinoma (GSE18668), atypical teratoid rhabdoid tumour (AT/RT): (GSE37373), prostatic adenocarcinoma (GSE74418), and ovarian

carcinoma (GSE53603). Expression profiles in synovial sarcoma significantly correlated with the previous studies as measured by GSEA (Figure 4.3A). A common core gene expression set was revealed by comparison analysis of significantly changed genes when comparing the synovial sarcoma study to the five additional studies; 501 genes were up-regulated and 678 genes were down-regulated in at least five studies (Figure 4.3B). Gene ontology analysis revealed the most significantly increased biological terms included cell development processes, regulation of exocytosis, nervous system development and response to ROS (Figure 4.3C). The most significantly down-regulated terms included cell cycle progression, macromolecule biogenesis and chromatin organization (Figure 4.3D). We summarized the core effects of HDAC inhibition in cancer cell lines with representative genes to include nervous system development, response to reactive oxygen species, cytostasis and developmental processes (Figure 4.3E).

4.3.3 HDAC inhibition in cell lines reactivated expression of genes repressed in synovial sarcoma tumour tissue

To relate cell line-based findings to the expression profile of synovial sarcoma patient tumour tissue, published RNA-seq expression profiles of patient specimens from the cancer genome atlas (TCGA) were examined differentially in comparison with the HDAC inhibitor-treated expression data revealing 1323 significantly up-regulated and 3368 significantly down-regulated genes (Figure 4.4A). In comparing average expression across the synovial sarcoma TCGA dataset to HDAC inhibition-mediated changes from the cell line data it was observed that globally, genes with low relative expression in the synovial sarcoma tumour data were reactivated in the treated cell line data while many highly-expressed targets in the

tumours decreased following HDAC inhibition in the cell lines (Figure 4.4B). Gene ontology analysis confirmed core effects of HDAC inhibition in synovial sarcoma to include up-regulation of mesenchymal cell differentiation, nervous system development, response to stress and apoptosis, as well as down-regulation of proliferation, macromolecule biogenesis and transcription (Figure 4.4C).

To demonstrate the specificity of this expression pattern reversal, the published primary tumour microarray expression profiles of patient specimens from the TCGA were examined in comparison with additional sarcoma subtypes liposarcoma and leiomyosarcoma. Human synovial sarcoma tumour expression data is characterized by a distinctive repression of several cyclin dependent kinase inhibitors: *CDKN2A* ($p16^{INK4a}$, $p14^{ARF}$), *CDKN2B* ($p15^{INK4b}$), *CDKN2D* ($p19^{INK4d}$), *CDKN1A* ($p21^{CIP1}$), *CDKN1C* ($p57^{KIP2}$) and tumour suppressors (*EGR1, PTEN*) as well as up-regulation of cell cycle (*CDK4, CDK6, CCND1*) and anti-apoptotic effectors (*BCL2*) (Figure 4.4D). Transcriptome analysis in the six synovial sarcoma cell lines comparing HDAC inhibitor treated to vehicle treated conditions demonstrated a drug-induced reversal of this proliferative phenotype concomitant with induction of pro-apoptotic effector expression (*BIK, BCL2L11 (BIM), BMF, ASK1, FOXO1, JUN, FOS*) (Figure 4.4E). Expression reversal was specific to synovial sarcoma most significantly in *CDKN2A* and *BIK* when compared with the five published transcriptome studies of HDAC inhibition in other cancer subtypes (Figure 4.4F).

4.3.4 HDAC inhibition induced ROS accumulation and activated a FOXO-mediated pro-apoptotic program

FOXO-regulated targets involved in apoptotic and cell cycle regulation (*BIM, BMF, GADD45*) were up-regulated in the transcriptome data following HDAC inhibition, whereas FOXO-regulated anti-oxidant factors were unchanged *(SOD1* and *SOD2*) suggesting a systemic switch toward apoptosis in response to ROS accumulation (Figure 4.5A). The transcriptome analysis further revealed an HDAC-inhibitor mediated significant increase in *FOXO* transcription factor levels in the six synovial sarcoma cell lines, particularly in *FOXO1* (Figure 4.5A).

Based on the observed modulation of factors related to the regulation of the cellular oxidative environment upon quisinostat treatment, we further investigated ROS levels. This revealed that quisinostat treatment induces ROS accumulation in a dose-dependent manner (Figure 4.5B) that can be attenuated by N-acetylcysteine (N-AC) treatment (Figure 4.5C). Recovering the ROS accumulation induced by HDAC inhibition with N-AC rescues synovial sarcoma cell lines from apoptosis by ~50% (Figure 4.5D).

Consistent with this observation, FOXO1, FOXO3 and FOXO4 translocate into the nucleus following quisinostat treatment, aligning with their activation in response to HDAC inhibition (Figure 4.5E). Under vehicle treated conditions FOXO1 exists phosphorylated in the cytoplasm, while following quisinostat treatment it was found to be acetylated and located in the nucleus (Figure 4.5F). In addition, we observed the decrease of FOXO1 acetylation by the addition of N-AC, suggesting FOXO1 was activated by the ROS accumulation (Figure 4.5G).

Following knockdown of *FOXO1* and *FOXO3* transcription factors, the quisinostat-induced activation of pro-apoptotic factors *BIM* and *BMF* was significantly attenuated (Figure 4.5H), whereas *FOXO4* depletion had no observable effect. FOXO knockdown rescues HDAC inhibitor induced apoptosis in synovial sarcoma cell lines, by ~50% for FOXO1 (Figure 4.5I).

4.3.5 HDAC inhibition shifted the ratio of *BCL2:BIK* and induced apoptosis in synovial sarcoma by mechanisms involving *CDKN2A*-mediated apoptosis pathways

BCL2 levels are known to be elevated in synovial sarcoma tumours resulting in an anti-apoptotic phenotype (Hirakawa et al., 1996). Following HDAC inhibition, mRNA levels of the pro-apoptotic factor *BIK* increased by an average of approximately 23-fold, significantly more than other pro-apoptotic factors (Figure 4.6A, 4.6B). This resulted in a shift in the average ratio of *BCL2:BIK* from approximately 58:1 pre-treatment down to almost 1:1 following HDAC inhibitor treatment, favoring apoptosis (Figure 4.6C). At the protein level, increases in BIK and BIM as well as the phosphorylation of BCL2 occurred in a dose-dependent manner with increasing levels of quisinostat treatment in synovial sarcoma cell lines (Figure 4.6D). Cleaved caspase 3/7 could be detected at increasing levels with increased doses of quisinostat over time, indicating apoptosis was occurring at much higher levels than with standard doxorubicin treatment assayed in this manner (Figure 4.6E). Cleaved caspase 3/7 levels were decreased with the depletion of *BIK*, *BIM* and *BMF* suggesting each was important for apoptosis induction following HDAC inhibition, with the most significant contribution by BIK (Figure 4.6F).

An inducible mouse model of synovial sarcoma was treated by HDAC inhibition to assess efficacy of apoptosis induction *in vivo*. At 7 days post treatment, the quisinostat treated tumours had decreased in volume by approximately 40% while vehicle treated tumours grew by approximately 30% (Figure 4.6G, 4.6H). In comparison with other pro-apoptotic factors, tumour *BIK* levels were found to be significantly higher following treatment than in the vehicle treated group, again resulting in a pro-apoptotic shift in the ratio of *BCL2:BIK* (Figure 4.6I). Tumour cell proliferation decreases with quisinostat treatment, as measured by Ki-67 staining (Figure 4.6J, 4.6K).

CDKN2A is a known target of SS18-SSX mediated repression. When depleting the oncoprotein or when treating with quisinostat, a reactivation at the protein level of $p14^{ARF}$ and $p16^{INK4A}$ was observed, and the loss of SS18-SSX protein in response to HDAC inhibition was confirmed (Figure 4.7A). *CDKN2A* knockdown attenuated BIK activation at the RNA (Figure 4.7B) and protein level (Figure 4.7C), and resulted in a decrease in cleaved caspase 3/7 induction following quisinostat treatment (Figure 4.7D), suggesting *CDKN2A* is necessary for BIK activity in response to HDAC inhibition. Following HDAC inhibition, $p14^{ARF}$ was observed to interact with repressor protein CtBP and ubiquitin ligase MDM2, while the interaction of MDM2 and p53 decreased (Figure 4.7E).

4.4 DISCUSSION

Current cytotoxic therapies offer limited benefit against synovial sarcoma; more targeted therapeutic approaches are needed to improve outcome when local control measures are not cureative. The synovial sarcoma fusion oncoprotein SS18-SSX disrupts gene

expression in a characteristic manner leading to a distinctive phenotype. Previous studies have shown HDAC inhibition disrupts the driving complex in synovial sarcoma, resulting in reactivated expression of tumour suppressors otherwise repressed by SS18-SSX (Laporte et al., 2017; Su et al., 2012). In the current study, we delineate the common transcriptional patterns present across studies of HDAC inhibition in six cancer subtypes to uncover core class effects, investigate the effects of HDAC inhibition specific to synovial sarcoma and uncover mechanisms of apoptosis induction in this cancer type, as summarized in Figure 5.1. Quisinostat treatment was found to bring about mesenchymal and neuronal differentiation transcriptional patterns. HDAC inhibition is thought to further counteract the proliferative and anti-apoptotic phenotype of synovial sarcoma by activating repressed gene targets, such as *CDKN2A* which in turn facilitate expression of cell cycle regulators and pro-apoptotic proteins. ROS accumulation in response to HDAC inhibition and pro-apoptotic protein-mediated mitochondrial permeabilization further drives apoptotic pathways.

Expression of cell cycle regulator *CCND1* (cyclin D1) and cyclin-dependent kinases *CDK4* and *CDK6* decreased with the up-regulation of *CDKN2A* and *CDKN2B* in response to quisinostat treatment. The cyclin D1/CDK4/CDK6 axis is required for cell cycle progression through G1/S phase and is known to be highly active in synovial sarcoma (Vlenterie et al., 2016). Under normal conditions, CDK4 and CDK6 are inhibited by $p16^{INK4A}$ (*CDKN2A*) and $p15^{INK4B}$ (*CDKN2B*), negatively regulating cell division. Hampering the cyclin D1/CDK4/CDK6 axis by reactivation of *CDKN2A* and *CDKN2B* may therefore contribute to the observed cell cycle arrest in response to HDAC inhibition.

The *CDKN2A* locus has been previously shown to be directly repressed by SS18-SSX in synovial sarcoma (Su et al., 2012). *CDKN2A* is normally regulated by polycomb group

proteins, repressing its expression in the recruitment of EZH2 (Bracken et al., 2007), and is activated by SWI/SNF-mediated polycomb eviction (Kia et al., 2008). In the current study, we validate the reactivation of *CDKN2A* encoded proteins $p16^{INK4A}$ and $p14^{ARF}$ in response to SS18-SSX knockdown and HDAC inhibition, and demonstrate an epistatic relationship between *CDKN2A* expression and BIK activation in synovial sarcoma. The transcriptome data revealed pro-apoptotic factor *BIK* activation to be significant in all studied synovial sarcoma cell lines and mouse model following HDAC inhibition. BIK has been shown in previous studies to be inhibited by BCL2, and when activated to function in initiating the mitochondrial apoptosis pathway (Chinnadurai, Vijayalingam, & Rashmi, 2008). $p14^{ARF}$ has been observed to increase BIK levels by inhibition of transcriptional repressor CtBP (Kovi et al., 2010) as well as to activate p53 by inhibiting MDM2, inducing mitochondrial-mediated apoptosis (Muer et al., 2012). HDAC inhibition may therefore impede SS18-SSX-mediated repression of the *CDKN2A* locus, allowing for reactivation of normal cell cycle regulation and induction of pro-apoptotic pathways.

In this study, we further find that ROS accumulation by HDAC inhibition results in an initiation of FOXO transcription factor activation in synovial sarcoma. FOXO class forkhead transcription factors are known to act as cellular redox sensors that become modified post-translationally in response to oxidative stress (Klotz et al., 2015). FOXOs are negatively regulated by PI3K/AKT signaling (Luo et al., 2013) and translocate to the nucleus when activated by ROS activity where they can initiate transcription of anti-oxidant effectors such as SOD2 (Superoxide Dismutase 2**)** to promote survival (Klotz et al., 2015). FOXO transcription factors are also important in initiating expression of pro-apoptotic effectors in response to ROS (Luo et al., 2013). As described herein, the induced FOXO program favored

expression of pro-apoptotic factors *BIM* and *BMF* and was important for apoptotic induction in response to quisinostat. PTEN-mediated repression of the PI3K/AKT pathway is important for FOXO activation (Luo et al., 2013), which may be promoted in synovial sarcoma by reactivation of repressed *EGR1* in response to HDAC inhibition (Lubieniecka et al., 2008; Su et al., 2010).

In synovial sarcoma, HDAC inhibition acts at multiple sites resulting in blocked cell cycle progression, ROS accumulation and initiation of pro-apoptotic programs regulated by FOXO transcription factors. Through HDAC-mediated reactivation of repressed *CDKN2A*, pro-apoptotic factors are able to counteract elevated BCL2 levels. Quisinostat also increases antigen presentation pathways, which may have implications for immune-oncology approaches in a tumour type that characteristically lacks an immunogenic phenotype. Our study provides mechanistic support for the use of HDAC inhibitors in the treatment of synovial sarcoma. While single-agent studies of HDAC inhibition in solid tumours have concluded with mixed results, combinatorial drug protocols are the subject of active investigation (Slingerland, Guchelaar, & Gelderblom, 2014). Rational drug combinations incorporating HDAC inhibitors may enhance tumour penetration and synergistically affect multiple pathways leading to apoptosis (Thurn, Thomas, Moore, & Munster, 2011). In synovial sarcoma, low dose combinations of HDAC and proteasome inhibitors are particularly efficacious in reactivating pro-apoptotic factors, inducing apoptosis and decreasing tumour burden *in vivo* (Laporte et al., 2017). As shown here, HDAC inhibition specifically reverses the proliferative and anti-apoptotic phenotype brought about by SS18-SSX.

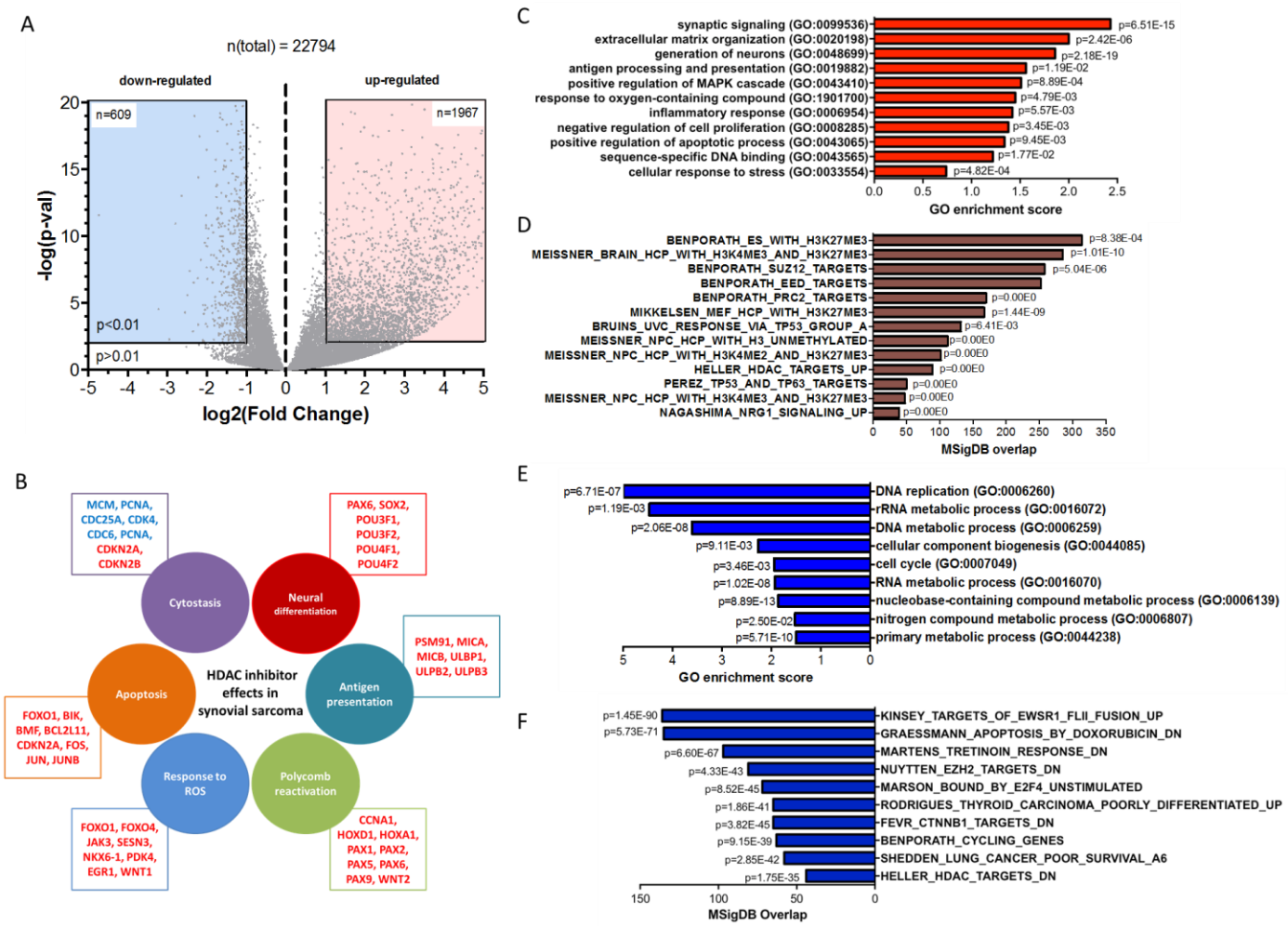

Figure 4.1: HDAC inhibition modulated common transcriptional programs across six synovial sarcoma cell lines. A) Average differential mRNA expression data with a greater than 2-fold change and *p*-value of less than 0.01 was used for further analysis, revealing 609 significantly down-regulated and 1967 significantly up-regulated gene targets in response to HDAC inhibition in six human synovial sarcoma cell lines. B) Summarized gene ontology and significantly enriched targets of up-regulated genes (red), down-regulated genes (blue) reveal effects of HDAC inhibition in synovial sarcoma to include neural differentiation, antigen presentation, polycomb reactivation, serum response, cytostasis and apoptosis. Detailed effects were observed by C) gene ontology and D) MSigDB analysis of up-regulated targets, as well as E) gene ontology and F) MSigDB analysis of down-regulated targets.

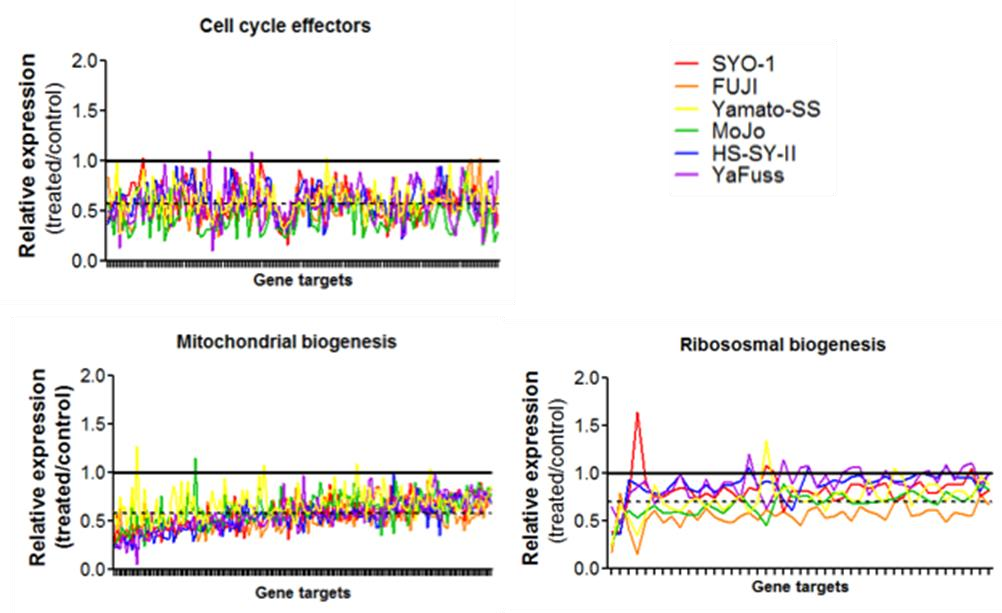

Figure 4.2: HDAC inhibition induces down-regulation of cell cycle effectors in six synovial sarcoma cell lines. Expression profile following HDAC inhibition demonstrates a class effect in the down-regulation of cell cycle progression effectors, ribosomal and mitochondrial biogenesis signals, suggesting cell cycle progression is blocked. Solid line represents relative pre-treatment expression, dotted line represents approximate average relative expression of gene category.

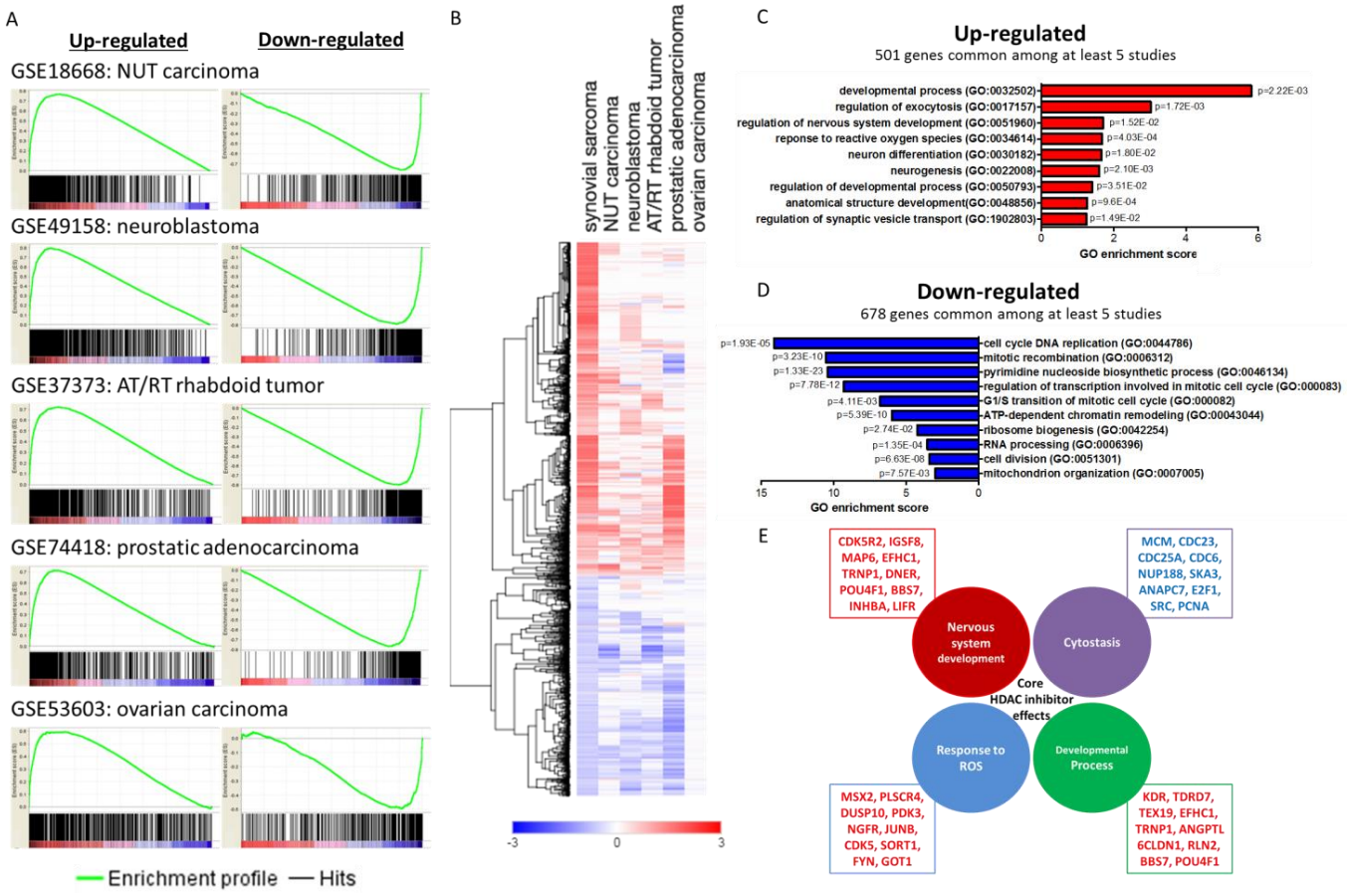

Figure 4.3: Correlation of expression data from six cancer cell line studies following HDAC inhibitor treatment. A) The expression data from five published individual cancer cell line studies was compared by GSEA to synovial sarcoma cell line data, demonstrating significant correlation in transcription changes following HDAC inhibition. B) The significant differentially expressed gene targets among the six studies were assembled to uncover a core set of transcriptional changes; unsupervised hierarchical clustering was done with GENE-E software. Among at least five studies, common gene targets were assessed to uncover the most significantly C) increased or decreased D) biological terms. E) Core transcriptional patterns brought on by HDAC inhibition-induced up- (red) and down- (blue) regulated genes were revealed.

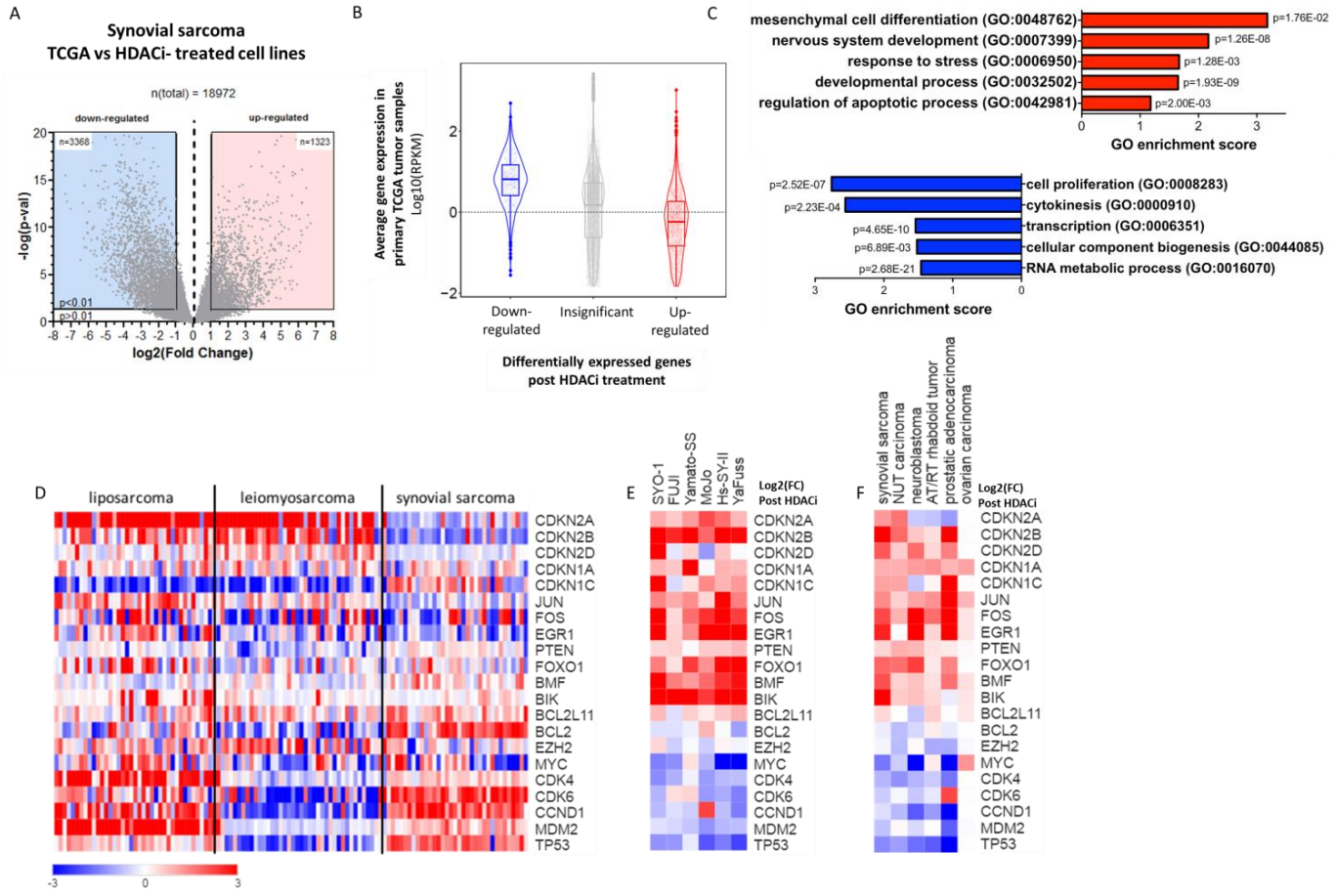

Figure 4.4: Expression profile characteristic of synovial sarcoma tumour phenotype was reversed by HDAC inhibition. A) Volcano plot demonstrating the differential expression of TCGA primary tumour mRNA sequencing data as compared with the post-HDAC inhibitor cell line data. B) Average expression across the synovial sarcoma TCGA dataset of HDAC inhibition-mediated up- (red), down-regulated (blue) and insignificantly changed (grey) genes. C) Gene ontology analysis confirmed core effects of HDAC inhibition in synovial sarcoma. D) The expression profiles of synovial sarcoma microarray tumour samples reveal characteristic repression of cell cycle regulators and up-regulation of anti-apoptotic targets, when compared to other sarcoma subtypes liposarcoma (subtype not specified) and leiomyosarcoma. E) This characteristic expression phenotype was reversed following HDAC inhibition in six synovial sarcoma cell lines. F) Expression reversal was specific to synovial sarcoma most significantly with *CDKN2A* and *BIK* gene expression when compared with five additional transcriptome studies of HDAC inhibition.

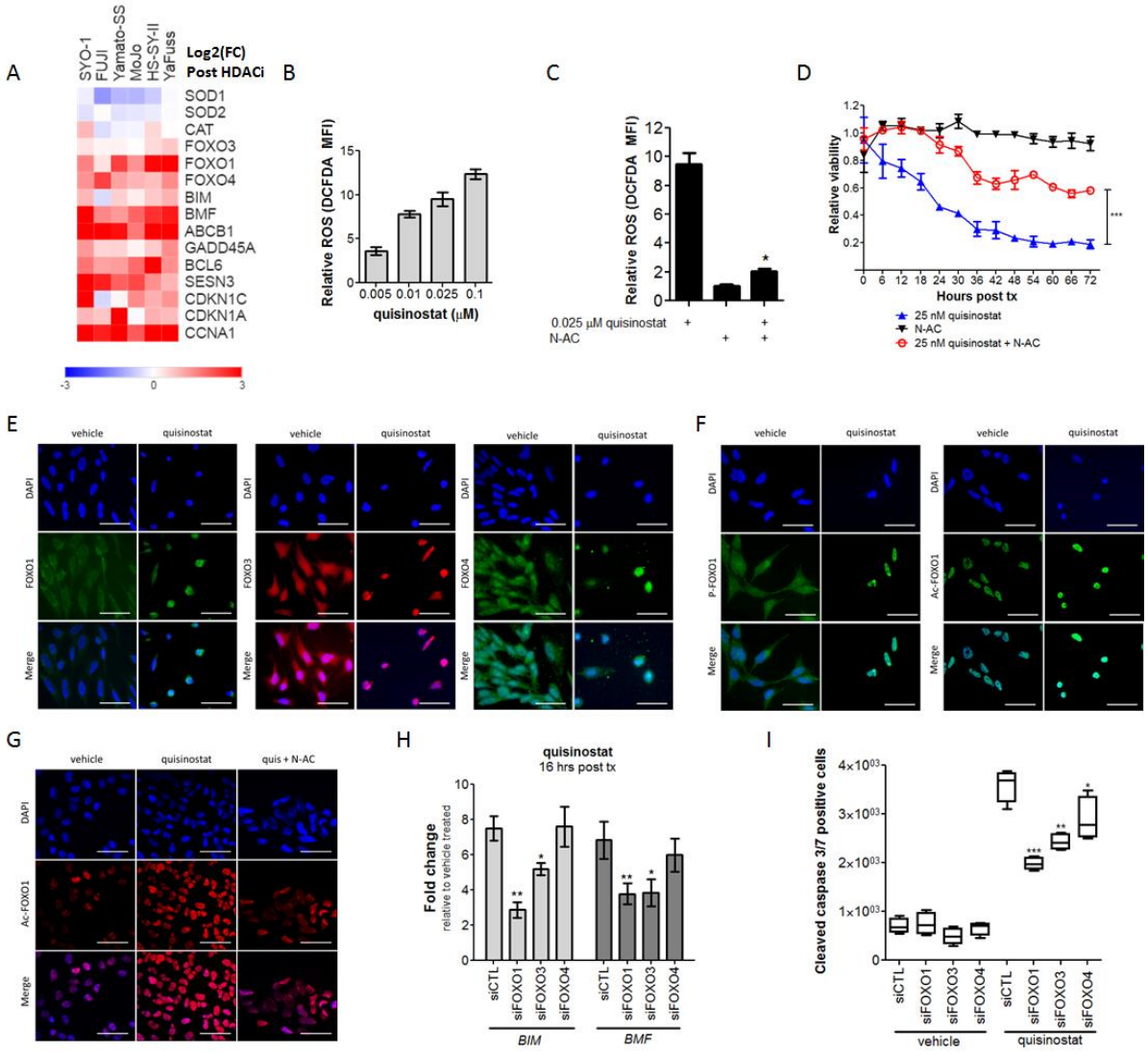

Figure 4.5: FOXO transcription activation by ROS accumulation initiates pro-apoptotic gene expression. A) mRNA expression profile following HDAC inhibition in six synovial sarcoma cell lines demonstrates an increase in *FOXO* transcription factors, pro-apoptotic and cell cycle regulation factors (*BIM, BMF, GADD45*), while anti-oxidant factors were not significantly affected (*SOD1* and *SOD2*). B) HDAC inhibition elicits ROS accumulation in a dose-dependent manner which C) is attenuated by 10 μM N-acetylcysteine (N-AC) treatments and D) rescues HDAC inhibitor induced apoptosis. E) FOXO proteins enter the nucleus following 0.025 μM quisinostat treatment. F) Under vehicle treated conditions phosphorylated FOXO1 is in the cytoplasm, and when treated with quisinostat it becomes translocated to the nucleus where it is acetylated. G) FOXO1 acetylation is decreased by the addition of N-AC. H) Knockdown of *FOXO*1 and *FOXO3* attenuates pro-apoptotic factor *BIM* and *BMF* activation. I) *FOXO1* knockdown rescues HDAC inhibitor induced apoptosis in synovial sarcoma cell lines. Scale bars represent 20 μm. Statistical significance compared to vehicle treatment controls was determined by Student t test: * denotes $p < 0.05$, ** denotes $p < 0.01$, *** denotes $p < 0.001$. Error bars represent standard error of mean from conditions performed in triplicate.

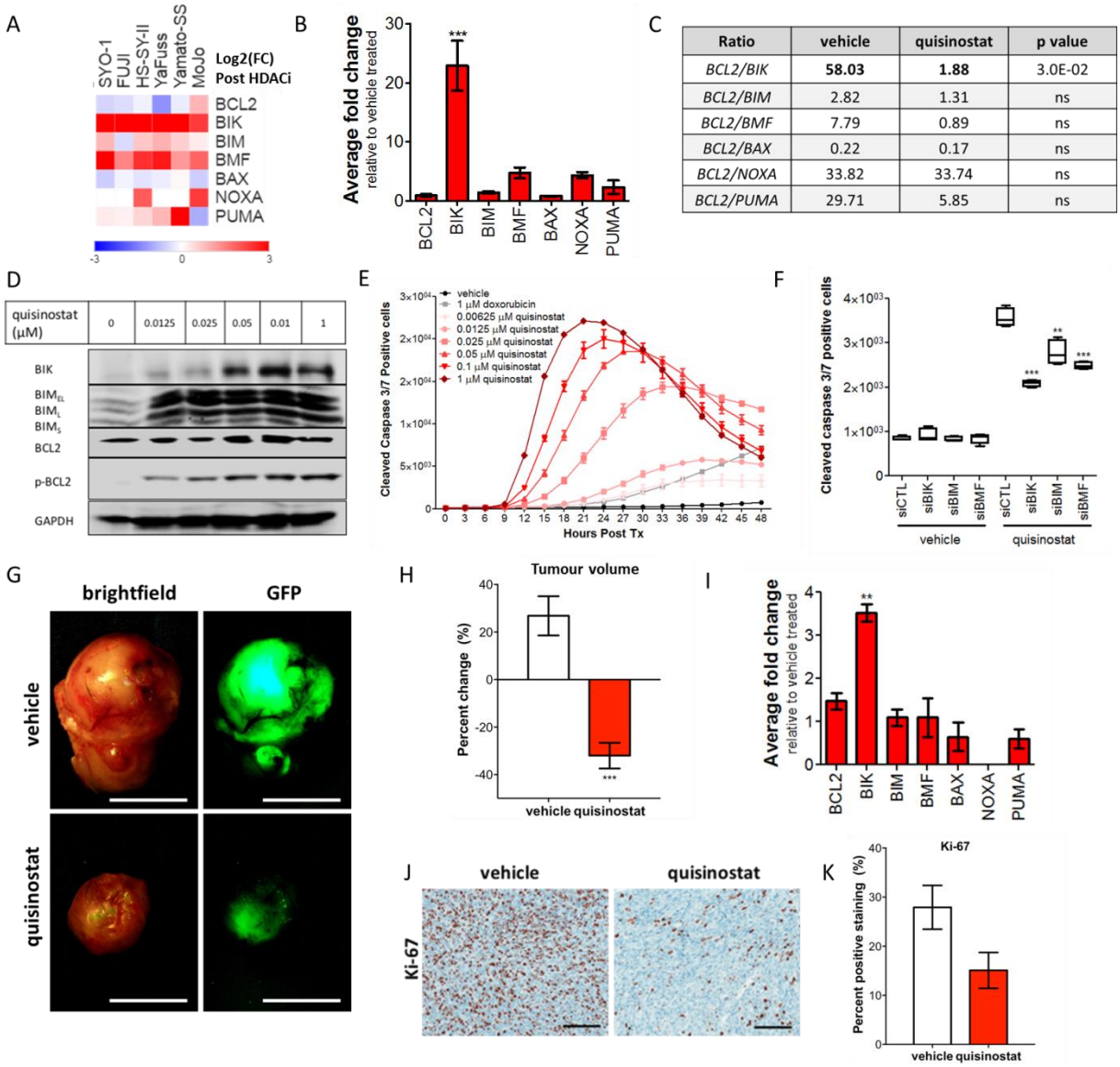

Ratio	vehicle	quisinostat	p value
BCL2/BIK	**58.03**	**1.88**	3.0E-02
BCL2/BIM	2.82	1.31	ns
BCL2/BMF	7.79	0.89	ns
BCL2/BAX	0.22	0.17	ns
BCL2/NOXA	33.82	33.74	ns
BCL2/PUMA	29.71	5.85	ns

Figure 4.6: HDAC inhibition shifted the *BCL2:BIK* ratio and induced apoptosis in synovial sarcoma. A) Differential expression profile of apoptosis regulators in six synovial sarcoma cell lines following HDAC inhibition demonstrates an increase in pro-apoptotic factor *BIK* expression. B) *BIK* expression increases by approximately 23-fold. C) The ratio of *BCL2/BIK* is decreased following quisinostat treatment. D) BIK, BIM and phosphorylation of BCL2 increase in a dose-dependent manner with increasing levels of quisinostat. E) Cleaved caspase 3/7 levels increase with increasing concentrations of quisinostat, significantly more so than doxorubicin treatment. F) Cleaved caspase 3/7 levels decrease with the knockdown of *BIK*, *BIM* and *BMF*. G) Tumours excised from *Pten*$^{fl/fl}$*;hSS2* mouse model of synovial sarcoma treated with quisinostat for 7 days. H) Quisinostat treated tumours shrunk by ~40%, while vehicle treated tumours grew by ~30%. I) RNA expression analysis demonstrated a significant increase in *BIK* levels in the quisinostat treatment group when compared to the vehicle treated tumours. J) Ki-67 staining by IHC was stronger in the vehicle treated mouse tumours than the quisinostat treated tumours; staining score was quantified in K). Scale bars in panel G represent 1 cm, and in panel J represent 100 μm. Statistical significance compared to vehicle treatment controls was determined by Student t test: ** denotes $p < 0.01$, *** denotes $p < 0.001$. Error bars represent standard error of mean from conditions performed in triplicate.

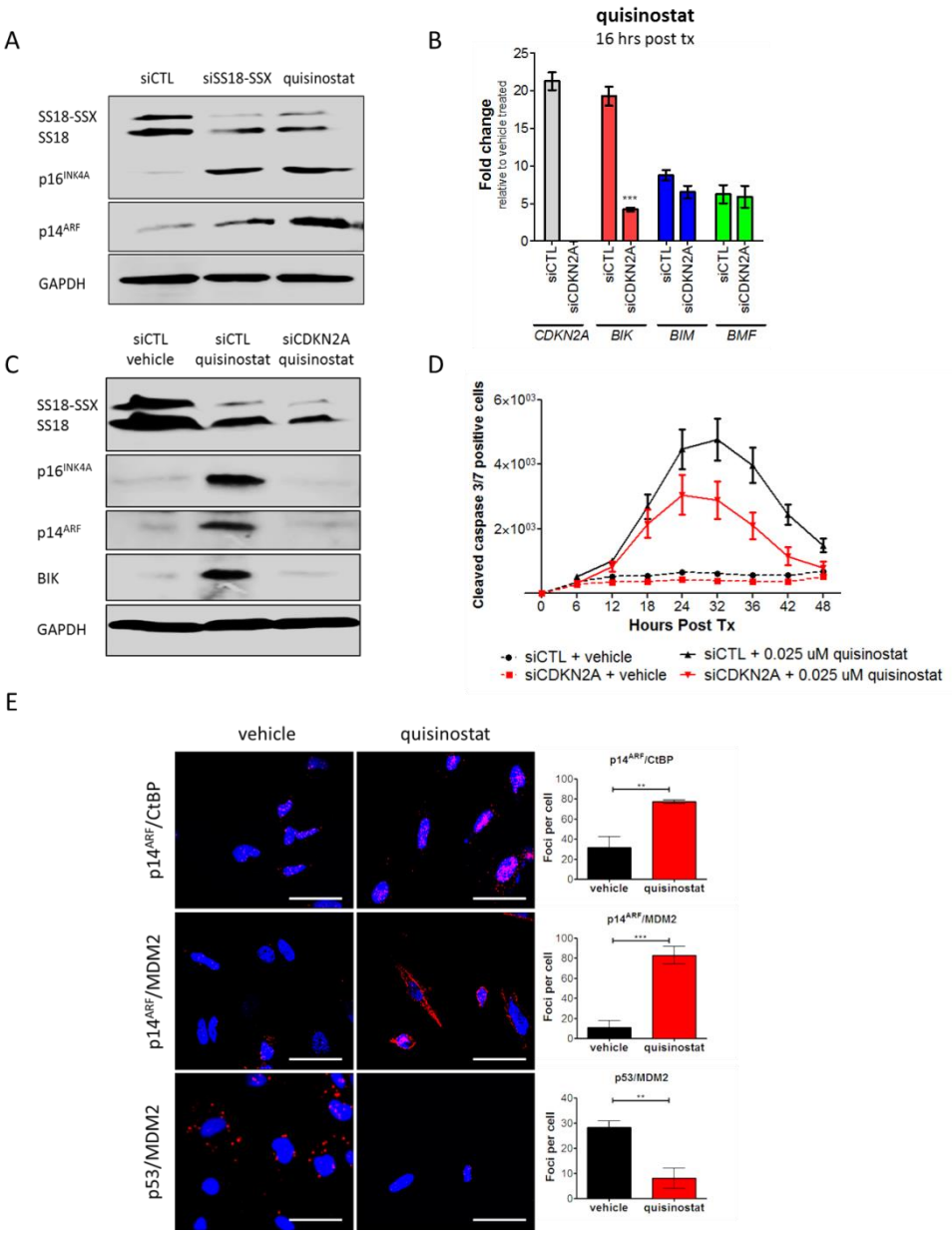

Figure 4.7: *CDKN2A* reactivation by HDAC inhibition is important for BIK expression and apoptosis induction. A) *CDKN2A*-encoded proteins $p14^{ARF}$ and $p16^{INK4A}$ were reactivated following SS18-SSX depletion and 0.025 μM quisinostat treatment in SYO-1 synovial sarcoma cells. SS18-SSX protein level was decreased following HDAC inhibition. B) Depletion of *CDKN2A* attenuated BIK activation at the RNA and C) protein level and D) inhibited cleaved caspase 3/7 induction in response to HDAC inhibition by 0.025 μM quisinostat in SYO-1 cells, suggesting *CDKN2A* was necessary for *BIK* activation in response to HDAC inhibition. E) Quisinostat reactivated $p14^{ARF}$ expression, allowing it to co-localize with repressor protein CtBP and ubiquitin ligase MDM2, as the interaction of MDM2 with p53 decreased. Statistical significance compared to vehicle treatment controls was determined by Student t test: ** denotes $p < 0.01$, *** denotes $p < 0.001$. Error bars represent standard error of mean from conditions performed in triplicate. Scale bars represent 20 μm.

CHAPTER 5: CONCLUSIONS AND DISCUSSION

5.1 Summary of findings

Synovial sarcomagenesis is driven by known oncoprotein SS18-SSX-mediated interactions with chromatin-modification proteins; however targeted therapies are not currently available. I hypothesized that the study of SS18-SSX complex disruption would facilitate drug discovery studies and that effective compounds would have clinical relevancy against synovial sarcoma. From my studies, the following novel advances in HDAC inhibitor-mediated drug development against synovial sarcoma were made.

I employed the proximity ligation assay to study the drug-mediated disruption of the SS18-SSX/TLE1 interaction and developed it for use in a high-throughput drug screening protocol. As a result of my work, PLA was found to be applicable to targeted drug discovery in translocation-associated sarcomas with known driving complexes. From this, the compound SXT1596 was found to be effective in disrupting the driving SS18-SSX/TLE1 interaction. However, this small molecule agent has not undergone advanced drug development studies and is considered likely to have potential off target effects and consequent toxicities. As it is therefore not currently a clinically useable agent for patient care, it was not pursued in further pre-clinical study, but could be revisited if toxicity studies eventually prove this compound or one of its derivatives can be used as an anticancer drug. I further confirmed several class I-targeting HDAC inhibitors to be able to disrupt the SS18-SSX/TLE1 complex and decrease cell viability in synovial sarcoma as well as bring about a loss of the oncoprotein, demonstrating the targeted effect of this class of drugs.

I then undertook a high-throughput drug screen of over 900 oncologic compounds and epigenetic modifiers in six synovial sarcoma cell lines to in order to uncover novel targetable pathways and sensitives brought about by SS18-SSX. From this, I found HDAC and proteasome inhibitors to be among the most potent targeted compounds in decreasing synovial sarcoma cell viability. In combination, I found these two drug classes to significantly synergize against synovial sarcoma, mechanistically attributable to inhibition of aggresome formation, endoplasmic reticulum cytosolic stress induction, and reactivation of pro-apoptotic factors. My pre-clinical studies were used as support for a novel Phase II investigational new drug (IND) clinical trial proposal to test the HDAC inhibitor quisinostat in combination with proteasome inhibitor bortezomib in synovial sarcoma and translocation-associated soft tissue sarcomas (Appendix II).

I also assessed the effects of HDAC inhibition on genome-wide transcription by RNA-seq. I demonstrated class effects of HDAC inhibition in various cancer cell line subtypes as well as effects unique to synovial sarcoma cells. I observed that HDAC inhibition leads to increased neuronal-based differentiation and cytostasis in cancer cells. My work uncovered that FOXO transcription factor activity is important in inducing pro-apoptotic *BMF* and *BIM* expression in response to ROS accumulation following HDAC inhibitor treatment in synovial sarcoma. My experiments further revealed, uniquely to synovial sarcoma, that HDAC inhibition provokes significant pro-apoptotic *BIK* expression correlating to *CDKN2A* reactivation. From this, the contributing roles of *CDKN2A* reactivation, pro-apoptotic factor expression and ROS accumulation in HDAC-inhibitor mediated apoptosis in synovial sarcoma were demonstrated.

5.2 HDAC inhibitor-induced effects in synovial sarcoma

I explored the impact of HDAC-inhibition in synovial sarcoma by genome-wide transcriptome analysis. From this, I found that HDAC inhibition reversed the synovial sarcoma-specific proliferative and anti-apoptotic phenotypical expression patterns. I further uncovered a mechanism by which HDAC inhibition disrupts the driving, repressive protein complexes of synovial sarcoma and elicits a loss of the oncoprotein, resulting in reactivation of SS18-SSX-repressed gene targets and pro-apoptotic factor induction.

It has been demonstrated that SMARCB1-deficient tumours are sensitive to HDAC inhibition, and low-dose treatment results in multi-lineage differentiation and cytostasis (Muscat et al., 2016). This is suggested to be due to the ability of HDAC inhibition to counteract the repression brought about by over-active PcG activity occurring as a result of ineffective polycomb eviction by SMARCB1-deficient SWI/SNF complexes. Resultant activation of differentiation and cell cycle regulators may thereby inhibit oncogenic development.

In the context of synovial sarcoma, SS18-SSX-mediated recruitment of PcG/HDAC complexes and SMARCB1-deficiency seem to result in a specific pattern of transcriptional repression, reversed by HDAC inhibition. HDAC inhibition further brings about a loss of SS18-SSX following dissociation of the SS18-SSX/PcG/HDAC complex. HDAC inhibition may then allow for histone acetylation activity to occur at these sites bringing about restored transcriptional expression.

Reactivation of SS18-SSX-repressed gene targets elicits activity of not only cell cycle regulators and differentiation effectors, but also pro-apoptotic activation that reverses the anti-apoptotic phenotype brought about by elevated BCL2, as well as bringing about ROS

accumulation and activation of redox-mediated apoptosis pathways (Figure 5.1). The activation of directly repressed gene targets by HDAC inhibitor-mediated dissociation of the PRC2/SS18-SSX complex is thereby important in the induction of apoptosis in synovial sarcoma.

5.3 Impact of SS18-SSX on the *CDKN2A* locus

Experimentally, I found HDAC inhibition to reactivate expression of both $p16^{INK4A}$ and $p14^{ARF}$ following disruption of the SS18-SSX/PcG/HDAC complex, and that this was important for BIK expression as well as apoptosis induction. $p14^{ARF}$ has been shown to be important in the induction of *BIK* transcription in the inhibition of repressor protein CtBP (Kovi et al., 2010). Repression at the *CDKN2A* locus by SS18-SSX-mediated polycomb activity accordingly promotes cell proliferation and survival. The re-expression of *CDKN2A/CDKN2B* and subsequent $p16^{INK4A}$, $p14^{ARF}$ and $p15^{INK4B}$ activity by HDAC inhibition therefore functions to bring about cytostasis and apoptotic control (Figure 5.2).

5.4 HDAC/proteasome inhibitor combination synergy

The combination of HDAC and proteasome inhibition in synovial sarcoma works congruently on multiple levels. SMARCB1-deficency may promote sensitivity to proteasome inhibition (Genovese et al., 2017), while HDAC inhibitor treatment promotes deregulated protein processing signatures, further sensitizing cells to proteasome inhibitors (Dupere-Richer et al., 2017). In this study, I found that HDAC inhibition reactivates expression of key SS18-SSX-repressed tumour-suppressors important for apoptosis and cell cycle regulation, as well as induces ROS accumulation. HDAC inhibitors further block formation of aggresomes

in response to proteasome inhibition supporting the induction of apoptosis in the blocking of these survival mechanisms (Figure 5.3). This represents a mechanism for their observed synergism.

5.5 Clinical relevance

My study provides a detailed pre-clinical and mechanistic rationale for testing HDAC inhibitors clinically against synovial sarcoma, specifically in the context of a combination with proteasome inhibition. This strategy targets the driving complex in synovial sarcoma and potently synergizes to induce apoptosis and decrease tumour burden *in vivo*. As a direct result of this thesis work, in collaboration with members of the Sarcoma Disease Site Committee of the Canadian Cancer Trials Group, I helped develop a clinical trial proposal for quisinostat and bortezomib in combination against translocation-associated soft tissue sarcomas (Appendix II). This strategy is expected to prove more efficacious than currently available therapeutics as it directly targets the SS18-SSX oncoprotein. In addition to synovial sarcoma, I found the HDAC/proteasome inhibitor combination to be effective in clear cell sarcoma, myxoid liposarcoma and desmoplastic small round cell tumour cell line models, but not in normal HEK293T cells or beast carcinoma MCF-7 cells (Figure II.1). This protocol is thereby hoped to elicit a therapeutic response in translocation-associated sarcomas wherein oncoproteins modulate transcriptional repression.

As leading drug classes against hematological malignancies, the combination of bortezomib and quisinostat has been studied clinically in a phase 1b trial against multiple myeloma (Moreau et al., 2016). This study successfully established the maximum tolerated dose (MTD) for the combination and demonstrated an acceptable safety profile with

manageable toxicity. Dose limiting toxicities at higher doses of quisinostat used in the combination included primarily cardiac electrophysiologic issues and thrombocytopenia. Unlike the situation that faces researchers when screens identify a "new" drug as active, this precedent allows future studies of the quisinostat/bortezomib combination to begin at phase II, an important practical consideration. Furthermore, the combination of HDAC inhibitor panobinostat and bortezomib has been assessed against multiple myeloma in a phase III study and brought about a significant increase in progression-free survival (PFS) when compared to the bortezomib/placebo arm, demonstrating the efficacy of this strategy (Richardson et al., 2016). Resistance mechanisms are expected to be hindered by the described combinational effects.

Quisinostat has been shown to induce prolonged inhibition of HDAC1 activity in solid tumours when compared to other HDAC inhibitors such as panobinostat, making it an optimal compound for sarcoma studies (Venugopal et al., 2013). Quisinostat is licensed by Janssen Pharmaceuticals to its subsidiary NewVac LLC, who are actively pursuing trials in solid tumour cancers. I found that proteasome inhibitors bortezomib, ixazomib and carfilzomib were all synergistic with quisinostat in pre-clinical studies, providing options for the combination partner. Bortezomib is now available as a generic drug and has clinical safety data allowing for the bypassing of phase I combination trials, whereas ixazomib and carfilzomib are second generation inhibitors with better expected solid tumour penetration but no toxicity studies of their combination with quisinostat.

The quisinostat/bortezomib combination phase II trial proposal is set as nonrandomized, due to limited accrual capacity of rare diseases that renders randomized designs impractical, and is designed with a 4 month PFS endpoint. The potential for

cytostatic effects of the study compounds determined the primary objective, as tumours may respond by not clinically progressing while not observably decreasing in size. A minimum of 21 patients are required to be enrolled to achieve statistical significance. With precedent from previous studies, a PFS rate of greater than 40% will be of interest and as such if 6 or more patients have PFS at 4 months a phase III trial would be considered.

Patients with validated synovial sarcoma, clear cell sarcoma, myxoid liposarcoma and desmoplastic small round cell tumour diagnoses, who have not received more than two previous lines of chemotherapy and with no prior exposure to HDAC or proteasome inhibitors will be eligible for trial inclusion. Dosing of quisinostat/bortezomib will follow the MTDs established from the phase Ib trial. Translational correlative studies will be undertaken to confirm diagnosis and determine if translocation-type correlates with response, and HDAC2 levels will be assessed by IHC to investigate drug activity and tumour penetrance using previously established methods (Chu et al., 2015).

The HDAC/proteasome inhibitor combination proposal has to-date received positive support from both NewVac LLC and the Canadian Cancer Trials Group (CCTG). The CCTG has polled site investigators from seven of the major accrual sites in Canada and 86% (6/7) are interested in participating in this trial, with no competing studies as of this writing. Patient accrual is estimated to be achievable within 18 months but due to the relative rarity of these diseases, accrual is not guaranteed and may require additional regional sarcoma centres to be added or additional disease subtypes to be included for accrual and study times to meet expected CCTG benchmarks

5.6 Future directions

Further investigation of targeted therapeutics in synovial sarcoma is expected to contribute to improved outcome, as more efficacious drugs become available. Currently, emerging drugs targeting the PRC2 complex are of great investigational interest with novel compounds against EZH2 and EED as well as more highly targeted HDAC inhibitors currently being developed. While EZH2 inhibitors may present minimal benefit in synovial sarcoma due to the importance of the non-catalytic EZH2 domain in SMARCB1-depleted cancers as well as residual SMARCB1 activity, efficacy may advance with improved drug candidates. HDAC inhibitors currently present the most active and clinically advanced epigenetic regulatory intervention against synovial sarcoma and their further clinical investigation in sarcomas is warranted.

In addition to generalized systemic-treatment drug trials, precision medicine experimental programs are becoming available in the context of personalized onco-genomics. In these studies, single patient tissues are evaluated by whole genome DNA and RNA sequencing analyses for aberrant signaling pathways that may be sensitive to available drug intervention. Similar programs rely on limited panel analyses of targetable pathways, making the whole genome approach more thorough. This approach may lead to personalized and targeted drug interventions specific to that individual and could reflect a promising tactic against synovial sarcoma for patients with progressive disease. This strategy may therefore compete for stage II accrual with HDAC inhibitor trials; however, this approach may also further support their use in individual patients.

Continued investigation of the role of *CDKN2A* silencing in synovial sarcoma specifically in the context of p53 regulation may further uncover important oncogenic

pathways. While p53 is known to remain intact in synovial sarcoma (D'Arcy, Ryan, & Brodin, 2009), its deregulation by inactivating effectors may play an important role in transformation by SS18-SSX. As the most commonly mutated gene in human cancer, genetic alterations to tumour suppressor *TP53* (p53) occur in half of all cancers (Rivlin, Brosh, Oren, & Rotter, 2011). In abrogating its tumour suppressive effects, p53 mutations promote anti-apoptotic phenotypes and therapy resistance as well as increase metastatic qualities (Oren, Tal, & Rotter, 2016). While not often mutated in synovial sarcoma, p53 may be functionally repressed by MDM2 inhibition, brought on by underactive $p14^{ARF}$ through repression of *CDKN2A*. Further investigation into the inactivation of p53 may provide further insight into SS18-SSX-mediated oncogenesis and reveal drug targets for improved therapeutics against synovial sarcoma.

Synovial sarcoma further represents an excellent disease model in the understanding of epigenetic oncogenesis as an emerging hallmark of cancer. More than 50% of all cancers have been reported to have some mutation to effectors that brings about dysregulated chromatin organization (P. A. Jones, Issa, & Baylin, 2016). This concept of a driving oncoprotein epigenetically modifying transcription is therefore relevant to many cancer subtypes, most specifically to the wide-range of translocation-associated soft tissue sarcomas. These mechanisms seem particularly relevant in adolescent and young adult cancers as cells undergo differentiation (Lawlor & Thiele, 2012), which are especially devastating in the field of pediatric oncology. Superior treatment options are needed to help improve the survival of these young patients. Further analysis of this epigenetic dysregulation hallmark and its role in transformation as uncovered in the synovial sarcoma model may provide increased biological insight and reveal novel therapeutic targets for a wide range of cancers.

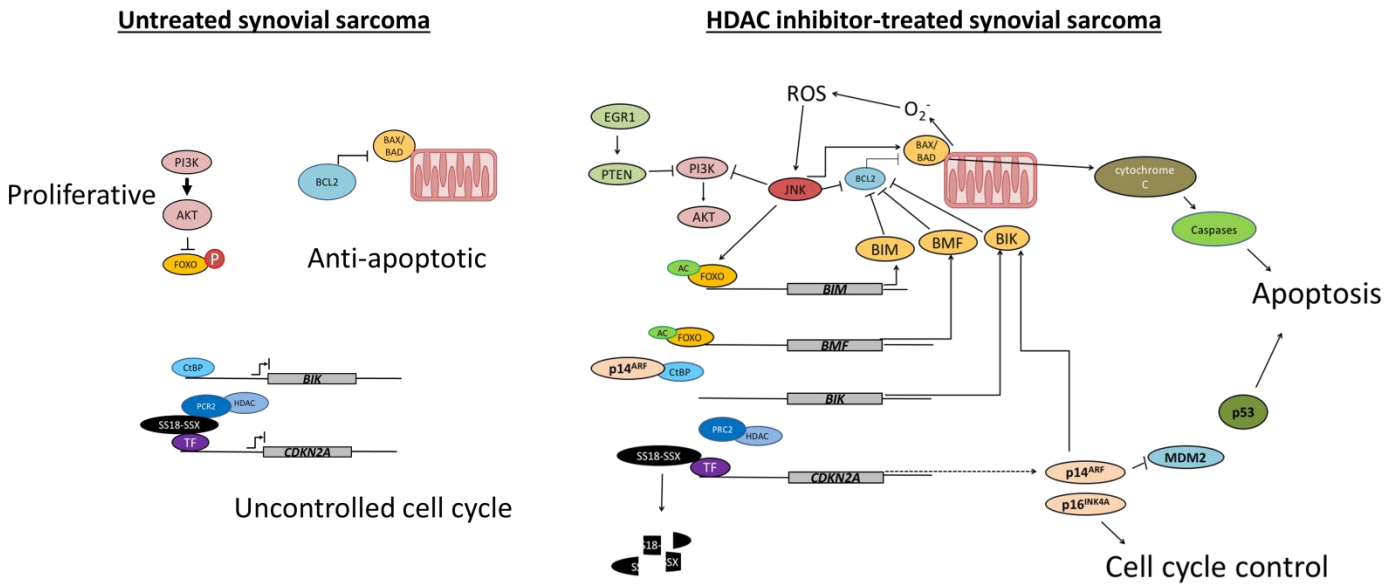

Figure 5.1: Proposed model of HDAC inhibitor induced apoptosis in synovial sarcoma. HDAC inhibition disrupts the driving, repressive protein complexes of synovial sarcoma and elicits a loss of the oncoprotein, resulting in reactivation of SS18-SSX-repressed gene targets and pro-apoptotic factor induction. HDAC inhibition results in expression of cell cycle regulators including $p16^{INK4A}$, and pro-apoptotic proteins, $p14^{ARF}$, BIK, BIM and BMF. $p14^{ARF}$ has been found to contribute to apoptosis induction activate BIK expression in the inhibition of transcriptional repressor CtBP, and to inhibit MDM2, activating p53. ROS accumulation in response to HDAC inhibition and pro-apoptotic protein-mediated mitochondrial permeabilization further drives apoptotic pathways, acetylating FOXO transcription factors to further express pro-apoptotic factors.

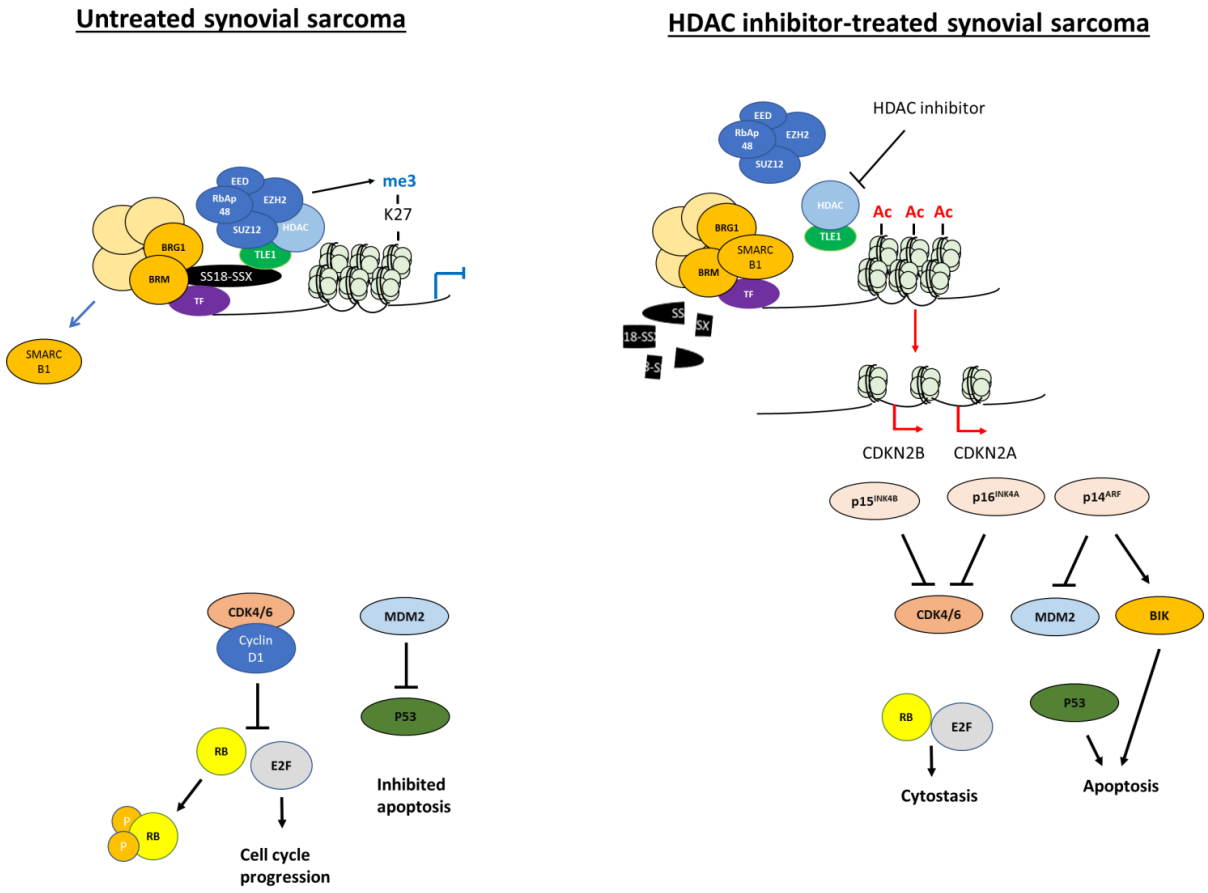

Figure 5.2: Proposed model of *CDKN2A* locus dysregulation in synovial sarcoma. HDAC inhibition disrupts the SS18-SSX/PcG/HDAC repressive complex and brings about a loss of the oncoprotein in synovial sarcoma. When CDKN2A is repressed, CDK4/6 interact with cyclin D1, together functioning to phosphorylate cell cycle regulator protein Rb, activating E2F transcription factors to initiate transcription of genes required for DNA replication, to initiate cell cycle progression. The p14 ^{ARF} protein inhibits the ubiquitin ligase MDM2, preventing its inactivation of tumour suppressor p53, which regulates expression of stress response gene targets and regulates apoptotic pathways. In addition, p14^{ARF} has been shown to be important in the induction of pro-apoptotic factor *BIK* transcription. This results in re-expression of *CDKN2A/CDKN2B* and subsequent p16^{INK4A}, p14^{ARF} and p15^{INK4B} activity induction, functioning to bring about cytostasis and apoptotic control.

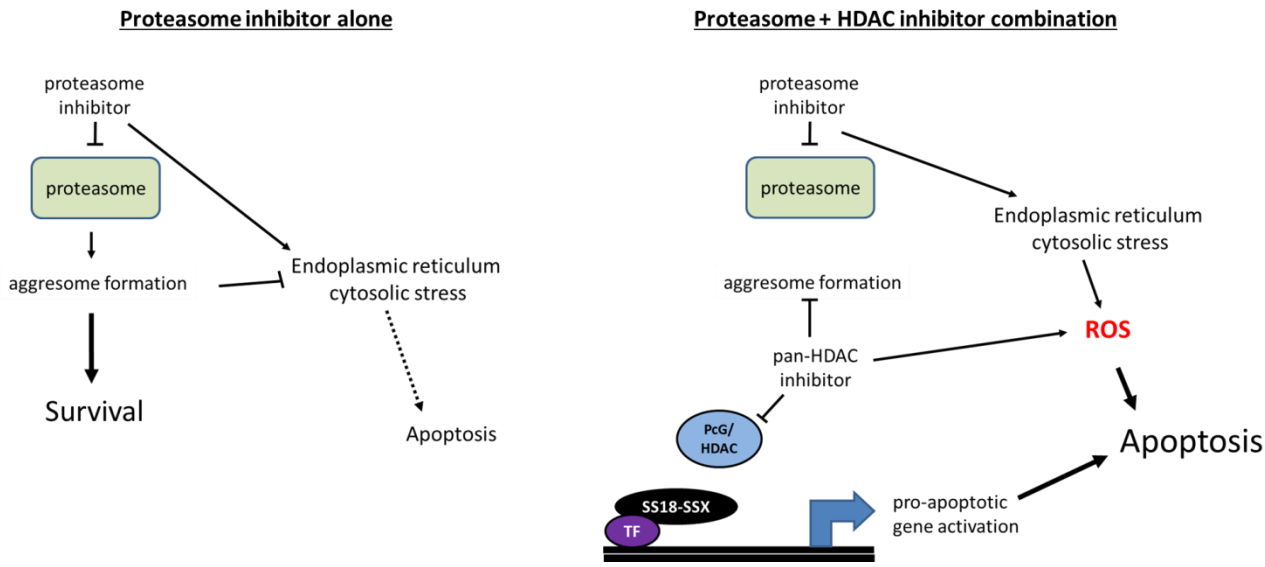

Figure 5.3: Proposed model of HDAC and proteasome inhibitor synergy in synovial sarcoma. HDAC inhibition reactivates expression of key SS18-SSX-repressed tumour-suppressors important for apoptosis and cell cycle regulation, as well as induces ROS accumulation. HDAC inhibitors further block formation of aggresomes in response to proteasome inhibition, supporting the induction of endoplasmic reticulum stress from loss of proteostasis and apoptosis. Figure reprinted with permission from Laporte *et al.*, 2017 PLoS ONE.

REFERENCES

Agaimy, A. (2014). The expanding family of SMARCB1(INI1)-deficient neoplasia: implications of phenotypic, biological, and molecular heterogeneity. *Adv Anat Pathol, 21*(6), 394-410. doi:10.1097/PAP.0000000000000038

Alberts, Bruce. (2010). *Essential cell biology* (3rd ed.). New York: Garland Science.

Aman, P. (2005). Fusion oncogenes in tumour development. *Semin Cancer Biol, 15*(3), 236-243. doi:10.1016/j.semcancer.2005.01.009

Anderson, J. L., Denny, C. T., Tap, W. D., & Federman, N. (2012). Pediatric sarcomas: translating molecular pathogenesis of disease to novel therapeutic possibilities. *Pediatr Res, 72*(2), 112-121. doi:10.1038/pr.2012.54

Anglesio, M. S., Wiegand, K. C., Melnyk, N., Chow, C., Salamanca, C., Prentice, L. M., . . . Huntsman, D. G. (2013). Type-specific cell line models for type-specific ovarian cancer research. *PLoS One, 8*(9), e72162. doi:10.1371/journal.pone.0072162

Antonescu, C. R., Kawai, A., Leung, D. H., Lonardo, F., Woodruff, J. M., Healey, J. H., & Ladanyi, M. (2000). Strong association of SYT-SSX fusion type and morphologic epithelial differentiation in synovial sarcoma. *Diagn Mol Pathol, 9*(1), 1-8.

Arnold, M. A., Arnold, C. A., Li, G., Chae, U., El-Etriby, R., Lee, C. C., & Tsokos, M. (2013). A unique pattern of INI1 immunohistochemistry distinguishes synovial sarcoma from its histologic mimics. *Hum Pathol, 44*(5), 881-887. doi:10.1016/j.humpath.2012.08.014

Arrighetti, N., Corno, C., & Gatti, L. (2015). Drug Combinations with HDAC Inhibitors in Antitumour Therapy. *Crit Rev Oncog, 20*(1-2), 83-117.

Bagchi, S., Fredriksson, R., & Wallen-Mackenzie, A. (2015). In Situ Proximity Ligation Assay (PLA). *Methods Mol Biol, 1318*, 149-159. doi:10.1007/978-1-4939-2742-5_15

Ballinger, M. L., Goode, D. L., Ray-Coquard, I., James, P. A., Mitchell, G., Niedermayr, E., . . . International Sarcoma Kindred, Study. (2016). Monogenic and polygenic determinants of sarcoma risk: an international genetic study. *Lancet Oncol, 17*(9), 1261-1271. doi:10.1016/S1470-2045(16)30147-4

Barco, R., Garcia, C. B., & Eid, J. E. (2009). The synovial sarcoma-associated SYT-SSX2 oncogene antagonizes the polycomb complex protein Bmi1. *PLoS One, 4*(4), e5060. doi:10.1371/journal.pone.0005060

Barham, W., Frump, A. L., Sherrill, T. P., Garcia, C. B., Saito-Diaz, K., VanSaun, M. N., . . . Eid, J. E. (2013). Targeting the Wnt pathway in synovial sarcoma models. *Cancer Discov, 3*(11), 1286-1301. doi:10.1158/2159-8290.CD-13-0138

Barrott, J. J., Illum, B. E., Jin, H., Zhu, J. F., Mosbruger, T., Monument, M. J., . . . Jones, K. B. (2015). beta-catenin stabilization enhances SS18-SSX2-driven synovial sarcomagenesis and blocks the mesenchymal to epithelial transition. *Oncotarget, 6*(26), 22758-22766. doi:10.18632/oncotarget.4283

Barrott, J. J., Kafchinski, L. A., Jin, H., Potter, J. W., Kannan, S. D., Kennedy, R., . . . Jones, K. B. (2016). Modeling synovial sarcoma metastasis in the mouse: PI3'-lipid signaling and inflammation. *J Exp Med, 213*(13), 2989-3005. doi:10.1084/jem.20160817

Barski, A., Cuddapah, S., Cui, K., Roh, T. Y., Schones, D. E., Wang, Z., . . . Zhao, K. (2007). High-resolution profiling of histone methylations in the human genome. *Cell, 129*(4), 823-837. doi:10.1016/j.cell.2007.05.009

Ben-Porath, I., Thomson, M. W., Carey, V. J., Ge, R., Bell, G. W., Regev, A., & Weinberg, R. A. (2008). An embryonic stem cell-like gene expression signature in poorly differentiated aggressive human tumours. *Nat Genet, 40*(5), 499-507. doi:10.1038/ng.127

Bhaskara, S., Chyla, B. J., Amann, J. M., Knutson, S. K., Cortez, D., Sun, Z. W., & Hiebert, S. W. (2008). Deletion of histone deacetylase 3 reveals critical roles in S phase progression and DNA damage control. *Mol Cell, 30*(1), 61-72. doi:10.1016/j.molcel.2008.02.030

Bolden, J. E., Peart, M. J., & Johnstone, R. W. (2006). Anticancer activities of histone deacetylase inhibitors. *Nat Rev Drug Discov, 5*(9), 769-784. doi:10.1038/nrd2133

Boone, D. N., Qi, Y., Li, Z., & Hann, S. R. (2011). Egr1 mediates p53-independent c-Myc-induced apoptosis via a noncanonical ARF-dependent transcriptional mechanism. *Proc Natl Acad Sci U S A, 108*(2), 632-637. doi:10.1073/pnas.1008848108

Bozzi, F., Ferrari, A., Negri, T., Conca, E., Luca da, R., Losa, M., . . . Pilotti, S. (2008). Molecular characterization of synovial sarcoma in children and adolescents: evidence of akt activation. *Transl Oncol, 1*(2), 95-101.

Bracken, A. P., Kleine-Kohlbrecher, D., Dietrich, N., Pasini, D., Gargiulo, G., Beekman, C., . . . Helin, K. (2007). The Polycomb group proteins bind throughout the INK4A-ARF locus and are disassociated in senescent cells. *Genes Dev, 21*(5), 525-530. doi:10.1101/gad.415507

Bramwell, V. H. (2012). Pazopanib and the treatment palette for soft-tissue sarcoma. *Lancet, 379*(9829), 1854-1856. doi:10.1016/S0140-6736(12)60739-9

Brennan, Antonescu, C., Alektiar, K., & Maki, R. (2016). Management of soft tissue sarcoma *Springerplus, 2*(2). doi:doi:10.1007/978-3-319-41906-0

Brennan, M. F., Antonescu, C. R., Moraco, N., & Singer, S. (2014). Lessons learned from the study of 10,000 patients with soft tissue sarcoma. *Ann Surg, 260*(3), 416-421; discussion 421-412. doi:10.1097/SLA.0000000000000869

Brett, D., Whitehouse, S., Antonson, P., Shipley, J., Cooper, C., & Goodwin, G. (1997). The SYT protein involved in the t(X;18) synovial sarcoma translocation is a transcriptional activator localised in nuclear bodies. *Hum Mol Genet, 6*(9), 1559-1564.

Bush, K. T., Goldberg, A. L., & Nigam, S. K. (1997). Proteasome inhibition leads to a heat-shock response, induction of endoplasmic reticulum chaperones, and thermotolerance. *J Biol Chem, 272*(14), 9086-9092.

Cai, W., Sun, Y., Wang, W., Han, C., Ouchida, M., Xia, W., . . . Sun, B. (2011). The effect of SYT-SSX and extracellular signal-regulated kinase (ERK) on cell proliferation in synovial sarcoma. *Pathol Oncol Res, 17*(2), 357-367. doi:10.1007/s12253-010-9334-y

Chinnadurai, G., Vijayalingam, S., & Rashmi, R. (2008). BIK, the founding member of the BH3-only family proteins: mechanisms of cell death and role in cancer and pathogenic processes. *Oncogene, 27 Suppl 1*, S20-29. doi:10.1038/onc.2009.40

Choi, J. H., Kwon, H. J., Yoon, B. I., Kim, J. H., Han, S. U., Joo, H. J., & Kim, D. Y. (2001). Expression profile of histone deacetylase 1 in gastric cancer tissues. *Jpn J Cancer Res, 92*(12), 1300-1304.

Chraybi, M., Abd Alsamad, I., Copie-Bergman, C., Baia, M., Andre, J., Dumaz, N., & Ortonne, N. (2013). Oncogene abnormalities in a series of primary melanomas of the sinonasal tract: NRAS mutations and cyclin D1 amplification are more frequent than KIT or BRAF mutations. *Hum Pathol, 44*(9), 1902-1911. doi:10.1016/j.humpath.2013.01.025

Chu, Q. S., Nielsen, T. O., Alcindor, T., Gupta, A., Endo, M., Goytain, A., . . . Eisenhauer, E. A. (2015). A phase II study of SB939, a novel pan-histone deacetylase inhibitor, in patients with translocation-associated recurrent/metastatic sarcomas-NCIC-CTG IND 200dagger. *Ann Oncol, 26*(5), 973-981. doi:10.1093/annonc/mdv033

Cironi, L., Petricevic, T., Fernandes Vieira, V., Provero, P., Fusco, C., Cornaz, S., . . . Stamenkovic, I. (2016). The fusion protein SS18-SSX1 employs core Wnt pathway transcription factors to induce a partial Wnt signature in synovial sarcoma. *Sci Rep, 6*, 22113. doi:10.1038/srep22113

Clark, J., Rocques, P. J., Crew, A. J., Gill, S., Shipley, J., Chan, A. M., . . . Cooper, C. S. (1994). Identification of novel genes, SYT and SSX, involved in the t(X;18)(p11.2;q11.2) translocation found in human synovial sarcoma. *Nat Genet, 7*(4), 502-508. doi:10.1038/ng0894-502

Clements, W. M., Lowy, A. M., & Groden, J. (2003). Adenomatous polyposis coli/beta-catenin interaction and downstream targets: altered gene expression in gastrointestinal tumours. *Clin Colorectal Cancer, 3*(2), 113-120.

D'Arcy, P., Maruwge, W., Ryan, B. A., & Brodin, B. (2008). The oncoprotein SS18-SSX1 promotes p53 ubiquitination and degradation by enhancing HDM2 stability. *Mol Cancer Res, 6*(1), 127-138. doi:10.1158/1541-7786.MCR-07-0176

D'Arcy, P., Maruwge, W., Wolahan, B., Ma, L., & Brodin, B. (2014). Oncogenic functions of the cancer-testis antigen SSX on the proliferation, survival, and signaling pathways of cancer cells. *PLoS One, 9*(4), e95136. doi:10.1371/journal.pone.0095136

D'Arcy, P., Ryan, B. A., & Brodin, B. (2009). Reactivation of p53 function in synovial sarcoma cells by inhibition of p53-HDM2 interaction. *Cancer Lett, 275*(2), 285-292. doi:10.1016/j.canlet.2008.10.030

Dahmen, R. P., Koch, A., Denkhaus, D., Tonn, J. C., Sorensen, N., Berthold, F., . . . Pietsch, T. (2001). Deletions of AXIN1, a component of the WNT/wingless pathway, in sporadic medulloblastomas. *Cancer Res, 61*(19), 7039-7043.

Dancsok, A. R., Asleh-Aburaya, K., & Nielsen, T. O. (2017). Advances in sarcoma diagnostics and treatment. *Oncotarget, 8*(4), 7068-7093. doi:10.18632/oncotarget.12548

de Bruijn, D. R., Allander, S. V., van Dijk, A. H., Willemse, M. P., Thijssen, J., van Groningen, J. J., . . . van Kessel, A. G. (2006). The synovial-sarcoma-associated SS18-SSX2 fusion protein induces epigenetic gene (de)regulation. *Cancer Res, 66*(19), 9474-9482. doi:10.1158/0008-5472.CAN-05-3726

Deleu, S., Lemaire, M., Arts, J., Menu, E., Van Valckenborgh, E., Vande Broek, I., . . . Vanderkerken, K. (2009). Bortezomib alone or in combination with the histone deacetylase inhibitor JNJ-26481585: effect on myeloma bone disease in the 5T2MM murine model of myeloma. *Cancer Res, 69*(13), 5307-5311. doi:10.1158/0008-5472.CAN-08-4472

Deng, X. M., Xiao, L., Lang, W. H., Gao, F. Q., Ruvolo, P., & May, W. S. (2001). Novel role for JNK as a stress-activated Bcl2 kinase. *Journal of Biological Chemistry, 276*(26), 23681-23688. doi:DOI 10.1074/jbc.M100279200

Deshmukh, R., Mankin, H. J., & Singer, S. (2004). Synovial sarcoma: the importance of size and location for survival. *Clin Orthop Relat Res*(419), 155-161.

dos Santos, N. R., de Bruijn, D. R., Kater-Baats, E., Otte, A. P., & van Kessel, A. G. (2000). Delineation of the protein domains responsible for SYT, SSX, and SYT-SSX nuclear localization. *Exp Cell Res, 256*(1), 192-202. doi:10.1006/excr.2000.4813

Dupere-Richer, D., Kinal, M., Pettersson, F., Emond, A., Calvo-Vidal, M. N., Nichol, J. N., . . . Mann, K. K. (2017). Increased protein processing gene signature in HDACi-resistant cells predicts response to proteasome inhibitors. *Leuk Lymphoma, 58*(1), 218-221. doi:10.1080/10428194.2016.1180684

Endo, M., de Graaff, M. A., Ingram, D. R., Lim, S., Lev, D. C., Briaire-de Bruijn, I. H., . . . Nielsen, T. O. (2015). NY-ESO-1 (CTAG1B) expression in mesenchymal tumours. *Mod Pathol, 28*(4), 587-595. doi:10.1038/modpathol.2014.155

Everett, J. R. (2015). Academic drug discovery: current status and prospects. *Expert Opin Drug Discov, 10*(9), 937-944. doi:10.1517/17460441.2015.1059816

Falkenberg, N., Anastasov, N., Hofig, I., Bashkueva, K., Lindner, K., Hofler, H., . . . Aubele, M. (2015). Additive impact of HER2-/PTK6-RNAi on interactions with HER3 or IGF-1R leads to reduced breast cancer progression in vivo. *Mol Oncol, 9*(1), 282-294. doi:10.1016/j.molonc.2014.08.012

Faustino-Rocha, A., Oliveira, P. A., Pinho-Oliveira, J., Teixeira-Guedes, C., Soares-Maia, R., da Costa, R. G., . . . Ginja, M. (2013). Estimation of rat mammary tumour volume using caliper and ultrasonography measurements. *Lab Anim (NY), 42*(6), 217-224. doi:10.1038/laban.254

Ferrari, A., De Salvo, G. L., Brennan, B., van Noesel, M. M., De Paoli, A., Casanova, M., . . . Orbach, D. (2015). Synovial sarcoma in children and adolescents: the European Pediatric Soft Tissue Sarcoma Study Group prospective trial (EpSSG NRSTS 2005). *Ann Oncol, 26*(3), 567-572. doi:10.1093/annonc/mdu562

Ferrari, A., Sultan, I., Huang, T. T., Rodriguez-Galindo, C., Shehadeh, A., Meazza, C., . . . Spunt, S. L. (2011). Soft tissue sarcoma across the age spectrum: a population-based study from the Surveillance Epidemiology and End Results database. *Pediatr Blood Cancer, 57*(6), 943-949. doi:10.1002/pbc.23252

Filippakopoulos, P., Muller, S., & Knapp, S. (2009). SH2 domains: modulators of nonreceptor tyrosine kinase activity. *Curr Opin Struct Biol, 19*(6), 643-649. doi:10.1016/j.sbi.2009.10.001

Fisher, C. (1998). Synovial sarcoma. *Ann Diagn Pathol, 2*(6), 401-421.

Flanders, K. C., Heger, C. D., Conway, C., Tang, B., Sato, M., Dengler, S. L., . . . Wakefield, L. M. (2014). Brightfield proximity ligation assay reveals both canonical and mixed transforming growth factor-beta/bone morphogenetic protein Smad signaling complexes in tissue sections. *J Histochem Cytochem, 62*(12), 846-863. doi:10.1369/0022155414550163

Fotheringham, S., Epping, M. T., Stimson, L., Khan, O., Wood, V., Pezzella, F., . . . La Thangue, N. B. (2009). Genome-wide loss-of-function screen reveals an important role for the proteasome in HDAC inhibitor-induced apoptosis. *Cancer Cell, 15*(1), 57-66. doi:10.1016/j.ccr.2008.12.001

Fredriksson, S., Gullberg, M., Jarvius, J., Olsson, C., Pietras, K., Gustafsdottir, S. M., . . . Landegren, U. (2002). Protein detection using proximity-dependent DNA ligation assays. *Nat Biotechnol, 20*(5), 473-477. doi:10.1038/nbt0502-473

Fribley, A., Zeng, Q., & Wang, C. Y. (2004). Proteasome inhibitor PS-341 induces apoptosis through induction of endoplasmic reticulum stress-reactive oxygen species in head and neck squamous cell carcinoma cells. *Mol Cell Biol, 24*(22), 9695-9704. doi:10.1128/MCB.24.22.9695-9704.2004

Friedrichs, N., Trautmann, M., Endl, E., Sievers, E., Kindler, D., Wurst, P., . . . Hartmann, W. (2011). Phosphatidylinositol-3'-kinase/AKT signaling is essential in synovial sarcoma. *Int J Cancer, 129*(7), 1564-1575. doi:10.1002/ijc.25829

Garcia, C. B., Shaffer, C. M., & Eid, J. E. (2012). Genome-wide recruitment to Polycomb-modified chromatin and activity regulation of the synovial sarcoma oncogene SYT-SSX2. *BMC Genomics, 13*, 189. doi:10.1186/1471-2164-13-189

Genovese, G., Carugo, A., Tepper, J., Robinson, F. S., Li, L., Svelto, M., . . . Chin, L. (2017). Synthetic vulnerabilities of mesenchymal subpopulations in pancreatic cancer. *Nature, 542*(7641), 362-366. doi:10.1038/nature21064

Giaginis, C., Damaskos, C., Koutsounas, I., Zizi-Serbetzoglou, A., Tsoukalas, N., Patsouris, E., . . . Theocharis, S. (2015). Histone deacetylase (HDAC)-1, -2, -4 and -6 expression in human pancreatic adenocarcinoma: associations with clinicopathological parameters, tumour proliferative capacity and patients' survival. *BMC Gastroenterol, 15*, 148. doi:10.1186/s12876-015-0379-y

Gjerstorff, M. F., Andersen, M. H., & Ditzel, H. J. (2015). Oncogenic cancer/testis antigens: prime candidates for immunotherapy. *Oncotarget, 6*(18), 15772-15787. doi:10.18632/oncotarget.4694

Goldblum, John R., Folpe, Andrew L., Weiss, Sharon W., Enzinger, Franz M., Weiss, Sharon W., & ClinicalKey Flex. (2014). *Enzinger and Weiss's soft tissue tumours*

Gravitz, L. (2011). Chemoprevention: First line of defence. *Nature, 471*(7339), S5-7. doi:10.1038/471S5a

Grayson, D. R., Kundakovic, M., & Sharma, R. P. (2010). Is there a future for histone deacetylase inhibitors in the pharmacotherapy of psychiatric disorders? *Mol Pharmacol, 77*(2), 126-135. doi:10.1124/mol.109.061333

Habibi, E., Masoudi-Nejad, A., Abdolmaleky, H. M., & Haggarty, S. J. (2011). Emerging roles of epigenetic mechanisms in Parkinson's disease. *Funct Integr Genomics, 11*(4), 523-537. doi:10.1007/s10142-011-0246-z

Haldar, M., Hancock, J. D., Coffin, C. M., Lessnick, S. L., & Capecchi, M. R. (2007). A conditional mouse model of synovial sarcoma: insights into a myogenic origin. *Cancer Cell, 11*(4), 375-388. doi:10.1016/j.ccr.2007.01.016

Haldar, M., Randall, R. L., & Capecchi, M. R. (2008). Synovial sarcoma: from genetics to genetic-based animal modeling. *Clin Orthop Relat Res, 466*(9), 2156-2167. doi:10.1007/s11999-008-0340-2

Hardwick, J. M., & Soane, L. (2013). Multiple functions of BCL-2 family proteins. *Cold Spring Harb Perspect Biol, 5*(2). doi:10.1101/cshperspect.a008722

Hasegawa, T., Yokoyama, R., Matsuno, Y., Shimoda, T., & Hirohashi, S. (2001). Prognostic significance of histologic grade and nuclear expression of beta-catenin in synovial sarcoma. *Hum Pathol, 32*(3), 257-263. doi:10.1053/hupa.2001.22764

Hidalgo, Manuel, Eckhardt, S. Gail, Garrett-Mayer, Elizabeth, & Clendeninn, Neil J. (2010). Principles of Anticancer Drug Development. *Springer Science & Business Media*. doi:10.1007/978-1-4419-7358-0

Hirakawa, N., Naka, T., Yamamoto, I., Fukuda, T., & Tsuneyoshi, M. (1996). Overexpression of bcl-2 protein in synovial sarcoma: a comparative study of other soft tissue spindle cell sarcomas and an additional analysis by fluorescence in situ hybridization. *Hum Pathol, 27*(10), 1060-1065.

Horvai, A. E., Kramer, M. J., & O'Donnell, R. (2006). Beta-catenin nuclear expression correlates with cyclin D1 expression in primary and metastatic synovial sarcoma: a tissue microarray study. *Arch Pathol Lab Med, 130*(6), 792-798. doi:10.1043/1543-2165(2006)130[792:CNECWC]2.0.CO;2

Hughes, J. P., Rees, S., Kalindjian, S. B., & Philpott, K. L. (2011). Principles of early drug discovery. *Br J Pharmacol, 162*(6), 1239-1249. doi:10.1111/j.1476-5381.2010.01127.x

IHle, M. A., Merkelbach-Bruse, S., Hartmann, W., Bauer, S. , Ratner, N., Sonobe, H., . . . Schildhaus, H. U. (2016). HR23b expression is a potential predictive biomarkerfor HDAC inhibitor treatment in mesenchymal tumoursand is associated with response to vorinostat. *J Path: Clin Res, 2*, 59–71.

Ikegaki, N., Katsumata, M., Minna, J., & Tsujimoto, Y. (1994). Expression of bcl-2 in small cell lung carcinoma cells. *Cancer Res, 54*(1), 6-8.

Ishibe, T., Nakayama, T., Okamoto, T., Aoyama, T., Nishijo, K., Shibata, K. R., . . . Toguchida, J. (2005). Disruption of fibroblast growth factor signal pathway inhibits the growth of synovial sarcomas: potential application of signal inhibitors to molecular target therapy. *Clin Cancer Res, 11*(7), 2702-2712. doi:10.1158/1078-0432.CCR-04-2057

Ishizaki, Y., Ikeda, S., Fujimori, M., Shimizu, Y., Kurihara, T., Itamoto, T., . . . Asahara, T. (2004). Immunohistochemical analysis and mutational analyses of beta-catenin, Axin family and APC genes in hepatocellular carcinomas. *Int J Oncol, 24*(5), 1077-1083.

Italiano, A., Di Mauro, I., Rapp, J., Pierron, G., Auger, N., Alberti, L., . . . Pedeutour, F. (2016). Clinical effect of molecular methods in sarcoma diagnosis (GENSARC): a prospective, multicentre, observational study. *Lancet Oncol, 17*(4), 532-538. doi:10.1016/S1470-2045(15)00583-5

Italiano, A., Penel, N., Robin, Y. M., Bui, B., Le Cesne, A., Piperno-Neumann, S., . . . Blay, J. Y. (2009). Neo/adjuvant chemotherapy does not improve outcome in resected primary synovial sarcoma: a study of the French Sarcoma Group. *Ann Oncol, 20*(3), 425-430. doi:10.1093/annonc/mdn678

Ito, T., Ouchida, M., Morimoto, Y., Yoshida, A., Jitsumori, Y., Ozaki, T., . . . Shimizu, K. (2005). Significant growth suppression of synovial sarcomas by the histone deacetylase inhibitor FK228 in vitro and in vivo. *Cancer Lett, 224*(2), 311-319. doi:10.1016/j.canlet.2004.10.030

Jackson, E. M., Sievert, A. J., Gai, X., Hakonarson, H., Judkins, A. R., Tooke, L., . . . Biegel, J. A. (2009). Genomic analysis using high-density single nucleotide polymorphism-based oligonucleotide arrays and multiplex ligation-dependent probe amplification provides a comprehensive analysis of INI1/SMARCB1 in malignant rhabdoid tumours. *Clin Cancer Res, 15*(6), 1923-1930. doi:10.1158/1078-0432.CCR-08-2091

Jagdis, A., Rubin, B. P., Tubbs, R. R., Pacheco, M., & Nielsen, T. O. (2009). Prospective evaluation of TLE1 as a diagnostic immunohistochemical marker in synovial sarcoma. *Am J Surg Pathol, 33*(12), 1743-1751. doi:10.1097/PAS.0b013e3181b7ed36

Jain, S., Xu, R., Prieto, V. G., & Lee, P. (2010). Molecular classification of soft tissue sarcomas and its clinical applications. *Int J Clin Exp Pathol, 3*(4), 416-428.

Jamshidi, F., Bashashati, A., Shumansky, K., Dickson, B., Gokgoz, N., Wunder, J. S., . . . Nielsen, T. O. (2016). The genomic landscape of epithelioid sarcoma cell lines and tumours. *J Pathol, 238*(1), 63-73. doi:10.1002/path.4636

Jarvius, M., Paulsson, J., Weibrecht, I., Leuchowius, K. J., Andersson, A. C., Wahlby, C., . . . Soderberg, O. (2007). In situ detection of phosphorylated platelet-derived growth factor receptor beta using a generalized proximity ligation method. *Mol Cell Proteomics, 6*(9), 1500-1509. doi:10.1074/mcp.M700166-MCP200

Johnston, J. A., Ward, C. L., & Kopito, R. R. (1998). Aggresomes: a cellular response to misfolded proteins. *J Cell Biol, 143*(7), 1883-1898.

Jones, K. B., Barrott, J. J., Xie, M., Haldar, M., Jin, H., Zhu, J. F., . . . Capecchi, M. R. (2016). The impact of chromosomal translocation locus and fusion oncogene coding sequence in synovial sarcomagenesis. *Oncogene*. doi:10.1038/onc.2016.38

Jones, K. B., Haldar, M., Schiffman, J. D., Cannon-Albright, L., Lessnick, S. L., Sharma, S., . . . Randall, R. L. (2011). Of mice and men: opportunities to use genetically engineered mouse models of synovial sarcoma for preclinical cancer therapeutic evaluation. *Cancer Control, 18*(3), 196-203.

Jones, K. B., Su, L., Jin, H., Lenz, C., Randall, R. L., Underhill, T. M., . . . Capecchi, M. R. (2013). SS18-SSX2 and the mitochondrial apoptosis pathway in mouse and human synovial sarcomas. *Oncogene, 32*(18), 2365-2371, 2375 e2361-2365. doi:10.1038/onc.2012.247

Jones, P. A., Issa, J. P., & Baylin, S. (2016). Targeting the cancer epigenome for therapy. *Nat Rev Genet, 17*(10), 630-641. doi:10.1038/nrg.2016.93

Joyner, D. E., Albritton, K. H., Bastar, J. D., & Randall, R. L. (2006). G3139 antisense oligonucleotide directed against antiapoptotic Bcl-2 enhances doxorubicin cytotoxicity in the FU-SY-1 synovial sarcoma cell line. *J Orthop Res, 24*(3), 474-480. doi:10.1002/jor.20087

Jurd, L., Narayanan, V. L., & Paull, K. D. (1987). In vivo antitumour activity of 6-benzyl-1,3-benzodioxole derivatives against the P388, L1210, B16, and M5076 murine models. *J Med Chem, 30*(10), 1752-1756.

Kaap, S., Quentin, I., Tamiru, D., Shaheen, M., Eger, K., & Steinfelder, H. J. (2003). Structure activity analysis of the pro-apoptotic, antitumour effect of nitrostyrene adducts and related compounds. *Biochem Pharmacol, 65*(4), 603-610.

Kadoch, C., & Crabtree, G. R. (2013). Reversible disruption of mSWI/SNF (BAF) complexes by the SS18-SSX oncogenic fusion in synovial sarcoma. *Cell, 153*(1), 71-85. doi:10.1016/j.cell.2013.02.036

Kadoch, C., Hargreaves, D. C., Hodges, C., Elias, L., Ho, L., Ranish, J., & Crabtree, G. R. (2013). Proteomic and bioinformatic analysis of mammalian SWI/SNF complexes identifies extensive roles in human malignancy. *Nat Genet, 45*(6), 592-601. doi:10.1038/ng.2628

Kaitu'u-Lino, T. J., Palmer, K. R., Whitehead, C. L., Williams, E., Lappas, M., & Tong, S. (2012). MMP-14 is expressed in preeclamptic placentas and mediates release of soluble endoglin. *Am J Pathol, 180*(3), 888-894. doi:10.1016/j.ajpath.2011.11.014

Kato, H., Tjernberg, A., Zhang, W., Krutchinsky, A. N., An, W., Takeuchi, T., . . . Roeder, R. G. (2002). SYT associates with human SNF/SWI complexes and the C-terminal region of its fusion partner SSX1 targets histones. *J Biol Chem, 277*(7), 5498-5505. doi:10.1074/jbc.M108702200

Kaufman, R. J., Scheuner, D., Schroder, M., Shen, X., Lee, K., Liu, C. Y., & Arnold, S. M. (2002). The unfolded protein response in nutrient sensing and differentiation. *Nat Rev Mol Cell Biol, 3*(6), 411-421. doi:10.1038/nrm829

Kawaguchi, Y., Kovacs, J. J., McLaurin, A., Vance, J. M., Ito, A., & Yao, T. P. (2003). The deacetylase HDAC6 regulates aggresome formation and cell viability in response to misfolded protein stress. *Cell, 115*(6), 727-738.

Kawai, A., Naito, N., Yoshida, A., Morimoto, Y., Ouchida, M., Shimizu, K., & Beppu, Y. (2004). Establishment and characterization of a biphasic synovial sarcoma cell line, SYO-1. *Cancer Lett, 204*(1), 105-113.

Kawano, S., Grassian, A. R., Tsuda, M., Knutson, S. K., Warholic, N. M., Kuznetsov, G., . . . Keilhack, H. (2016). Preclinical Evidence of Anti-Tumour Activity Induced by EZH2 Inhibition in Human Models of Synovial Sarcoma. *PLoS One, 11*(7), e0158888. doi:10.1371/journal.pone.0158888

Kawasaki, H., Schiltz, L., Chiu, R., Itakura, K., Taira, K., Nakatani, Y., & Yokoyama, K. K. (2000). ATF-2 has intrinsic histone acetyltransferase activity which is modulated by phosphorylation. *Nature, 405*(6783), 195-200. doi:10.1038/35012097

Khan, O., Fotheringham, S., Wood, V., Stimson, L., Zhang, C., Pezzella, F., . . . La Thangue, N. B. (2010). HR23B is a biomarker for tumour sensitivity to HDAC inhibitor-based therapy. *Proc Natl Acad Sci U S A, 107*(14), 6532-6537. doi:10.1073/pnas.0913912107

Kia, S. K., Gorski, M. M., Giannakopoulos, S., & Verrijzer, C. P. (2008). SWI/SNF mediates polycomb eviction and epigenetic reprogramming of the INK4b-ARF-INK4a locus. *Mol Cell Biol, 28*(10), 3457-3464. doi:10.1128/MCB.02019-07

Kim, J. H., Kim, J. H., Lee, G. E., Lee, J. E., & Chung, I. K. (2003). Potent inhibition of human telomerase by nitrostyrene derivatives. *Mol Pharmacol, 63*(5), 1117-1124.

Kim, K. H., Kim, W., Howard, T. P., Vazquez, F., Tsherniak, A., Wu, J. N., . . . Roberts, C. W. (2015). SWI/SNF-mutant cancers depend on catalytic and non-catalytic activity of EZH2. *Nat Med, 21*(12), 1491-1496. doi:10.1038/nm.3968

Kim, Y. B., Ki, S. W., Yoshida, M., & Horinouchi, S. (2000). Mechanism of cell cycle arrest caused by histone deacetylase inhibitors in human carcinoma cells. *J Antibiot (Tokyo), 53*(10), 1191-1200.

Klotz, L. O., Sanchez-Ramos, C., Prieto-Arroyo, I., Urbanek, P., Steinbrenner, H., & Monsalve, M. (2015). Redox regulation of FoxO transcription factors. *Redox Biol, 6*, 51-72. doi:10.1016/j.redox.2015.06.019

Kohno, K., Normington, K., Sambrook, J., Gething, M. J., & Mori, K. (1993). The promoter region of the yeast KAR2 (BiP) gene contains a regulatory domain that responds to the presence of unfolded proteins in the endoplasmic reticulum. *Mol Cell Biol, 13*(2), 877-890.

Kovar, H. (2011). Dr. Jekyll and Mr. Hyde: The Two Faces of the FUS/EWS/TAF15 Protein Family. *Sarcoma, 2011*, 837474. doi:10.1155/2011/837474

Kovi, R. C., Paliwal, S., Pande, S., & Grossman, S. R. (2010). An ARF/CtBP2 complex regulates BH3-only gene expression and p53-independent apoptosis. *Cell Death Differ, 17*(3), 513-521. doi:10.1038/cdd.2009.140

Kreiger, P. A., Judkins, A. R., Russo, P. A., Biegel, J. A., Lestini, B. J., Assanasen, C., & Pawel, B. R. (2009). Loss of INI1 expression defines a unique subset of pediatric undifferentiated soft tissue sarcomas. *Mod Pathol, 22*(1), 142-150. doi:10.1038/modpathol.2008.185

Krieg, A. H., Hefti, F., Speth, B. M., Jundt, G., Guillou, L., Exner, U. G., . . . Siebenrock, K. A. (2010). Synovial sarcomas usually metastasize after >5 years: a multicenter retrospective analysis with minimum follow-up of 10 years for survivors. *Annals of Oncology*. doi:10.1093/annonc/mdq394

Krskova, L., Kalinova, M., Brizova, H., Mrhalova, M., Sumerauer, D., & Kodet, R. (2009). Molecular and immunohistochemical analyses of BCL2, KI-67, and cyclin D1 expression in synovial sarcoma. *Cancer Genet Cytogenet, 193*(1), 1-8. doi:10.1016/j.cancergencyto.2009.03.008

Kuwahara, Y., Wei, D., Durand, J., & Weissman, B. E. (2013). SNF5 reexpression in malignant rhabdoid tumours regulates transcription of target genes by recruitment of SWI/SNF complexes and RNAPII to the transcription start site of their promoters. *Mol Cancer Res, 11*(3), 251-260. doi:10.1158/1541-7786.MCR-12-0390

Ladanyi, M. (2001). Fusions of the SYT and SSX genes in synovial sarcoma. *Oncogene, 20*(40), 5755-5762. doi:DOI 10.1038/sj.onc.1204601

Lai, J. P., Robbins, P. F., Raffeld, M., Aung, P. P., Tsokos, M., Rosenberg, S. A., . . . Lee, C. C. (2012). NY-ESO-1 expression in synovial sarcoma and other mesenchymal tumours: significance for NY-ESO-1-based targeted therapy and differential diagnosis. *Mod Pathol, 25*(6), 854-858. doi:10.1038/modpathol.2012.31

Laporte, A. N., Barrott, J. J., Yao, R. J., Poulin, N. M., Brodin, B. A., Jones, K. B., . . . Nielsen, T. O. (2017). HDAC and Proteasome Inhibitors Synergize to Activate Pro-Apoptotic Factors in Synovial Sarcoma. *PLoS One, 12*(1), e0169407. doi:10.1371/journal.pone.0169407

Laporte, A. N., Ji, J. X., Ma, L., Nielsen, T. O., & Brodin, B. A. (2016). Identification of cytotoxic agents disrupting synovial sarcoma oncoprotein interactions by proximity ligation assay. *Oncotarget, 7*(23), 34384-34394. doi:10.18632/oncotarget.8882

Lawlor, E. R., & Thiele, C. J. (2012). Epigenetic changes in pediatric solid tumours: promising new targets. *Clin Cancer Res, 18*(10), 2768-2779. doi:10.1158/1078-0432.CCR-11-1921

Le Cesne, A., Ouali, M., Leahy, M. G., Santoro, A., Hoekstra, H. J., Hohenberger, P., . . . Van Der Graaf, W. T. (2014). Doxorubicin-based adjuvant chemotherapy in soft tissue sarcoma: pooled analysis of two STBSG-EORTC phase III clinical trials. *Ann Oncol, 25*(12), 2425-2432. doi:10.1093/annonc/mdu460

Le Tourneau, C., Lee, J. J., & Siu, L. L. (2009). Dose escalation methods in phase I cancer clinical trials. *J Natl Cancer Inst, 101*(10), 708-720. doi:10.1093/jnci/djp079

Lee, K., Tirasophon, W., Shen, X., Michalak, M., Prywes, R., Okada, T., . . . Kaufman, R. J. (2002). IRE1-mediated unconventional mRNA splicing and S2P-mediated ATF6

cleavage merge to regulate XBP1 in signaling the unfolded protein response. *Genes Dev, 16*(4), 452-466. doi:10.1101/gad.964702

Leppa, S., & Bohmann, D. (1999). Diverse functions of JNK signaling and c-Jun in stress response and apoptosis. *Oncogene, 18*(45), 6158-6162. doi:10.1038/sj.onc.1203173

Leuchowius, K. J., Jarvius, M., Wickstrom, M., Rickardson, L., Landegren, U., Larsson, R., . . . Jarvius, J. (2010). High content screening for inhibitors of protein interactions and post-translational modifications in primary cells by proximity ligation. *Mol Cell Proteomics, 9*(1), 178-183. doi:10.1074/mcp.M900331-MCP200

Levanon, D., Goldstein, R. E., Bernstein, Y., Tang, H., Goldenberg, D., Stifani, S., . . . Groner, Y. (1998). Transcriptional repression by AML1 and LEF-1 is mediated by the TLE/Groucho corepressors. *Proc Natl Acad Sci U S A, 95*(20), 11590-11595.

Li, C., Li, R., Grandis, J. R., & Johnson, D. E. (2008). Bortezomib induces apoptosis via Bim and Bik up-regulation and synergizes with cisplatin in the killing of head and neck squamous cell carcinoma cells. *Mol Cancer Ther, 7*(6), 1647-1655. doi:10.1158/1535-7163.MCT-07-2444

Li, X. N., Shu, Q., Su, J. M., Perlaky, L., Blaney, S. M., & Lau, C. C. (2005). Valproic acid induces growth arrest, apoptosis, and senescence in medulloblastomas by increasing histone hyperacetylation and regulating expression of p21Cip1, CDK4, and CMYC. *Mol Cancer Ther, 4*(12), 1912-1922. doi:10.1158/1535-7163.MCT-05-0184

Li, Y., & Seto, E. (2016). HDACs and HDAC Inhibitors in Cancer Development and Therapy. *Cold Spring Harb Perspect Med, 6*(10). doi:10.1101/cshperspect.a026831

Liu, P., Cheng, H., Roberts, T. M., & Zhao, J. J. (2009). Targeting the phosphoinositide 3-kinase pathway in cancer. *Nat Rev Drug Discov, 8*(8), 627-644. doi:10.1038/nrd2926

Llambi, F., Moldoveanu, T., Tait, S. W., Bouchier-Hayes, L., Temirov, J., McCormick, L. L., . . . Green, D. R. (2011). A unified model of mammalian BCL-2 protein family interactions at the mitochondria. *Mol Cell, 44*(4), 517-531. doi:10.1016/j.molcel.2011.10.001

Love, M. I., Huber, W., & Anders, S. (2014). Moderated estimation of fold change and dispersion for RNA-seq data with DESeq2. *Genome Biol, 15*(12), 550. doi:10.1186/s13059-014-0550-8

Lu, H., Li, G., Zhou, C., Jin, W., Qian, X., Wang, Z., . . . Wang, X. (2016). Regulation and role of post-translational modifications of enhancer of zeste homologue 2 in cancer development. *Am J Cancer Res, 6*(12), 2737-2754.

Lubieniecka, J. M., de Bruijn, D. R., Su, L., van Dijk, A. H., Subramanian, S., van de Rijn, M., . . . Nielsen, T. O. (2008). Histone deacetylase inhibitors reverse SS18-SSX-mediated polycomb silencing of the tumour suppressor early growth response 1 in synovial sarcoma. *Cancer Res, 68*(11), 4303-4310. doi:10.1158/0008-5472.CAN-08-0092

Luo, H., Yang, Y., Duan, J., Wu, P., Jiang, Q., & Xu, C. (2013). PTEN-regulated AKT/FoxO3a/Bim signaling contributes to reactive oxygen species-mediated apoptosis in selenite-treated colorectal cancer cells. *Cell Death Dis, 4*, e481. doi:10.1038/cddis.2013.3

Maher, Christopher A., Kumar-Sinha, Chandan, Cao, Xuhong, Kalyana-Sundaram, Shanker, Han, Bo, Jing, Xiaojun, . . . Chinnaiyan, Arul M. (2009). Transcriptome sequencing to detect gene fusions in cancer. *Nature, 458*(7234), 97-101. doi:http://www.nature.com/nature/journal/v458/n7234/suppinfo/nature07638_S1.html

Mancuso, T., Mezzelani, A., Riva, C., Fabbri, A., Dal Bo, L., Sampietro, G., . . . Pilotti, S. (2000). Analysis of SYT-SSX fusion transcripts and bcl-2 expression and phosphorylation status in synovial sarcoma. *Lab Invest, 80*(6), 805-813.

Mani, R. S., & Chinnaiyan, A. M. (2010). Triggers for genomic rearrangements: insights into genomic, cellular and environmental influences. *Nat Rev Genet, 11*(12), 819-829. doi:10.1038/nrg2883

Marks, P. A. (2010). The clinical development of histone deacetylase inhibitors as targeted anticancer drugs. *Expert Opin Investig Drugs, 19*(9), 1049-1066. doi:10.1517/13543784.2010.510514

Marks, P. A., Richon, V. M., & Rifkind, R. A. (2000). Histone deacetylase inhibitors: inducers of differentiation or apoptosis of transformed cells. *J Natl Cancer Inst, 92*(15), 1210-1216.

McWilliams, R. R., Wieben, E. D., Rabe, K. G., Pedersen, K. S., Wu, Y., Sicotte, H., & Petersen, G. M. (2011). Prevalence of CDKN2A mutations in pancreatic cancer patients: implications for genetic counseling. *Eur J Hum Genet, 19*(4), 472-478. doi:10.1038/ejhg.2010.198

Meissner, A., Mikkelsen, T. S., Gu, H., Wernig, M., Hanna, J., Sivachenko, A., . . . Lander, E. S. (2008). Genome-scale DNA methylation maps of pluripotent and differentiated cells. *Nature, 454*(7205), 766-770. doi:10.1038/nature07107

Mertens, F., Antonescu, C. R., Hohenberger, P., Ladanyi, M., Modena, P., D'Incalci, M., . . . Alvegard, T. (2009). Translocation-related sarcomas. *Semin Oncol, 36*(4), 312-323. doi:10.1053/j.seminoncol.2009.06.004

Messerschmitt, P. J., Rettew, A. N., Schroeder, N. O., Brookover, R. E., Jakatdar, A. P., Getty, P. J., & Greenfield, E. M. (2012). Osteosarcoma Phenotype Is Inhibited by 3,4-Methylenedioxy-beta-nitrostyrene. *Sarcoma, 2012*, 479712. doi:10.1155/2012/479712

Mi, H., Muruganujan, A., Casagrande, J. T., & Thomas, P. D. (2013). Large-scale gene function analysis with the PANTHER classification system. *Nat Protoc, 8*(8), 1551-1566. doi:10.1038/nprot.2013.092

Micale, N., Zappala, M., & Grasso, S. (2002). Synthesis and antitumour activity of 1,3-benzodioxole derivatives. *Farmaco, 57*(10), 853-859.

Middeljans, E., Wan, X., Jansen, P. W., Sharma, V., Stunnenberg, H. G., & Logie, C. (2012). SS18 together with animal-specific factors defines human BAF-type SWI/SNF complexes. *PLoS One, 7*(3), e33834. doi:10.1371/journal.pone.0033834

Mikkelsen, T. S., Ku, M., Jaffe, D. B., Issac, B., Lieberman, E., Giannoukos, G., . . . Bernstein, B. E. (2007). Genome-wide maps of chromatin state in pluripotent and lineage-committed cells. *Nature, 448*(7153), 553-560. doi:10.1038/nature06008

Mills, A. A. (2010). Throwing the cancer switch: reciprocal roles of polycomb and trithorax proteins. *Nat Rev Cancer, 10*(10), 669-682. doi:10.1038/nrc2931

Mohan, R., Rastogi, N., Namboothiri, I. N., Mobin, S. M., & Panda, D. (2006). Synthesis and evaluation of alpha-hydroxymethylated conjugated nitroalkenes for their anticancer activity: inhibition of cell proliferation by targeting microtubules. *Bioorg Med Chem, 14*(23), 8073-8085. doi:10.1016/j.bmc.2006.07.035

Monni, O., Joensuu, H., Franssila, K., Klefstrom, J., Alitalo, K., & Knuutila, S. (1997). BCL2 overexpression associated with chromosomal amplification in diffuse large B-cell lymphoma. *Blood, 90*(3), 1168-1174.

Mora-Blanco, E. L., Mishina, Y., Tillman, E. J., Cho, Y. J., Thom, C. S., Pomeroy, S. L., . . . Roberts, C. W. (2014). Activation of beta-catenin/TCF targets following loss of the tumour suppressor SNF5. *Oncogene, 33*(7), 933-938. doi:10.1038/onc.2013.37

Moreau, P., Facon, T., Touzeau, C., Benboubker, L., Delain, M., Badamo-Dotzis, J., . . . Leleu, X. (2016). Quisinostat, bortezomib, and dexamethasone combination therapy for relapsed multiple myeloma. *Leuk Lymphoma*, 1-14. doi:10.3109/10428194.2015.1117611

Moreno-Bueno, G., Rodriguez-Perales, S., Sanchez-Estevez, C., Hardisson, D., Sarrio, D., Prat, J., . . . Palacios, J. (2003). Cyclin D1 gene (CCND1) mutations in endometrial cancer. *Oncogene, 22*(38), 6115-6118. doi:10.1038/sj.onc.1206868

Muer, A., Overkamp, T., Gillissen, B., Richter, A., Pretzsch, T., Milojkovic, A., . . . Hemmati, P. (2012). p14(ARF)-induced apoptosis in p53 protein-deficient cells is mediated by BH3-only protein-independent derepression of Bak protein through down-regulation of Mcl-1 and Bcl-xL proteins. *J Biol Chem, 287*(21), 17343-17352. doi:10.1074/jbc.M111.314898

Muscat, A., Popovski, D., Jayasekara, W. S., Rossello, F. J., Ferguson, M., Marini, K. D., . . . Ashley, D. M. (2016). Low-Dose Histone Deacetylase Inhibitor Treatment Leads to Tumour Growth Arrest and Multi-Lineage Differentiation of Malignant Rhabdoid Tumours. *Clin Cancer Res, 22*(14), 3560-3570. doi:10.1158/1078-0432.CCR-15-2260

Nair, P., Muthukkumar, S., Sells, S. F., Han, S. S., Sukhatme, V. P., & Rangnekar, V. M. (1997). Early growth response-1-dependent apoptosis is mediated by p53. *J Biol Chem, 272*(32), 20131-20138.

Naka, N., Takenaka, S., Araki, N., Miwa, T., Hashimoto, N., Yoshioka, K., . . . Itoh, K. (2010). Synovial sarcoma is a stem cell malignancy. *Stem Cells, 28*(7), 1119-1131. doi:10.1002/stem.452

Nawrocki, S. T., Carew, J. S., Pino, M. S., Highshaw, R. A., Andtbacka, R. H., Dunner, K., Jr., . . . McConkey, D. J. (2006). Aggresome disruption: a novel strategy to enhance bortezomib-induced apoptosis in pancreatic cancer cells. *Cancer Res, 66*(7), 3773-3781. doi:10.1158/0008-5472.CAN-05-2961

Neuville, A., Chibon, F., & Coindre, J. M. (2014). Grading of soft tissue sarcomas: from histological to molecular assessment. *Pathology, 46*(2), 113-120. doi:10.1097/PAT.0000000000000048

Ng, T. L., Gown, A. M., Barry, T. S., Cheang, M. C., Chan, A. K., Turbin, D. A., . . . Nielsen, T. O. (2005). Nuclear beta-catenin in mesenchymal tumours. *Mod Pathol, 18*(1), 68-74. doi:10.1038/modpathol.3800272

Nielsen, T. O., Poulin, N. M., & Ladanyi, M. (2015). Synovial sarcoma: recent discoveries as a roadmap to new avenues for therapy. *Cancer Discov, 5*(2), 124-134. doi:10.1158/2159-8290.CD-14-1246

Noh, K. M., Allis, C. D., & Li, H. (2016). Reading between the Lines: "ADD"-ing Histone and DNA Methylation Marks toward a New Epigenetic "Sum". *ACS Chem Biol, 11*(3), 554-563. doi:10.1021/acschembio.5b00830

Nojima, T., Wang, Y. S., Abe, S., Matsuno, T., Yamawaki, S., & Nagashima, K. (1990). Morphological and cytogenetic studies of a human synovial sarcoma xenotransplanted into nude mice. *Acta Pathol Jpn, 40*(7), 486-493.

Novo, F. J., & Vizmanos, J. L. (2006). Chromosome translocations in cancer: computational evidence for the random generation of double-strand breaks. *Trends Genet, 22*(4), 193-196. doi:10.1016/j.tig.2006.02.001

Nuytten, M., Beke, L., Van Eynde, A., Ceulemans, H., Beullens, M., Van Hummelen, P., . . . Bollen, M. (2008). The transcriptional repressor NIPP1 is an essential player in EZH2-mediated gene silencing. *Oncogene, 27*(10), 1449-1460. doi:10.1038/sj.onc.1210774

Okcu, M. F., Despa, S., Choroszy, M., Berrak, S. G., Cangir, A., Jaffe, N., & Raney, R. B. (2001). Synovial sarcoma in children and adolescents: thirty three years of experience with multimodal therapy. *Med Pediatr Oncol, 37*(2), 90-96. doi:10.1002/mpo.1175

Oren, M., Tal, P., & Rotter, V. (2016). Targeting mutant p53 for cancer therapy. *Aging (Albany NY), 8*(6), 1159-1160. doi:10.18632/aging.100992

Ormanns, S., Neumann, J., Horst, D., Kirchner, T., & Jung, A. (2014). WNT signaling and distant metastasis in colon cancer through transcriptional activity of nuclear beta-Catenin depend on active PI3K signaling. *Oncotarget, 5*(10), 2999-3011. doi:10.18632/oncotarget.1626

Ozdag, H., Teschendorff, A. E., Ahmed, A. A., Hyland, S. J., Blenkiron, C., Bobrow, L., . . . Caldas, C. (2006). Differential expression of selected histone modifier genes in human solid cancers. *BMC Genomics, 7*, 90. doi:10.1186/1471-2164-7-90

Papadopoulou, T., Kaymak, A., Sayols, S., & Richly, H. (2016). Dual role of Med12 in PRC1-dependent gene repression and ncRNA-mediated transcriptional activation. *Cell Cycle, 15*(11), 1479-1493. doi:10.1080/15384101.2016.1175797

Park, J., & Pei, D. (2004). trans-Beta-nitrostyrene derivatives as slow-binding inhibitors of protein tyrosine phosphatases. *Biochemistry, 43*(47), 15014-15021. doi:10.1021/bi0486233

Park, T. S., Groh, E. M., Patel, K., Kerkar, S. P., Lee, C. C., & Rosenberg, S. A. (2016). Expression of MAGE-A and NY-ESO-1 in Primary and Metastatic Cancers. *J Immunother, 39*(1), 1-7. doi:10.1097/CJI.0000000000000101

Pedersen, E. A., Menon, R., Bailey, K. M., Thomas, D. G., Van Noord, R. A., Tran, J., . . . Lawlor, E. R. (2016). Activation of Wnt/beta-Catenin in Ewing Sarcoma Cells Antagonizes EWS/ETS Function and Promotes Phenotypic Transition to More Metastatic Cell States. *Cancer Res, 76*(17), 5040-5053. doi:10.1158/0008-5472.CAN-15-3422

Peng, C., Guo, W., Yang, Y., & Zhao, H. (2008). Downregulation of SS18-SSX1 expression by small interfering RNA inhibits growth and induces apoptosis in human synovial sarcoma cell line HS-SY-II in vitro. *Eur J Cancer Prev, 17*(5), 392-398. doi:10.1097/CEJ.0b013e328305a11b

Peng, C. L., Guo, W., Ji, T., Ren, T., Yang, Y., Li, D. S., . . . Tang, X. D. (2009). Sorafenib induces growth inhibition and apoptosis in human synovial sarcoma cells via inhibiting the RAF/MEK/ERK signaling pathway. *Cancer Biol Ther, 8*(18), 1729-1736.

Pifl, C., Nagy, G., Berenyi, S., Kattinger, A., Reither, H., & Antus, S. (2005). Pharmacological characterization of ecstasy synthesis byproducts with recombinant human monoamine transporters. *J Pharmacol Exp Ther, 314*(1), 346-354. doi:10.1124/jpet.105.084426

Pomerantz, J., Schreiber-Agus, N., Liegeois, N. J., Silverman, A., Alland, L., Chin, L., . . . DePinho, R. A. (1998). The Ink4a tumour suppressor gene product, p19Arf, interacts with MDM2 and neutralizes MDM2's inhibition of p53. *Cell, 92*(6), 713-723.

Porta, C., Paglino, C., & Mosca, A. (2014). Targeting PI3K/Akt/mTOR Signaling in Cancer. *Front Oncol, 4*, 64. doi:10.3389/fonc.2014.00064

Qi, Y., Wang, C. C., He, Y. L., Zou, H., Liu, C. X., Pang, L. J., . . . Li, F. (2013). The correlation between morphology and the expression of TGF-beta signaling pathway proteins and epithelial-mesenchymal transition-related proteins in synovial sarcomas. *Int J Clin Exp Pathol, 6*(12), 2787-2799.

Quelle, D. E., Zindy, F., Ashmun, R. A., & Sherr, C. J. (1995). Alternative reading frames of the INK4a tumour suppressor gene encode two unrelated proteins capable of inducing cell cycle arrest. *Cell, 83*(6), 993-1000.

Rekhi, B., & Vogel, U. (2015). Utility of characteristic 'Weak to Absent' INI1/SMARCB1/BAF47 expression in diagnosis of synovial sarcomas. *APMIS, 123*(7), 618-628. doi:10.1111/apm.12395

Richardson, P. G., Hungria, V. T., Yoon, S. S., Beksac, M., Dimopoulos, M. A., Elghandour, A., . . . San-Miguel, J. F. (2016). Panobinostat plus bortezomib and dexamethasone in previously treated multiple myeloma: outcomes by prior treatment. *Blood, 127*(6), 713-721. doi:10.1182/blood-2015-09-665018

Rikimaru, T., Taketomi, A., Yamashita, Y., Shirabe, K., Hamatsu, T., Shimada, M., & Maehara, Y. (2007). Clinical significance of histone deacetylase 1 expression in patients with hepatocellular carcinoma. *Oncology, 72*(1-2), 69-74. doi:10.1159/000111106

Ritchie, M. E., Phipson, B., Wu, D., Hu, Y., Law, C. W., Shi, W., & Smyth, G. K. (2015). limma powers differential expression analyses for RNA-sequencing and microarray studies. *Nucleic Acids Res, 43*(7), e47. doi:10.1093/nar/gkv007

Rivlin, N., Brosh, R., Oren, M., & Rotter, V. (2011). Mutations in the p53 Tumour Suppressor Gene: Important Milestones at the Various Steps of Tumourigenesis. *Genes Cancer, 2*(4), 466-474. doi:10.1177/1947601911408889

Robbins, P. F., Kassim, S. H., Tran, T. L., Crystal, J. S., Morgan, R. A., Feldman, S. A., . . . Rosenberg, S. A. (2015). A pilot trial using lymphocytes genetically engineered with an NY-ESO-1-reactive T-cell receptor: long-term follow-up and correlates with response. *Clin Cancer Res, 21*(5), 1019-1027. doi:10.1158/1078-0432.CCR-14-2708

Sabah, M., Cummins, R., Leader, M., & Kay, E. (2005). Loss of p16INK4A expression is associated with allelic imbalance/loss of heterozygosity of chromosome 9p21 in microdissected synovial sarcomas. *Virchows Arch, 447*(5), 842-848. doi:10.1007/s00428-005-0024-1

Saito, T., Nagai, M., & Ladanyi, M. (2006). SYT-SSX1 and SYT-SSX2 interfere with repression of E-cadherin by snail and slug: a potential mechanism for aberrant mesenchymal to epithelial transition in human synovial sarcoma. *Cancer Res, 66*(14), 6919-6927. doi:10.1158/0008-5472.CAN-05-3697

Sakuma, T., Uzawa, K., Onda, T., Shiiba, M., Yokoe, H., Shibahara, T., & Tanzawa, H. (2006). Aberrant expression of histone deacetylase 6 in oral squamous cell carcinoma. *Int J Oncol, 29*(1), 117-124.

Sandberg, A. A., & Bridge, J. A. (2002). Updates on the cytogenetics and molecular genetics of bone and soft tissue tumours. Synovial sarcoma. *Cancer Genet Cytogenet, 133*(1), 1-23.

Santos, C. X., Tanaka, L. Y., Wosniak, J., & Laurindo, F. R. (2009). Mechanisms and implications of reactive oxygen species generation during the unfolded protein response: roles of endoplasmic reticulum oxidoreductases, mitochondrial electron transport, and NADPH oxidase. *Antioxid Redox Signal, 11*(10), 2409-2427. doi:10.1089/ARS.2009.2625

Sarrut, D., Badel, J. N., Halty, A., Garin, G., Perol, D., Cassier, P., . . . Giraudet, A. L. (2017). 3D absorbed dose distribution estimated by Monte Carlo simulation in radionuclide therapy with a monoclonal antibody targeting synovial sarcoma. *EJNMMI Phys, 4*(1), 6. doi:10.1186/s40658-016-0172-1

Schoenwaelder, S. M., & Jackson, S. P. (2012). Bcl-xL-inhibitory BH3 mimetics (ABT-737 or ABT-263) and the modulation of cytosolic calcium flux and platelet function. *Blood, 119*(5), 1320-1321; author reply 1321-1322. doi:10.1182/blood-2011-10-387399

Schweitzer, B., Wiltshire, S., Lambert, J., O'Malley, S., Kukanskis, K., Zhu, Z., . . . Ward, D. C. (2000). Immunoassays with rolling circle DNA amplification: a versatile platform for ultrasensitive antigen detection. *Proc Natl Acad Sci U S A, 97*(18), 10113-10119. doi:10.1073/pnas.170237197

Setsu, N., Kohashi, K., Fushimi, F., Endo, M., Yamamoto, H., Takahashi, Y., . . . Oda, Y. (2013). Prognostic impact of the activation status of the Akt/mTOR pathway in synovial sarcoma. *Cancer, 119*(19), 3504-3513. doi:10.1002/cncr.28255

Sharpless, N. E., & Sherr, C. J. (2015). Forging a signature of in vivo senescence. *Nat Rev Cancer, 15*(7), 397-408. doi:10.1038/nrc3960

Shen, J. K., Cote, G. M., Gao, Y., Choy, E., Mankin, H. J., Hornicek, F. J., & Duan, Z. (2016). Targeting EZH2-mediated methylation of H3K27 inhibits proliferation and migration of Synovial Sarcoma in vitro. *Sci Rep, 6*, 25239. doi:10.1038/srep25239

Shtutman, M., Zhurinsky, J., Simcha, I., Albanese, C., D'Amico, M., Pestell, R., & Ben-Ze'ev, A. (1999). The cyclin D1 gene is a target of the beta-catenin/LEF-1 pathway. *Proc Natl Acad Sci U S A, 96*(10), 5522-5527.

Shukla, N., Somwar, R., Smith, R. S., Ambati, S., Munoz, S., Merchant, M., . . . Ladanyi, M. (2016). Proteasome Addiction Defined in Ewing Sarcoma Is Effectively Targeted by a Novel Class of 19S Proteasome Inhibitors. *Cancer Res*. doi:10.1158/0008-5472.CAN-16-1040

Siegel, D. S., Dimopoulos, M., Jagannath, S., Goldschmidt, H., Durrant, S., Kaufman, J. L., . . . Anderson, K. C. (2016). VANTAGE 095: An International, Multicenter, Open-Label Study of Vorinostat (MK-0683) in Combination With Bortezomib in Patients With Relapsed and Refractory Multiple Myeloma. *Clin Lymphoma Myeloma Leuk*. doi:10.1016/j.clml.2016.02.042

Skytting, B., Nilsson, G., Brodin, B., Xie, Y., Lundeberg, J., Uhlen, M., & Larsson, O. (1999). A novel fusion gene, SYT-SSX4, in synovial sarcoma. *J Natl Cancer Inst, 91*(11), 974-975.

Slingerland, M., Guchelaar, H. J., & Gelderblom, H. (2014). Histone deacetylase inhibitors: an overview of the clinical studies in solid tumours. *Anticancer Drugs, 25*(2), 140-149. doi:10.1097/CAD.0000000000000040

Soderberg, O., Gullberg, M., Jarvius, M., Ridderstrale, K., Leuchowius, K. J., Jarvius, J., . . . Landegren, U. (2006). Direct observation of individual endogenous protein complexes in situ by proximity ligation. *Nat Methods, 3*(12), 995-1000. doi:10.1038/nmeth947

Soderberg, O., Leuchowius, K. J., Gullberg, M., Jarvius, M., Weibrecht, I., Larsson, L. G., & Landegren, U. (2008). Characterizing proteins and their interactions in cells and tissues using the in situ proximity ligation assay. *Methods, 45*(3), 227-232. doi:10.1016/j.ymeth.2008.06.014

Song, Y., Madahar, V., & Liao, J. (2011). Development of FRET assay into quantitative and high-throughput screening technology platforms for protein-protein interactions. *Ann Biomed Eng, 39*(4), 1224-1234. doi:10.1007/s10439-010-0225-x

Sonobe, H., Manabe, Y., Furihata, M., Iwata, J., Oka, T., Ohtsuki, Y., . . . Abe, S. (1992). Establishment and characterization of a new human synovial sarcoma cell line, HS-SY-II. *Lab Invest, 67*(4), 498-505.

Soulez, M., Saurin, A. J., Freemont, P. S., & Knight, J. C. (1999). SSX and the synovial-sarcoma-specific chimaeric protein SYT-SSX co-localize with the human Polycomb group complex. *Oncogene, 18*(17), 2739-2746. doi:10.1038/sj.onc.1202613

Spence, S., Deurinck, M., Ju, H., Traebert, M., McLean, L., Marlowe, J., . . . Friedrichs, G. S. (2016). Histone Deacetylase Inhibitors Prolong Cardiac Repolarization through Transcriptional Mechanisms. *Toxicol Sci, 153*(1), 39-54. doi:10.1093/toxsci/kfw104

Spiegel, S., Milstien, S., & Grant, S. (2012). Endogenous modulators and pharmacological inhibitors of histone deacetylases in cancer therapy. *Oncogene, 31*(5), 537-551. doi:10.1038/onc.2011.267

Su, L., Cheng, H., Sampaio, A. V., Nielsen, T. O., & Underhill, T. M. (2010). EGR1 reactivation by histone deacetylase inhibitors promotes synovial sarcoma cell death through the PTEN tumour suppressor. *Oncogene, 29*(30), 4352-4361. doi:10.1038/onc.2010.204

Su, L., Sampaio, A. V., Jones, K. B., Pacheco, M., Goytain, A., Lin, S., . . . Nielsen, T. O. (2012). Deconstruction of the SS18-SSX fusion oncoprotein complex: insights into disease etiology and therapeutics. *Cancer Cell, 21*(3), 333-347. doi:10.1016/j.ccr.2012.01.010

Subramanian, A., Tamayo, P., Mootha, V. K., Mukherjee, S., Ebert, B. L., Gillette, M. A., . . . Mesirov, J. P. (2005). Gene set enrichment analysis: a knowledge-based approach for interpreting genome-wide expression profiles. *Proc Natl Acad Sci U S A, 102*(43), 15545-15550. doi:10.1073/pnas.0506580102

Subramanian, S., Bates, S. E., Wright, J. J., Espinoza-Delgado, I., & Piekarz, R. L. (2010). Clinical Toxicities of Histone Deacetylase Inhibitors. *Pharmaceuticals (Basel), 3*(9), 2751-2767. doi:10.3390/ph3092751

Sulong, S., Moorman, A. V., Irving, J. A., Strefford, J. C., Konn, Z. J., Case, M. C., . . . Harrison, C. J. (2009). A comprehensive analysis of the CDKN2A gene in childhood acute lymphoblastic leukemia reveals genomic deletion, copy number neutral loss of heterozygosity, and association with specific cytogenetic subgroups. *Blood, 113*(1), 100-107. doi:10.1182/blood-2008-07-166801

Sun, W. J., Zhou, X., Zheng, J. H., Lu, M. D., Nie, J. Y., Yang, X. J., & Zheng, Z. Q. (2012). Histone acetyltransferases and deacetylases: molecular and clinical implications to

gastrointestinal carcinogenesis. *Acta Biochim Biophys Sin (Shanghai), 44*(1), 80-91. doi:10.1093/abbs/gmr113

Takebe, N., Miele, L., Harris, P. J., Jeong, W., Bando, H., Kahn, M., . . . Ivy, S. P. (2015). Targeting Notch, Hedgehog, and Wnt pathways in cancer stem cells: clinical update. *Nat Rev Clin Oncol, 12*(8), 445-464. doi:10.1038/nrclinonc.2015.61

Takenaka, S., Naka, N., Araki, N., Hashimoto, N., Ueda, T., Yoshioka, K., . . . Itoh, K. (2010). Downregulation of SS18-SSX1 expression in synovial sarcoma by small interfering RNA enhances the focal adhesion pathway and inhibits anchorage-independent growth in vitro and tumour growth in vivo. *Int J Oncol, 36*(4), 823-831.

Tallarida, R. J. (2011). Quantitative methods for assessing drug synergism. *Genes Cancer, 2*(11), 1003-1008. doi:10.1177/1947601912440575

Tamaki, S., Fukuta, M., Sekiguchi, K., Jin, Y., Nagata, S., Hayakawa, K., . . . Toguchida, J. (2015). SS18-SSX, the Oncogenic Fusion Protein in Synovial Sarcoma, Is a Cellular Context-Dependent Epigenetic Modifier. *PLoS One, 10*(11), e0142991. doi:10.1371/journal.pone.0142991

Tang, L., Nogales, E., & Ciferri, C. (2010). Structure and function of SWI/SNF chromatin remodeling complexes and mechanistic implications for transcription. *Prog Biophys Mol Biol, 102*(2-3), 122-128. doi:10.1016/j.pbiomolbio.2010.05.001

Taylor, B. S., Barretina, J., Maki, R. G., Antonescu, C. R., Singer, S., & Ladanyi, M. (2011). Advances in sarcoma genomics and new therapeutic targets. *Nat Rev Cancer, 11*(8), 541-557. doi:10.1038/nrc3087

Terry, J., Saito, T., Subramanian, S., Ruttan, C., Antonescu, C. R., Goldblum, J. R., . . . Nielsen, T. O. (2007). TLE1 as a diagnostic immunohistochemical marker for synovial sarcoma emerging from gene expression profiling studies. *Am J Surg Pathol, 31*(2), 240-246. doi:10.1097/01.pas.0000213330.71745.39

Thaete, C., Brett, D., Monaghan, P., Whitehouse, S., Rennie, G., Rayner, E., . . . Goodwin, G. (1999). Functional domains of the SYT and SYT-SSX synovial sarcoma translocation proteins and co-localization with the SNF protein BRM in the nucleus. *Hum Mol Genet, 8*(4), 585-591.

Thurn, K. T., Thomas, S., Moore, A., & Munster, P. N. (2011). Rational therapeutic combinations with histone deacetylase inhibitors for the treatment of cancer. *Future Oncol, 7*(2), 263-283. doi:10.2217/fon.11.2

Trapnell, C., Roberts, A., Goff, L., Pertea, G., Kim, D., Kelley, D. R., . . . Pachter, L. (2012). Differential gene and transcript expression analysis of RNA-seq experiments with TopHat and Cufflinks. *Nat Protoc, 7*(3), 562-578. doi:10.1038/nprot.2012.016

Trautmann, M., Sievers, E., Aretz, S., Kindler, D., Michels, S., Friedrichs, N., . . . Hartmann, W. (2014). SS18-SSX fusion protein-induced Wnt/beta-catenin signaling is a therapeutic target in synovial sarcoma. *Oncogene, 33*(42), 5006-5016. doi:10.1038/onc.2013.443

Tsang, KH, Chan, WSW, Chan, MK, Lai, KC, & Chan, ACL. (2016). Synovial Sarcoma: Epidemiology, Prognosis, and Imaging in a Tertiary Referral Centre. *Hong Kong J Radiol, 19*, 19-27. doi:10.12809/hkjr1615298

Tsao, H., & Niendorf, K. (2004). Genetic testing in hereditary melanoma. *J Am Acad Dermatol, 51*(5), 803-808. doi:10.1016/j.jaad.2004.04.045

Tsujimoto, Y., Cossman, J., Jaffe, E., & Croce, C. M. (1985). Involvement of the bcl-2 gene in human follicular lymphoma. *Science, 228*(4706), 1440-1443.

Ungerstedt, J. S., Sowa, Y., Xu, W. S., Shao, Y., Dokmanovic, M., Perez, G., . . . Marks, P. A. (2005). Role of thioredoxin in the response of normal and transformed cells to histone deacetylase inhibitors. *Proc Natl Acad Sci U S A, 102*(3), 673-678. doi:10.1073/pnas.0408732102

Vadlakonda, L., Pasupuleti, M., & Pallu, R. (2013). Role of PI3K-AKT-mTOR and Wnt Signaling Pathways in Transition of G1-S Phase of Cell Cycle in Cancer Cells. *Front Oncol, 3*, 85. doi:10.3389/fonc.2013.00085

Valente, A. L., Tull, J., & Zhang, S. (2013). Specificity of TLE1 expression in unclassified high-grade sarcomas for the diagnosis of synovial sarcoma. *Appl Immunohistochem Mol Morphol, 21*(5), 408-413. doi:10.1097/PAI.0b013e318279f9ee

van der Graaf, W. T., Blay, J. Y., Chawla, S. P., Kim, D. W., Bui-Nguyen, B., Casali, P. G., . . . group, Palette study. (2012). Pazopanib for metastatic soft-tissue sarcoma (PALETTE): a randomised, double-blind, placebo-controlled phase 3 trial. *Lancet, 379*(9829), 1879-1886. doi:10.1016/S0140-6736(12)60651-5

Varambally, S., Dhanasekaran, S. M., Zhou, M., Barrette, T. R., Kumar-Sinha, C., Sanda, M. G., . . . Chinnaiyan, A. M. (2002). The polycomb group protein EZH2 is involved in progression of prostate cancer. *Nature, 419*(6907), 624-629. doi:10.1038/nature01075

Velazquez, E. F., Jungbluth, A. A., Yancovitz, M., Gnjatic, S., Adams, S., O'Neill, D., . . . Bhardwaj, N. (2007). Expression of the cancer/testis antigen NY-ESO-1 in primary and metastatic malignant melanoma (MM)--correlation with prognostic factors. *Cancer Immun, 7*, 11.

Venugopal, B., Baird, R., Kristeleit, R. S., Plummer, R., Cowan, R., Stewart, A., . . . Banerji, U. (2013). A phase I study of quisinostat (JNJ-26481585), an oral hydroxamate histone deacetylase inhibitor with evidence of target modulation and antitumour activity, in patients with advanced solid tumours. *Clin Cancer Res, 19*(15), 4262-4272. doi:10.1158/1078-0432.CCR-13-0312

Virolle, T., Adamson, E. D., Baron, V., Birle, D., Mercola, D., Mustelin, T., & de Belle, I. (2001). The Egr-1 transcription factor directly activates PTEN during irradiation-induced signalling. *Nat Cell Biol, 3*(12), 1124-1128. doi:10.1038/ncb1201-1124

Vlenterie, M., Hillebrandt-Roeffen, M. H., Schaars, E. W., Flucke, U. E., Fleuren, E. D., Navis, A. C., . . . van der Graaf, W. T. (2016). Targeting Cyclin-Dependent Kinases in Synovial Sarcoma: Palbociclib as a Potential Treatment for Synovial Sarcoma Patients. *Ann Surg Oncol, 23*(9), 2745-2752. doi:10.1245/s10434-016-5341-x

Wei, M. C., Zong, W. X., Cheng, E. H., Lindsten, T., Panoutsakopoulou, V., Ross, A. J., . . . Korsmeyer, S. J. (2001). Proapoptotic BAX and BAK: a requisite gateway to mitochondrial dysfunction and death. *Science, 292*(5517), 727-730. doi:10.1126/science.1059108

West, A. C., & Johnstone, R. W. (2014). New and emerging HDAC inhibitors for cancer treatment. *J Clin Invest, 124*(1), 30-39. doi:10.1172/JCI69738

Wilson, B. G., Wang, X., Shen, X., McKenna, E. S., Lemieux, M. E., Cho, Y. J., . . . Roberts, C. W. (2010). Epigenetic antagonism between polycomb and SWI/SNF complexes during oncogenic transformation. *Cancer Cell, 18*(4), 316-328. doi:10.1016/j.ccr.2010.09.006

Xie, B., Wang, C., Zheng, Z., Song, B., Ma, C., Thiel, G., & Li, M. (2011). Egr-1 transactivates Bim gene expression to promote neuronal apoptosis. *J Neurosci, 31*(13), 5032-5044. doi:10.1523/JNEUROSCI.5504-10.2011

Xie, Y., Skytting, B., Nilsson, G., Gasbarri, A., Haslam, K., Bartolazzi, A., . . . Larsson, O. (2002). SYT-SSX is critical for cyclin D1 expression in synovial sarcoma cells: a gain of function of the t(X;18)(p11.2;q11.2) translocation. *Cancer Res, 62*(13), 3861-3867.

Xie, Y., Skytting, B., Nilsson, G., Grimer, R. J., Mangham, C. D., Fisher, C., . . . Larsson, O. (2002). The SYT-SSX1 fusion type of synovial sarcoma is associated with increased expression of cyclin A and D1. A link between t(X;18)(p11.2; q11.2) and the cell cycle machinery. *Oncogene, 21*(37), 5791-5796. doi:10.1038/sj.onc.1205700

Yamamoto, K., Ichijo, H., & Korsmeyer, S. J. (1999). BCL-2 is phosphorylated and inactivated by an ASK1/Jun N-terminal protein kinase pathway normally activated at G(2)/M. *Molecular and Cellular Biology, 19*(12), 8469-8478.

Yao, D., Dai, C., & Peng, S. (2011). Mechanism of the mesenchymal-epithelial transition and its relationship with metastatic tumour formation. *Mol Cancer Res, 9*(12), 1608-1620. doi:10.1158/1541-7786.MCR-10-0568

Yasui, H., Imura, Y., Outani, H., Hamada, K., Nakai, T., Yamada, S., . . . Naka, N. (2016). Trabectedin is a promising antitumour agent for synovial sarcoma. *J Chemother, 28*(5), 417-424. doi:10.1080/1120009X.2015.1133013

Yokota, S., Kitahara, M., & Nagata, K. (2000). Benzylidene lactam compound, KNK437, a novel inhibitor of acquisition of thermotolerance and heat shock protein induction in human colon carcinoma cells. *Cancer Res, 60*(11), 2942-2948.

Yu, Q., Geng, Y., & Sicinski, P. (2001). Specific protection against breast cancers by cyclin D1 ablation. *Nature, 411*(6841), 1017-1021. doi:10.1038/35082500

Zhu, H., Zhang, L., Dong, F., Guo, W., Wu, S., Teraishi, F., . . . Fang, B. (2005). Bik/NBK accumulation correlates with apoptosis-induction by bortezomib (PS-341, Velcade) and other proteasome inhibitors. *Oncogene, 24*(31), 4993-4999. doi:10.1038/sj.onc.1208683

Zinszner, H., Kuroda, M., Wang, X., Batchvarova, N., Lightfoot, R. T., Remotti, H., . . . Ron, D. (1998). CHOP is implicated in programmed cell death in response to impaired function of the endoplasmic reticulum. *Genes Dev, 12*(7), 982-995.

Zupkovitz, G., Grausenburger, R., Brunmeir, R., Senese, S., Tischler, J., Jurkin, J., . . . Seiser, C. (2010). The cyclin-dependent kinase inhibitor p21 is a crucial target for histone deacetylase 1 as a regulator of cellular proliferation. *Mol Cell Biol, 30*(5), 1171-1181. doi:10.1128/MCB.01500-09

APPENDIX I

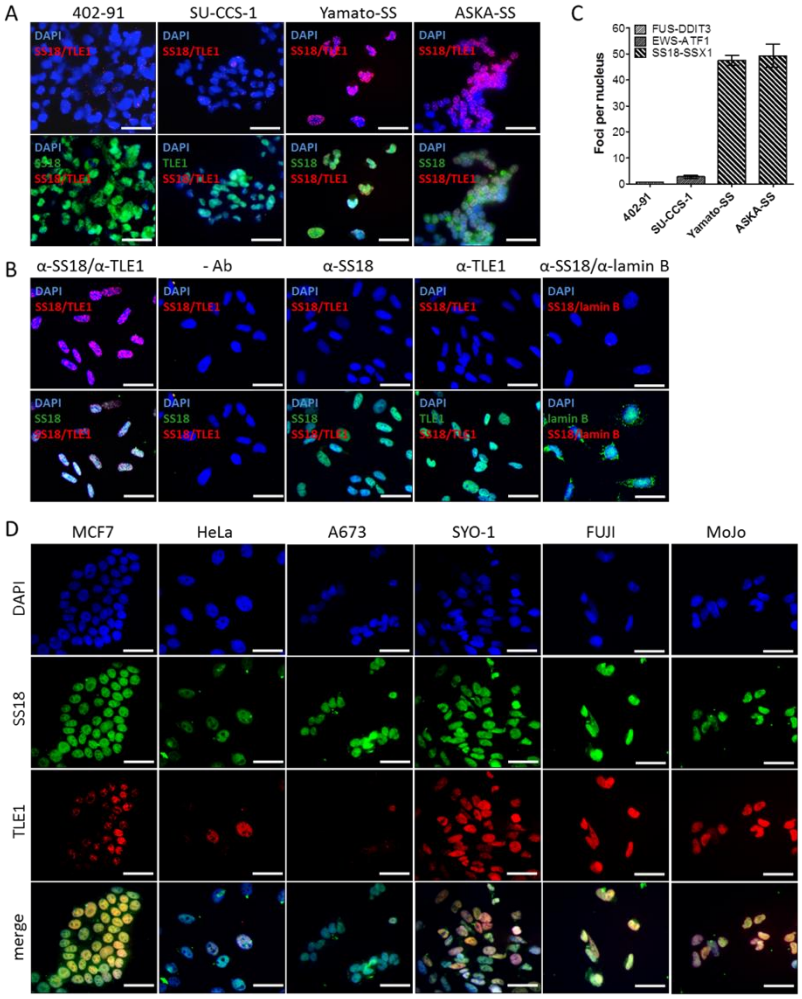

Figure I.1: The proximity ligation assay (PLA) demonstrated SS18-SSX/TLE1 co-localization selectively when SS18 (rabbit) and TLE1 (mouse) antibodies were included. (A, C) Beyond the cell lines that could be shown in Figure 2.1, additional SS18-SSX-containing synovial sarcoma cell lines Yamato-SS and ASKA-SS were also positive for SS18-SSX/TLE1 co-localization, whereas additional translocation-associated sarcoma cell lines (402-91 myxoid liposarcoma, SU-CCS-1 clear cell sarcoma) were not. (B) Control experiments with no antibody, single antibody or non-specific antibody inclusion resulted in little to no nuclear signal in SYO-1 cells. (D) All these cell lines, including control lines (MCF7, HeLa, A673) expressed some level of detectable SS18 (green channel) and TLE (red channel), but only SS18-SSX positive lines stain positive for nuclear PLA signals, indicating signal was a result of the SS18-SSX/TLE1 interaction and was not likely a result of wild-type protein interactions. Scale bars represent 20 μm. Error bars represent standard error of mean from three images.

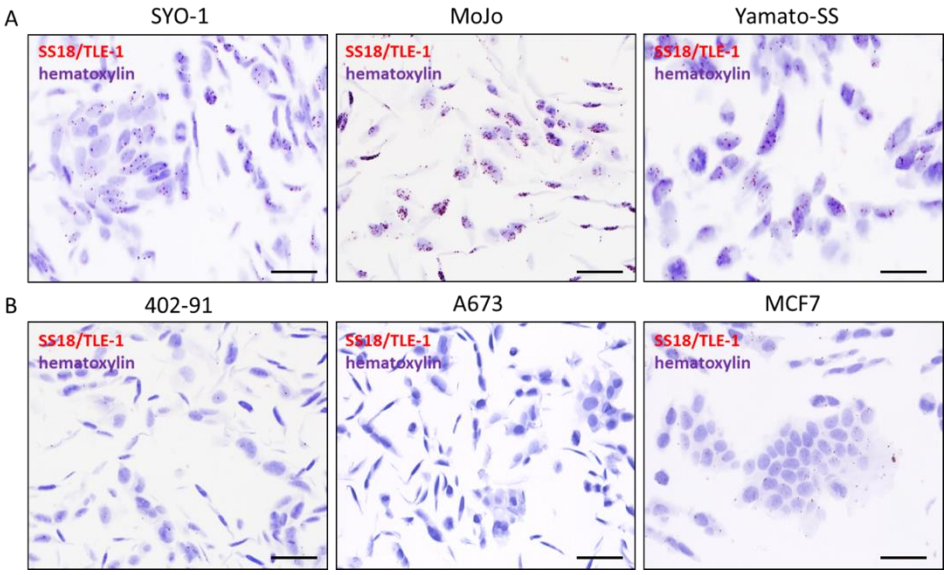

Figure I.2: The PLA assay could detect SS18-SSX/TLE1 co-localization in formalin fixed paraffin embedded (FFPE) pelleted cell samples. (A) Nuclear PLA signal was selectively detected in synovial sarcoma cell lines, (B) and not in cell lines from other types of cancer: 402-91 myxoid liposarcoma, A673 Ewing sarcoma, MCF7 breast cancer. Scale bars represent 20 μm.

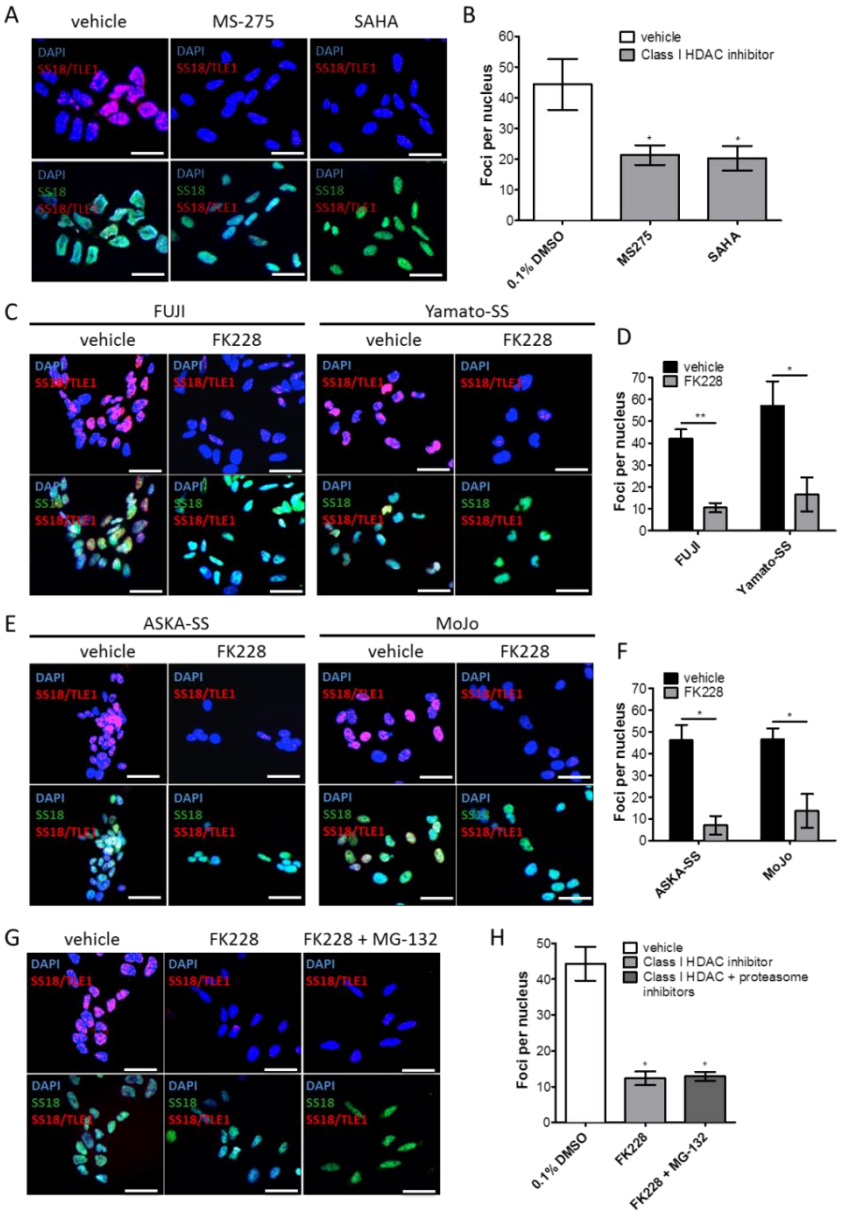

Figure I.3: Class I HDAC inhibitors significantly decreased nuclear PLA signal for SS18-SSX/TLE1 in synovial sarcoma. (A, B) At 12-hours post treatment in SYO-1 cells, nuclear PLA signal was decreased following incubation with IC_{50} doses of MS-275 and SAHA. (C-F) Class I HDAC inhibition consistently brought about a significant decrease in PLA signal in four additional human synovial sarcoma cell lines: FUJI, Yamato-SS, ASKA-SS and MoJo. (G, H) Class I HDAC inhibition dissociated SS18 from TLE1, consistently with and without the addition of a proteasome inhibitor, suggesting loss of PLA signal was not solely due to a loss of SS18-SSX protein. Scale bars represent 20 μm. Statistical significance compared to vehicle treated controls was determined by Student t test: * denotes $p < 0.05$; * denotes $p < 0.05$; ** denotes $p < 0.01$. Error bars represent standard error of mean from three images.

APPENDIX II

Proposal Concept: Phase II study of quisinostat in combination with bortezomib in translocation-associated soft tissue sarcomas

Lead Group: CCTG **Agents**: quisinostat (JNJ 26481585), bortezomib
Diseases: Synovial sarcoma (SS), clear cell sarcoma (CCS), myxoid liposarcoma (MLS), desmoplastic small round cell tumour (DSRCT)
Hypothesis: The HDAC inhibitor quisinostat in combination with the proteasome inhibitor bortezomib will improve progression-free survival in patients with SS, CCS, MLS and DSRCT, all translocation-associated sarcomas with a predilection for adolescents & young adults (AYA).
Objectives: The primary objective is to determine the activity of bortezomib plus quisinostat as defined by the 4-month progression-free survival (PFS) rate in patients with advanced or metastatic soft tissue sarcoma. Secondary objectives are (a) to determine the safety and tolerability of bortezomib plus quisinostat as defined by the frequency and severity of adverse events, (b) to determine the objective response rate and duration using RECIST criteria, and (c) to perform correlative studies that may define patients with a superior/inferior PFS.
Background and Rationale
Disease Setting: SS, CCS, MLS and DSRCT are aggressive soft-tissue malignancies that affect primarily AYA. Their limited chemo-sensitivity and high risk of local and metastatic recurrence, including late events, result in long-term disease-specific mortality rates of approximately 50% (SS), 65% (CCS), 15% (MLS) and 85% (DSRCT). Laboratory experiments *in vitro* indicate that the characteristic SS18/SSX fusion oncoprotein of SS, resulting from a pathognomonic t(X;18) translocation event, represses expression of EGR1, a key positive regulator of the tumour suppressor PTEN. This permits up-regulation of the PI3K/AKT/mTOR signaling pathway, resulting in a proliferative, anti-apoptotic phenotype. HDAC activity evokes this abnormal gene transcription in complex with PRC2 in SS, as a result of interactions with the driver fusion oncoprotein SS18/SSX. Similarly, CCS (EWS/ATF1), MLS (FUS/DDIT3) and DSRCT (EWS/WT1) have driving fusion oncoproteins, which epigenetically mediate oncogenesis.

New drug screens applied to multiple translocation-associated sarcoma cell lines found HDAC, PI3K/Akt and proteasome inhibitors to be the top hits from among more than 100 drug classes. At minute doses, the combination of HDAC inhibition and proteasome inhibition was observed to synergize and elicit significant apoptosis in SS, CCS, MLS and DSRCT *in vitro*. Utilizing a novel proximity ligation assay, the association of SS18/SSX with its effector complex was found to be specifically disrupted by this drug combination. Quisinostat inhibits HDAC activity, restoring transcription of abnormally-repressed tumour suppressors and differentiation genes. Bortezomib elicits cell apoptosis by preventing the breakdown of ubiquitinated proteins and synergizes with quisinostat in eliciting cell death. Their combination leads to an accumulation of ubiquitin-tagged SS18/SSX oncoprotein in SS cells at doses similar to those used in multiple myeloma, disrupting oncogenesis. Furthermore, aggresome-mediated resistance to bortezomib is obstructed by quisinostat via its inhibition of HDAC6 activity. This provides a second mechanistic rationale for the special synergism of the proposed drug combination.

Restoration of normal *EGR1* transcription and degradation of the driving oncoprotein have been observed to occur following HDAC inhibition *in vitro*, and in our recent IND.200 trial of the HDAC inhibitor SB939, most evaluable cases of SS (N=3), CCS (N=1), MLS (N=4) and DSRCT (N=2) achieved stable disease (Chu Q et al. *Ann Oncol* 2015, PMID: 25632070). This trial was able to establish a network of adult CCTG affiliated hospitals in Canada able to activate sarcoma subtype-specific trials and to accrue patients with translocation-associated sarcomas, but

was one of three trials that had to be terminated early due to financial restructuring at the supplier of SB939. Accrual rates in Canada were exceeding targets at the time of study closure.
Drug Information: The FDA has approved bortezomib (Velcade) for use in myeloma and mantle cell lymphoma. Quisinostat is a new HDAC inhibitor the FDA has approved for use in human clinical trials. The individual effectiveness of HDAC and proteasome inhibitors in myeloma, together with the rationale for synergistic action on the pathway for dealing with ubiquitinated proteins, led to a phase Ib trial utilizing the quisinostat-bortezomib combination being undertaken for patients with relapsed multiple myeloma: NCT01464112. This drug combination, here independently proposed for sarcoma treatment, was found to be active for treatment of relapsed multiple myeloma and was observed to have an acceptable safety profile (PMID: 26758913).
Eligibility Criteria: Recurrent and/or metastatic SS, CCS, MLS or DSRCT in patients ≥ 13 years of age; measurable disease by RECIST 1.1; adequate hematological parameters (ANC >1.5 x 109/L, platelet >100 x 109/L), liver (total bilirubin < ULN and AST/ALT <2.5 x ULN), renal (serum creatinine, potassium, calcium and magnesium within normal limits) and cardiac functions (QTc <450 msec, LVEF >50% by echocardiogram or MUGA and normal Troponin); availability of FFPE tissue for molecular confirmation of the diagnosis.
Ineligibility Criteria: Greater than two previous lines of chemotherapy; ECOG status >2, prior exposure to proteasome inhibitors or HDAC inhibitors.
Treatment Plan: quisinostat 10 mg po on days 1-3-5 weekly + bortezomib 1.3 mg/m^2 SQ on days 1-4-8-11 of a 3-week cycle. Patients will be treated until disease progression, unacceptable toxicity, consent withdrawal or a maximum of six cycles for stable disease (SD) or 12 cycles for complete response or partial response (as maintenance therapy beyond best radiological response has no established clinical benefit).
Translational Studies: The exon-specific translocation present in each case will be delineated using a NanoString-based assay recently developed in the Nielsen lab with funding from a Canadian Cancer Society Impact grant. This will molecularly-confirm the diagnosis as an integrated biomarker, and allow exploratory analyses as to whether the translocation subtype correlates with drug response. Additionally, we will use a pre-established, published assessment and scoring system for HDAC2 protein expression to test the correlative science hypothesis that an HDAC2 expression score >=5 will predict the group of patients who achieve 4 month PFS.
Statistical Considerations: The primary objective of this trial is to evaluate PFS at 4 months. The combination will not be of additional interest in this population if the true 4 month PFS probability is <15% (p0), whereas a true PFS of >40% (p1) will be of interest. A minimum of 21 patients would be needed, with the drug combination considered to be of interest if 6 or more are progression free at 4 months. This design has a significance level of 10% and a power of 90%.
Milestones and deliverables: The precedent for recruitment of AYA patients will follow the successful experience of CCTG IND.200, a trial of similar translocation-associated sarcomas which, after central activation, was able to open at 8 centres, registering 24 patients in 18 months. The current proposal would offer a new study to this population from both pediatric and adult hospitals through NCIC/C17.
Funding: The principal investigators (Drs. T Nielsen and T Alcindor) co-chair the CCTG sarcoma committee and will work through its established mechanisms to provide partial funding support. NewVac and Torrey Pines, makers of quisinostat, will supply drug and partial funding support. Proteasome inhibitor manufacturers (Janssen, Amgen, and Takeda) have been approached by ourselves and by Torrey Pines on several occasions over the past few months, but so far have not committed to provide funding support. Canadian Cancer Society funds (Impact grant to PI Nielsen) are available to support molecular correlative sciences, and Nielsen will personally provide pathology review support.

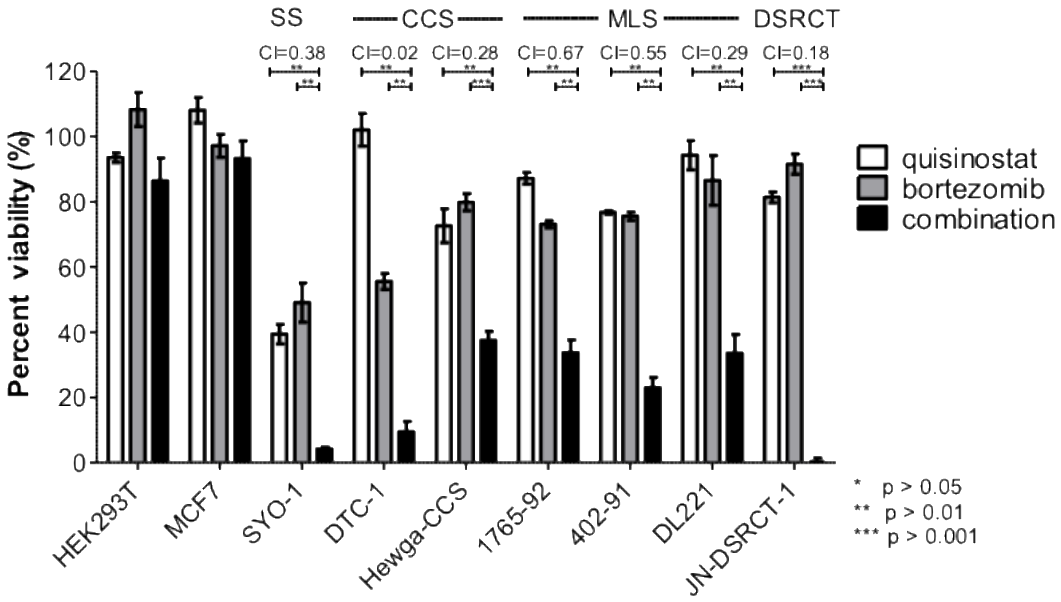

Figure II.1: Quisinostat and bortezomib synergized in translocation-associated soft tissue sarcomas. Combination index (CI) numbers of less than 1 are considered to be synergistic. The combination was synergistic in SS (synovial sarcoma), CCS (clear cell sarcoma), MLS (myxoid liposarcoma), DSRCT (desmoplastic small round cell tumour) but not in normal HEK293T cells or beast carcinoma MCF-7 cells. Statistical significance compared to vehicle treated controls was determined by Student t test: * denotes $p < 0.05$; * denotes $p < 0.05$; ** denotes $p < 0.01$. Error bars represent standard error of mean from three images.